# Heavy ion physics: what do we know at the start of NICA

Alexey Aparin, LHEP JINR

## Part 1 Setting the scene

Introduction
Model description of HIC
Equation of State
Phase diagram of QCD

# How do we study nuclear matter?

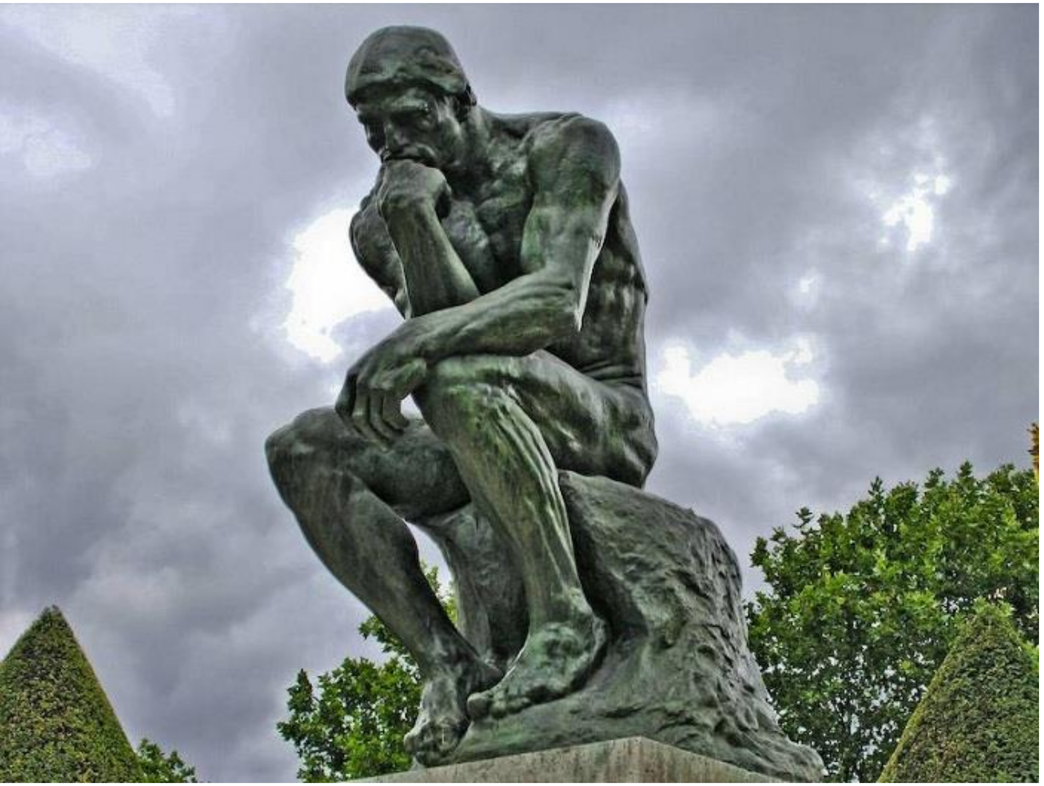

# How do we study nuclear matter?

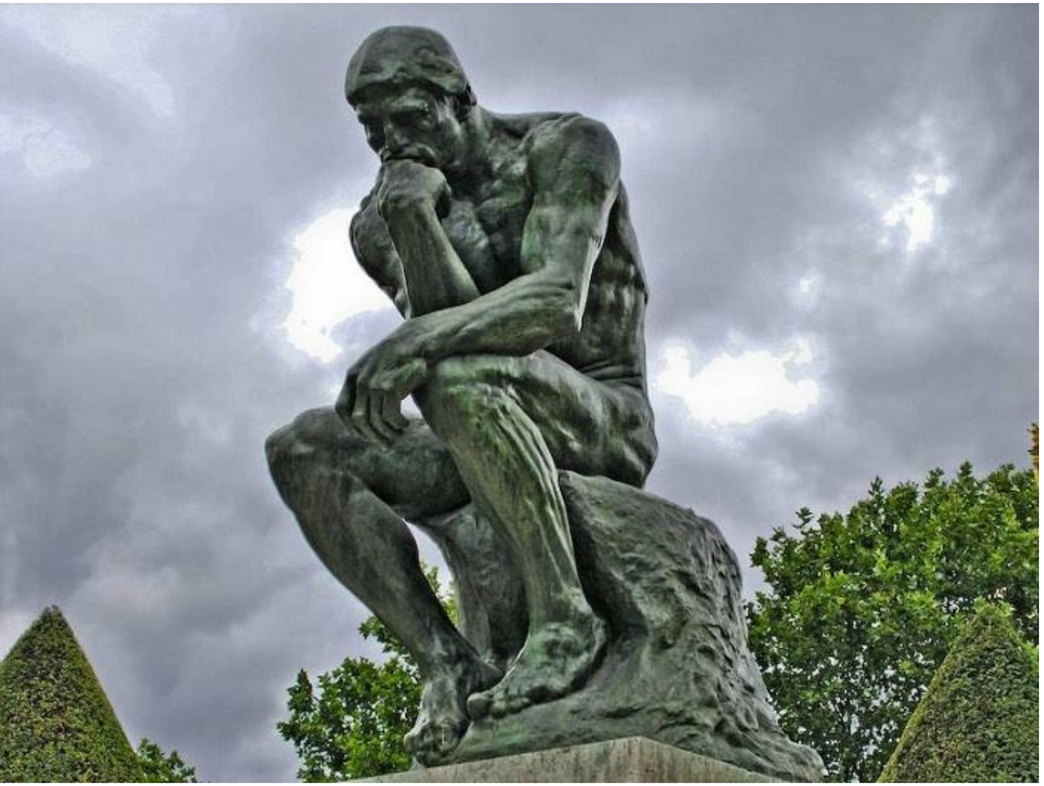

Typical scale of high energy experiment 1 fm = $10^{-13}$ sm
Typical timeframe ~ 1 – 100 fm/c = 0.3 – 30 * $10^{-23}$ sec

We need to use some beam of test particles to collide it into the sample we want to investigate

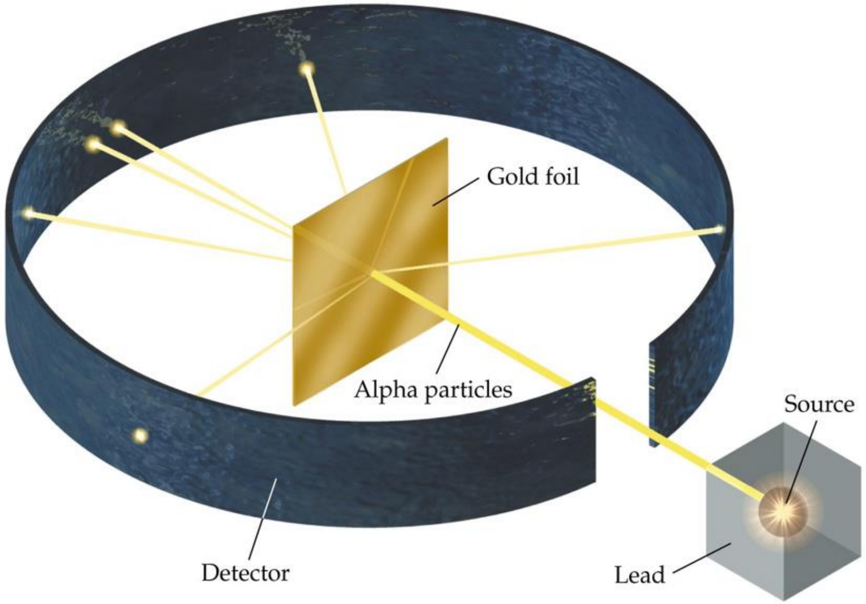

# How do we study nuclear matter?

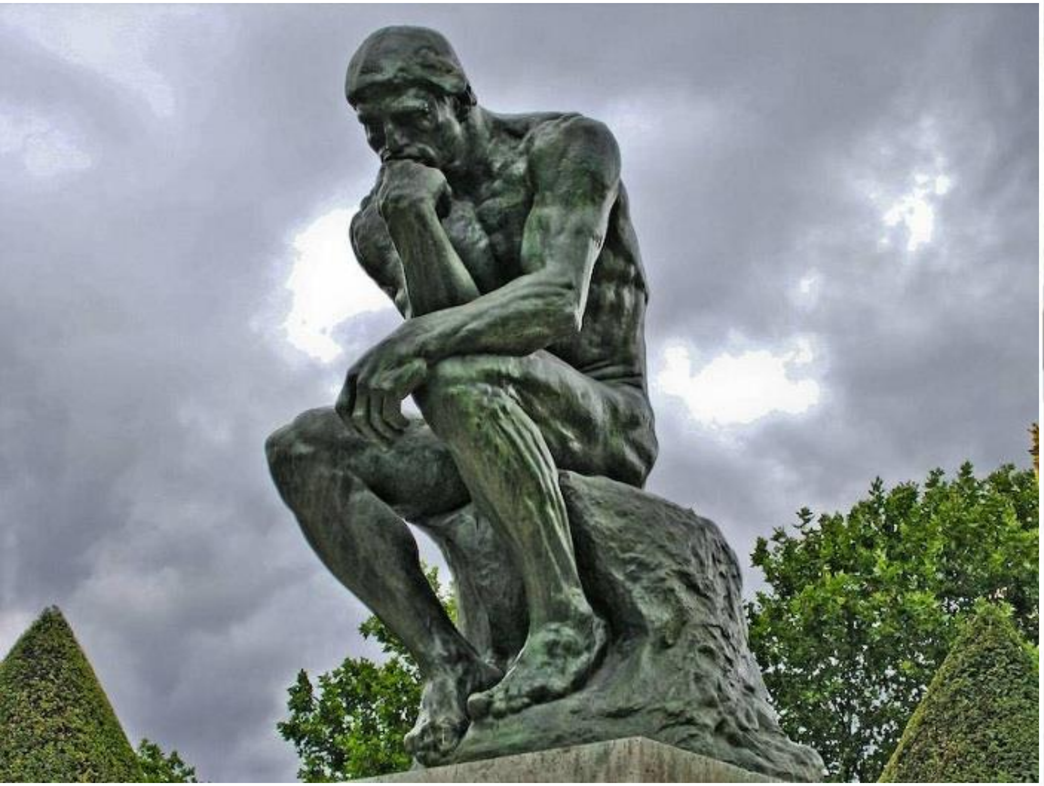


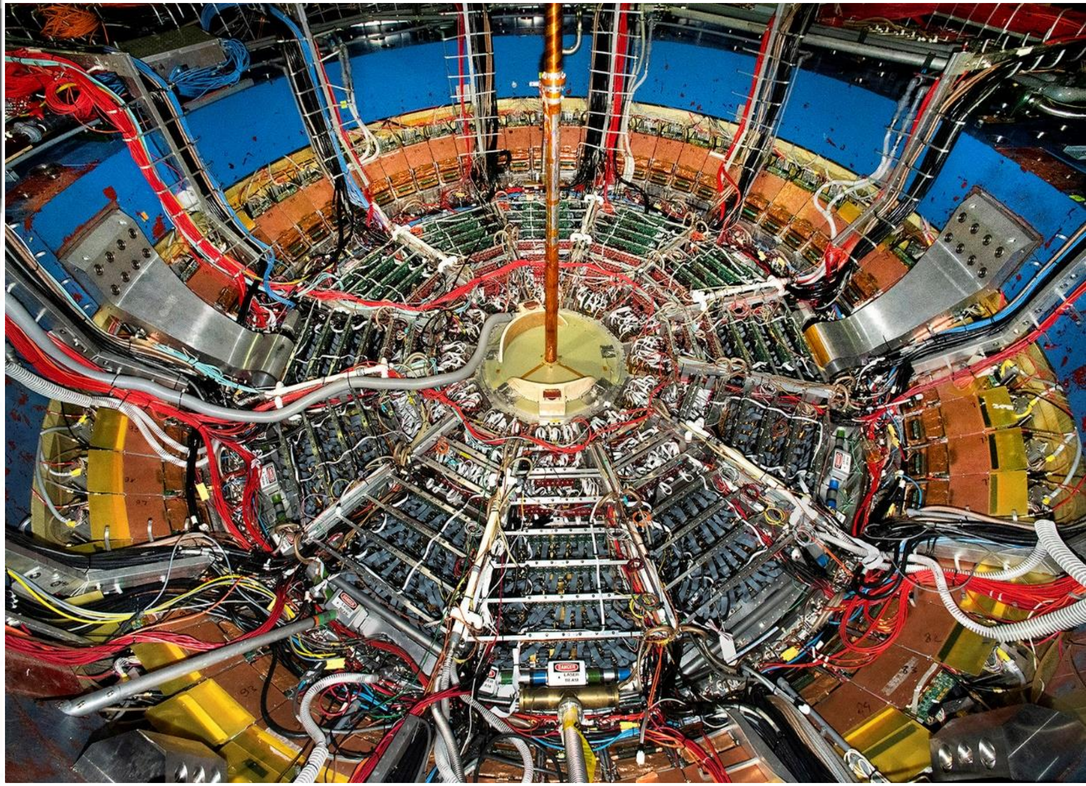

We need to understand well what we are going to collide!

# How does the nucleus look like?

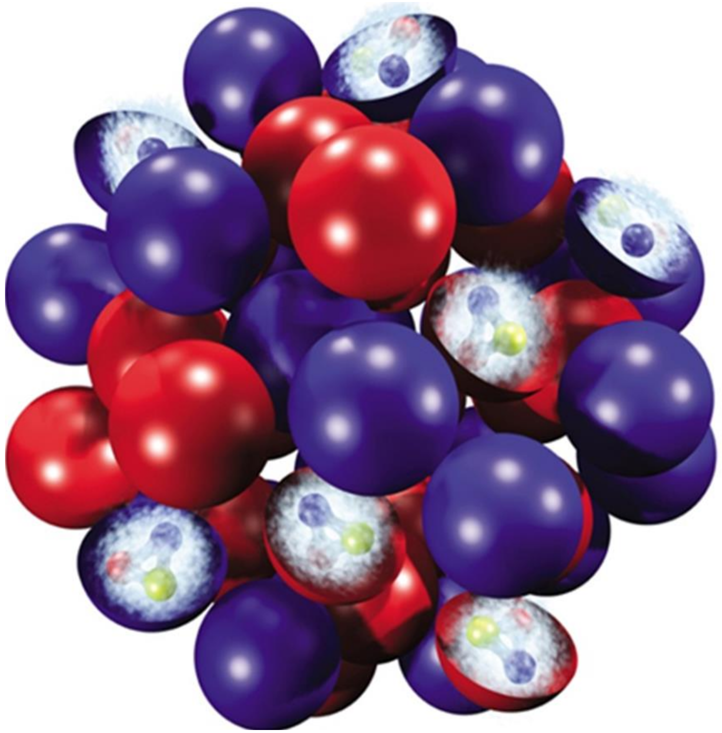

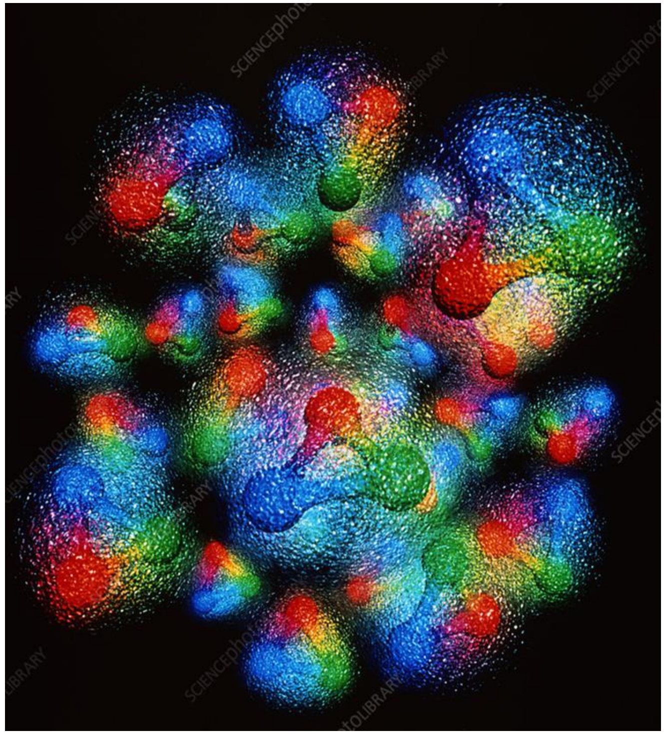

Which of the Si nucleus models is more realistic and why?

# How does the nucleus look like – it depends!

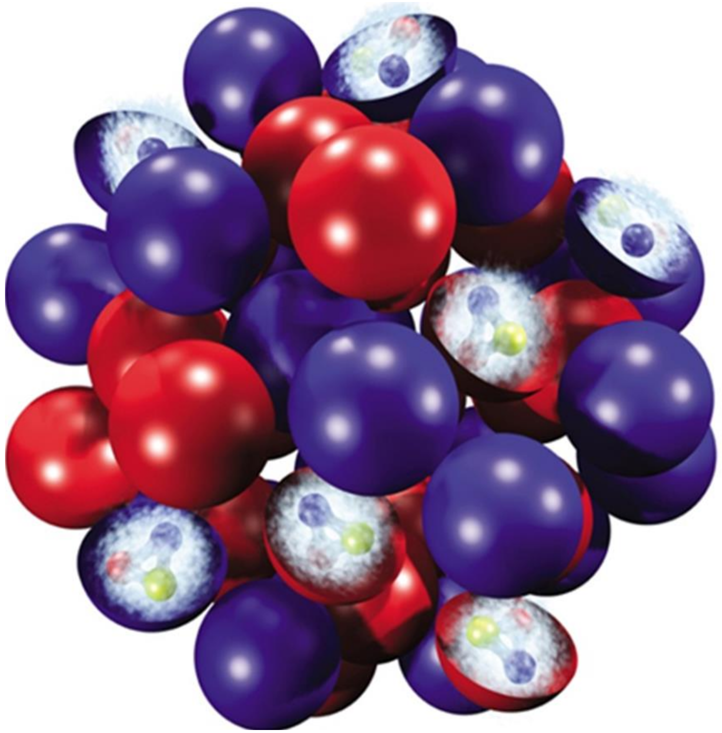

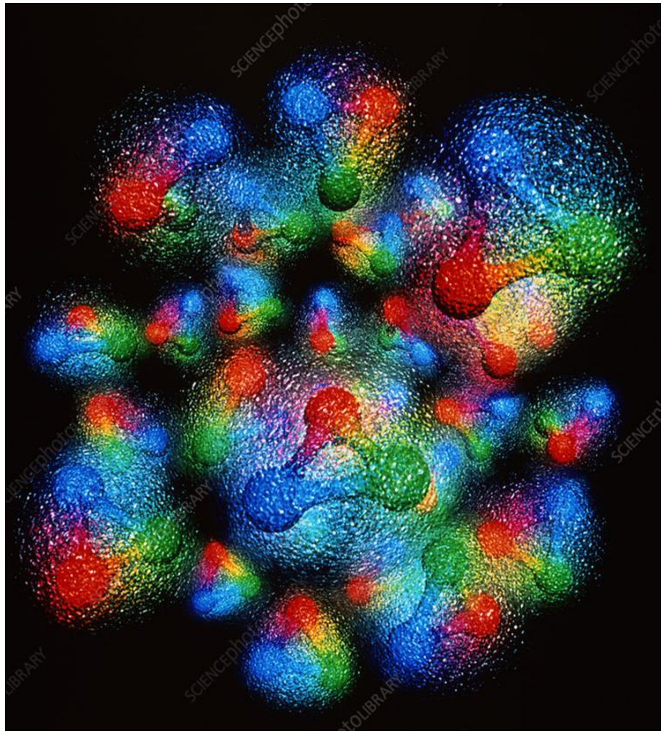

• deBroglie wavelength of constituent partons is effected by the beam energy.

$$\lambda = h/p \quad E = h\nu$$

At lower energy, nucleons are opaque, and the valence quarks are stopped in the fireball.
Excess quarks ➔ higher $\mu_B$

At higher energy, nucleons are transparent, and the valence quarks are pass through and exit the fireball.
Equal quarks and anti-quarks ➔ lower $\mu_B$

# Two regimes of the strong force

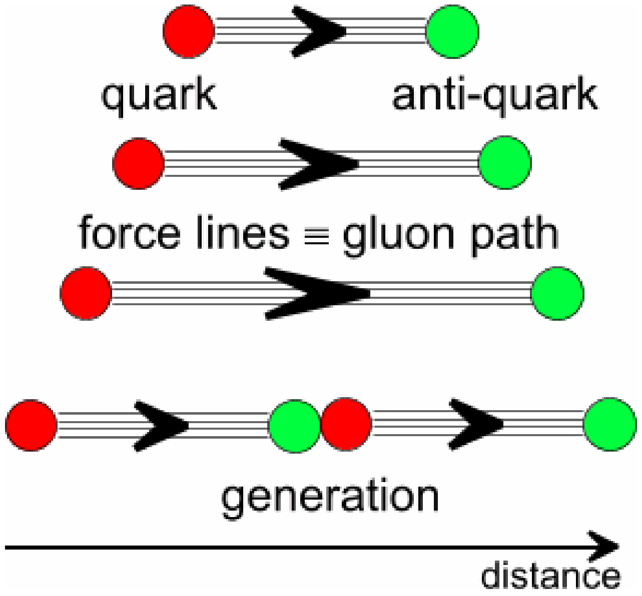


Confinement for color objects
Attraction force can create new quark – antiquark pair from vacuum to remain color neutral

Asymptotic freedom at very small scales/large energies

$$\alpha_s(k^2) \stackrel{\text{def}}{=} \frac{g_s^2(k^2)}{4\pi} \approx \frac{1}{\beta_0 \ln\left(\frac{k^2}{\Lambda^2}\right)}$$

(Wilczek, Gross and Politzer)
Nobel prize 2004

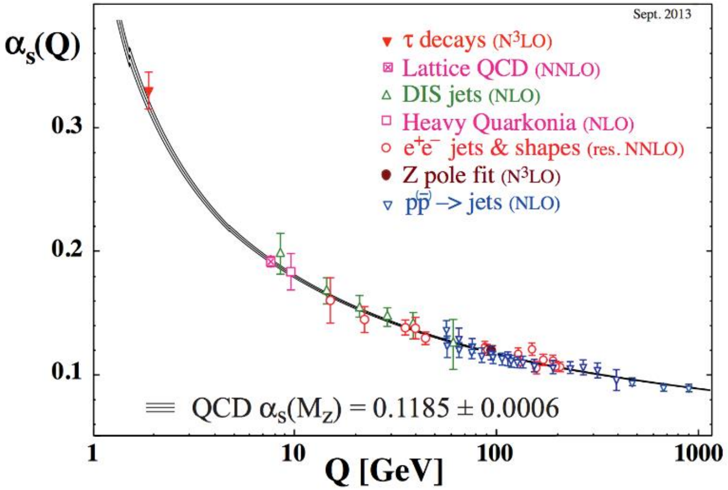


$\Lambda_{QCD} \simeq 1\ \text{fm}^{-1}$ – sets scale most important parameter in QCD

# Strong interaction potentials

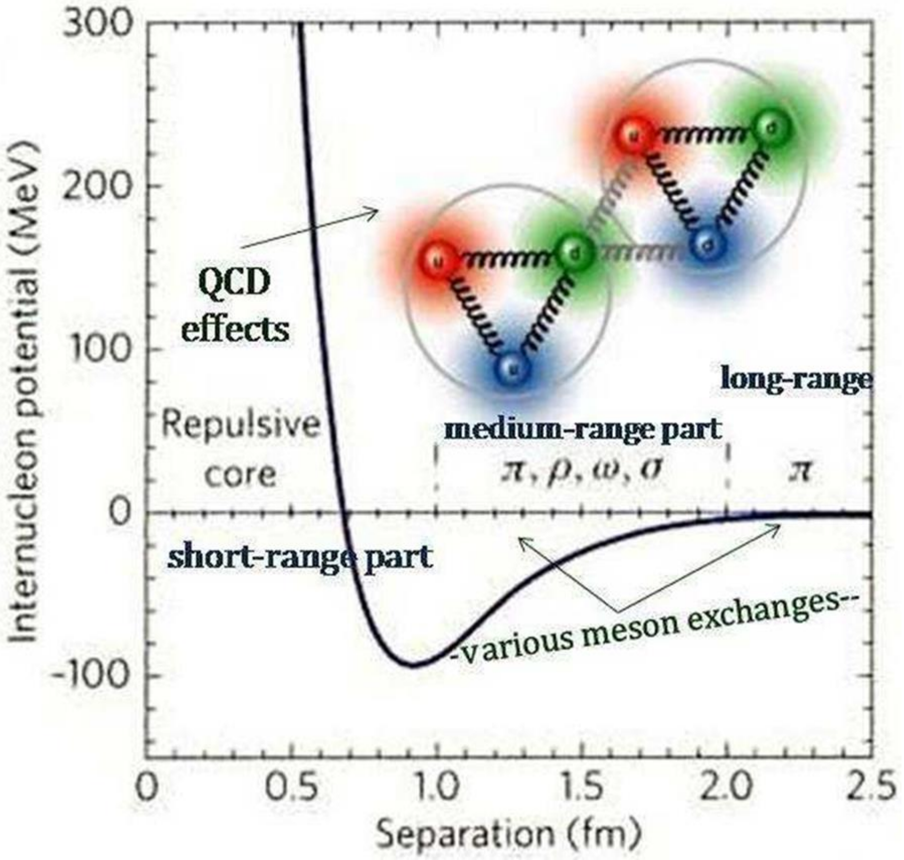


Gold nucleus

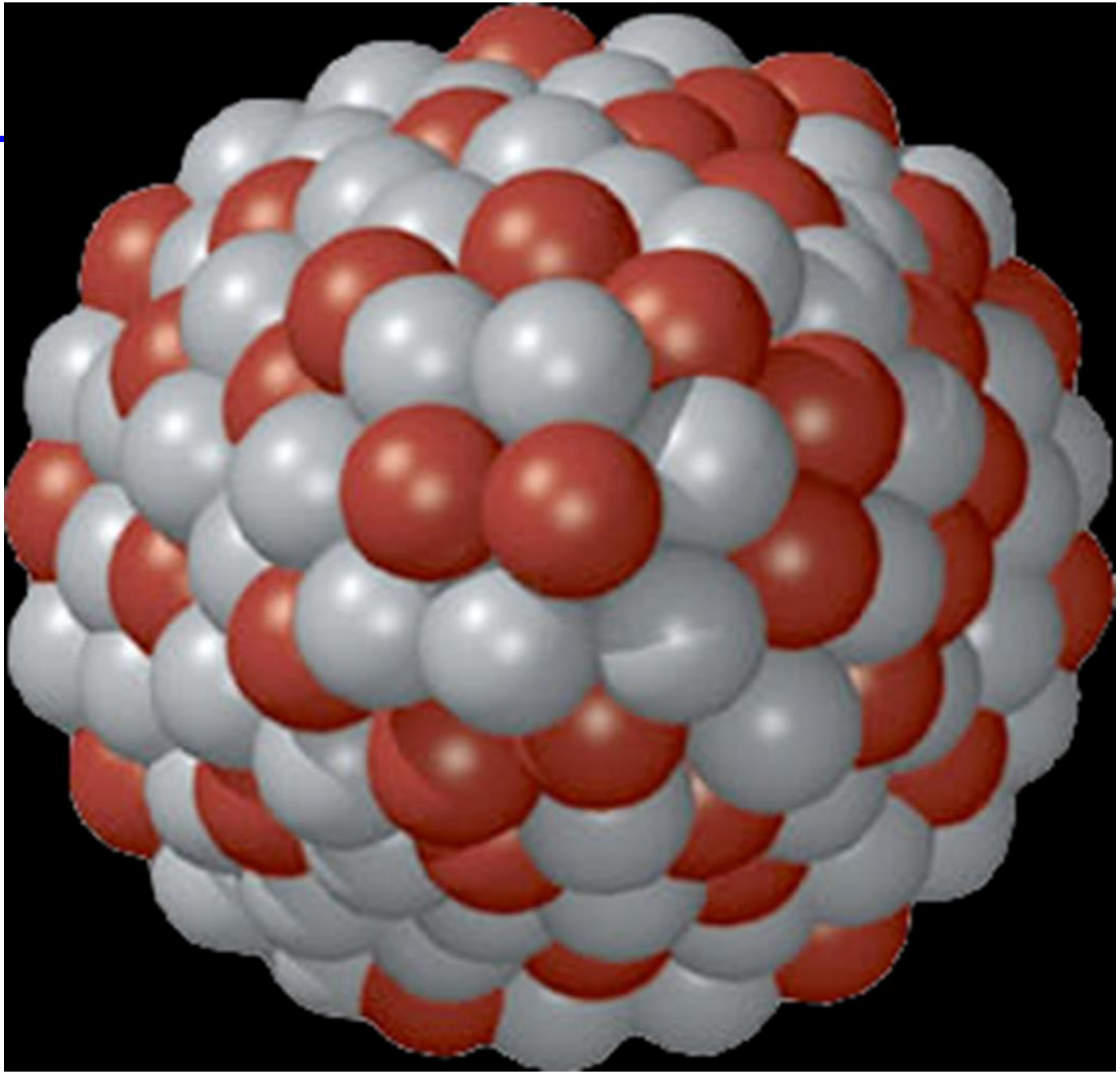

# Strong interaction potentials

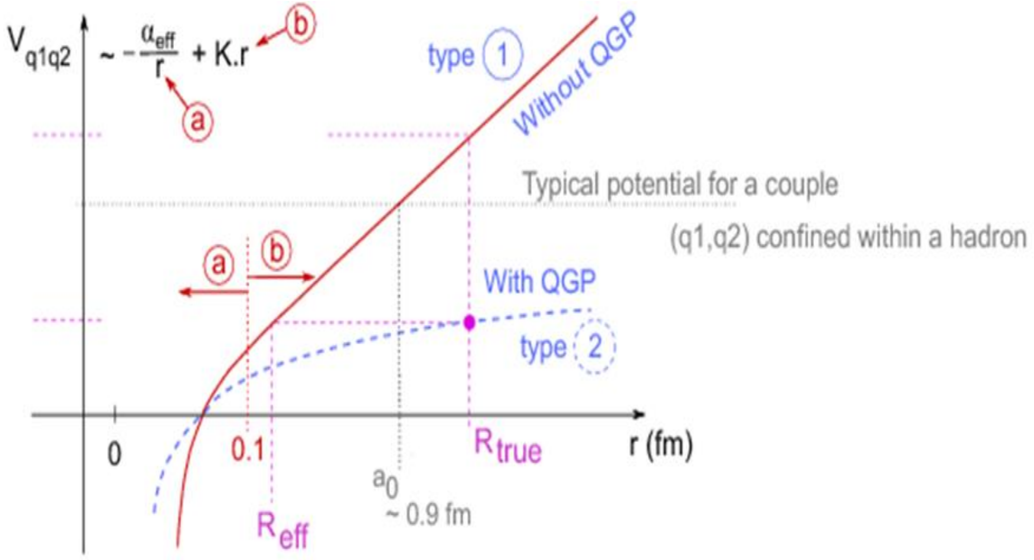


Gold nucleus

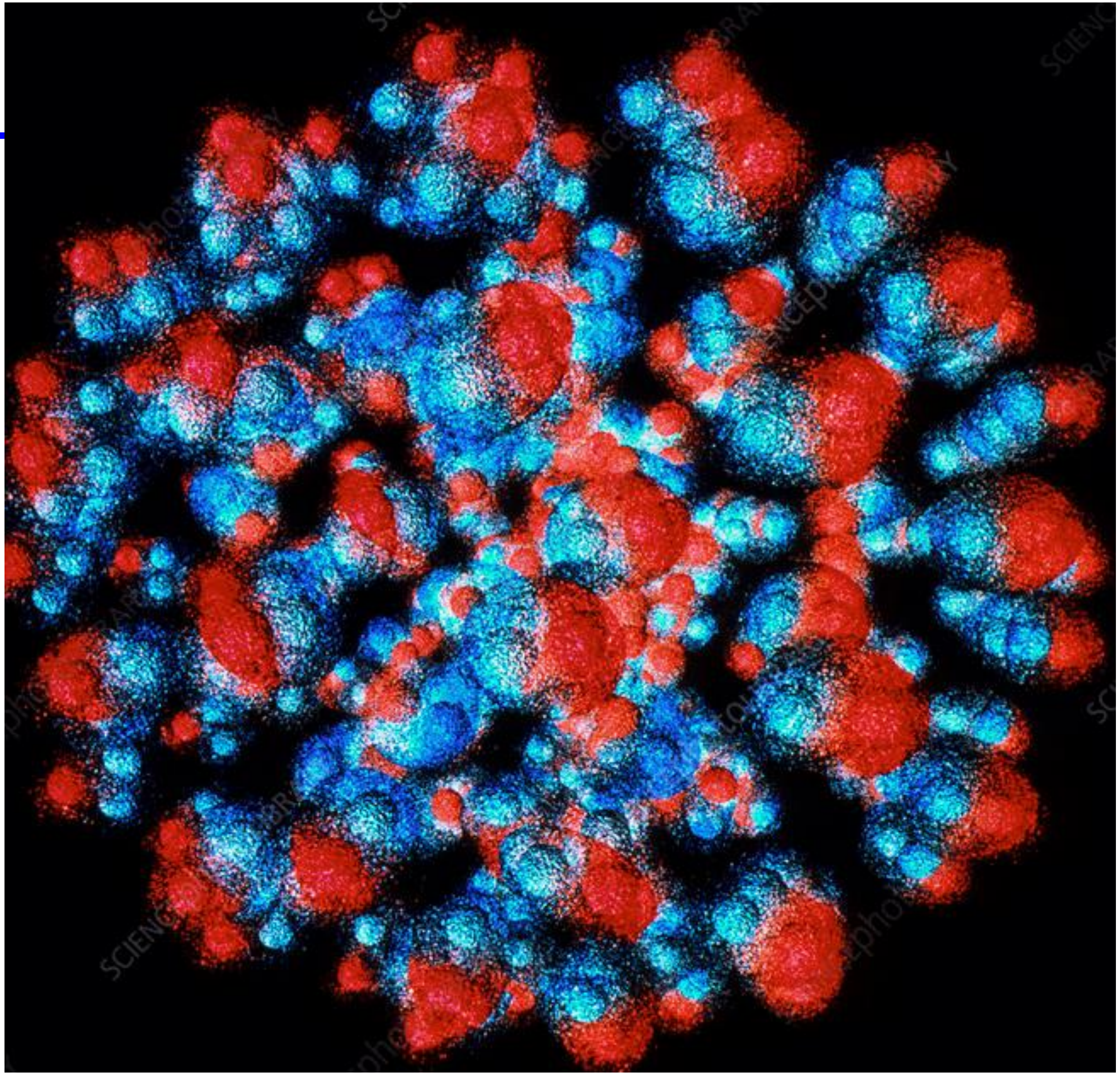

# Antiproton discovery at Bevatron 1955

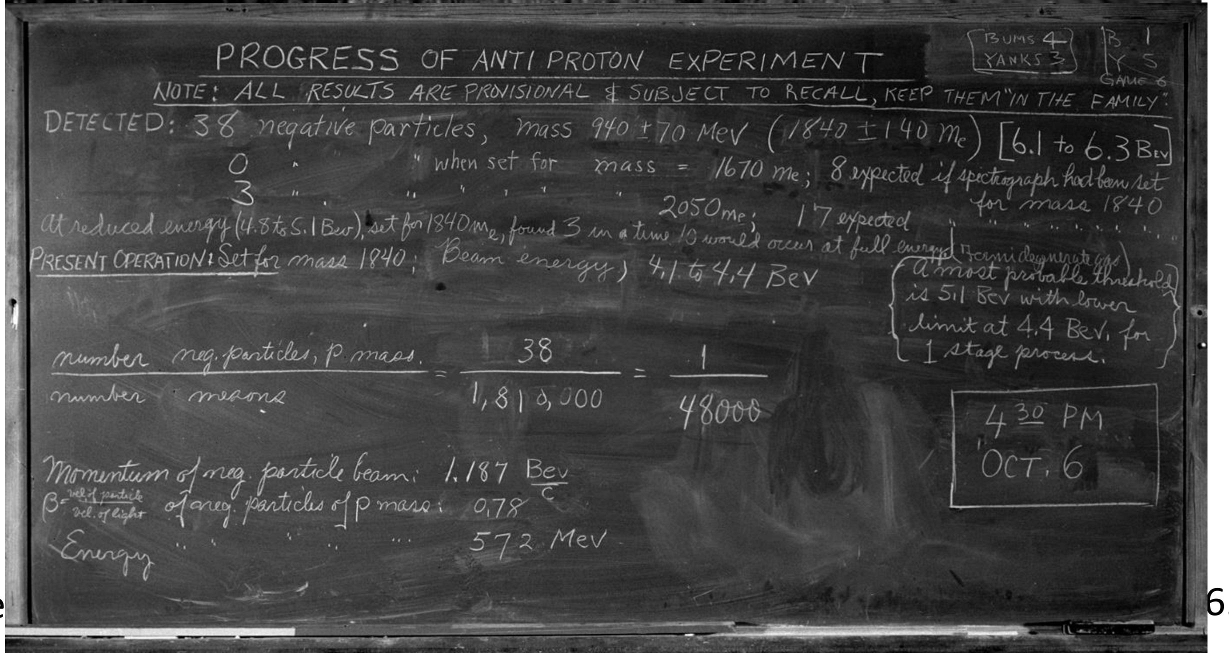


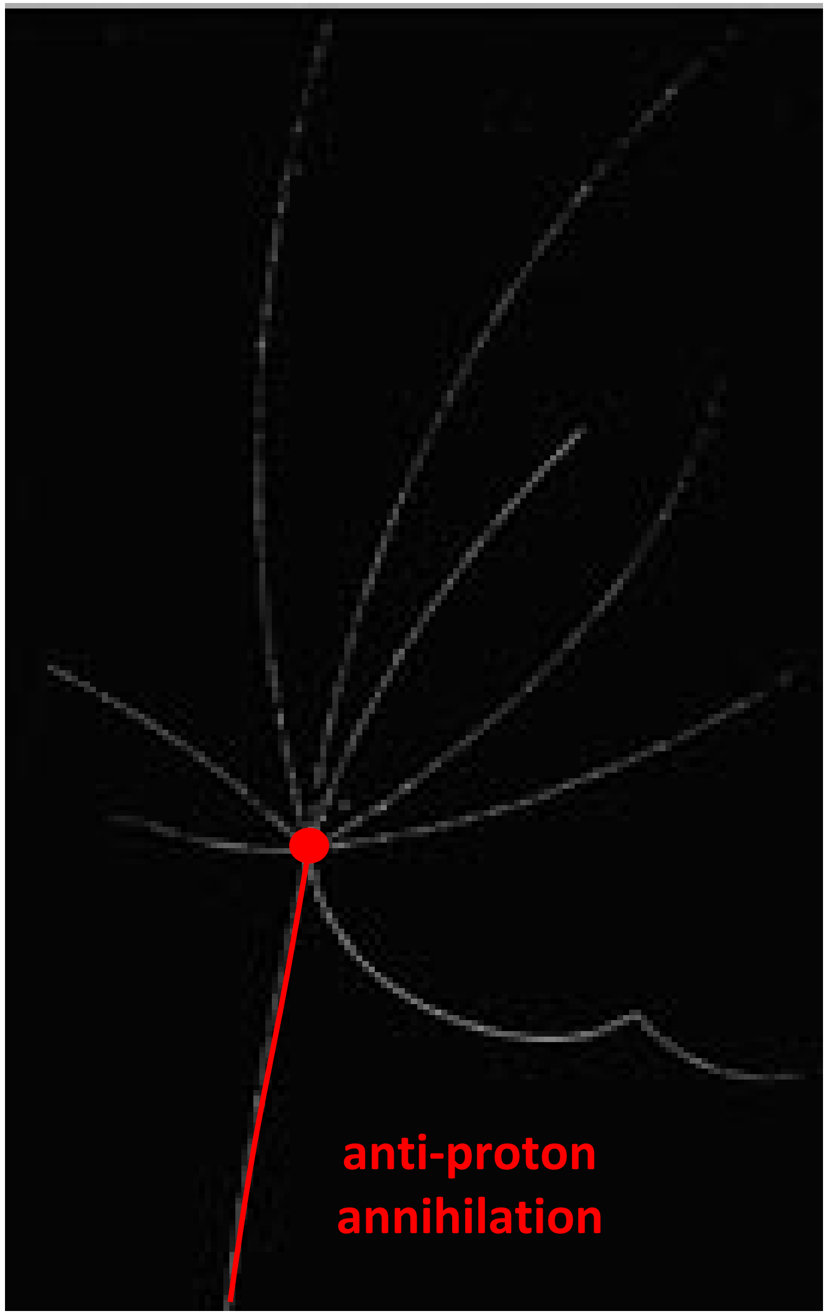

# Reactions on the threshold

Lab.: $p_A = (E_A, \vec{p}_A)$ $\quad p_B = (m_B, \vec{0})$ $\rightarrow$ $p_{tot}^{\text{Lab.}} = (E_A + m_B, \vec{p}_A)$

c.m.: $p_A = (E, \vec{p})$ $\quad p_B = (E, -\vec{p})$ $\rightarrow$ $p_{tot}^{\text{c.m.}} = (2E, \vec{0})$ (assumed $m_A$=$m_B$ ...)

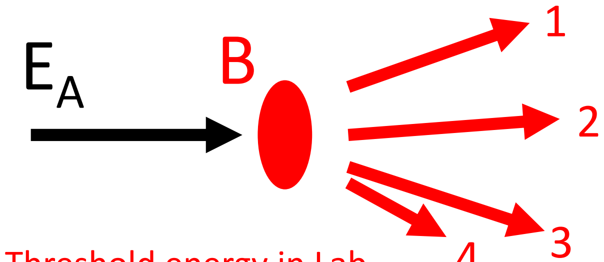


Threshold energy in c.m. frame: all particles produced at rest!

$\forall i : \quad \vec{p}_i = \vec{0}$ $\Rightarrow$ energy in c.m. frame:

$$E_1 + E_2 + E_3 + \ldots = m_1 + m_2 + m_3 + \ldots \equiv M \quad \Rightarrow \quad p_{tot}^{\text{c.m.}} = (M, \vec{0})$$

Use this minimum energy (M) in the c.m.

to calculate threshold energy in Lab.:

$$M^2 = (E_A + m_B)^2 - \vec{p}_A^2 = m_A^2 + m_B^2 + 2m_B E_A$$

$$\Rightarrow \quad E_A^{drempel} = \frac{M^2 - m_A^2 - m_B^2}{2m_B}$$

**Example: anti-proton**

$p+p \rightarrow \bar{p}+p+p+p$

$$\frac{(4m_p)^2 - m_p^2 - m_p^2}{2m_p} = 7m_p \sim 6.4 \text{ GeV}$$

# High baryon density region

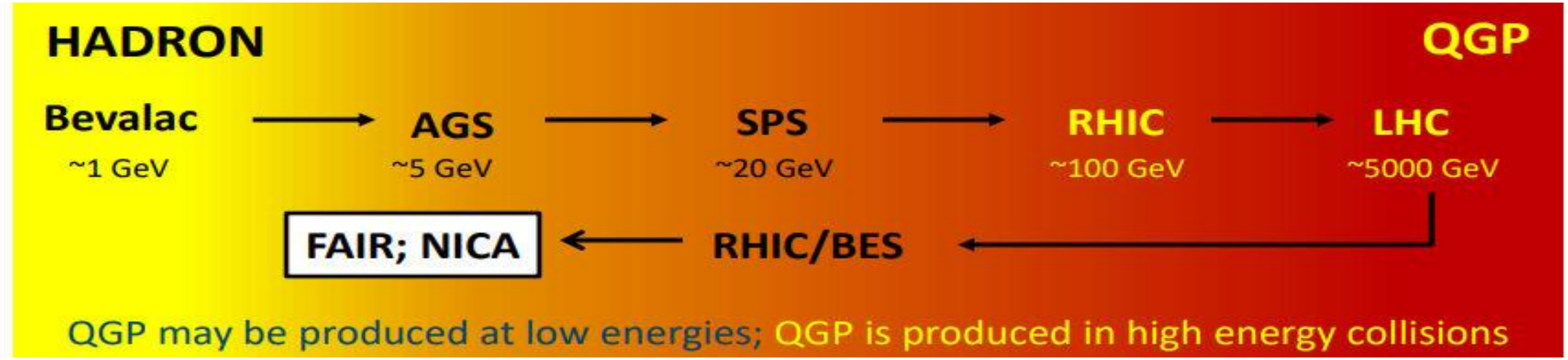


- ✓ Study of the QCD medium at extreme net baryon densities, phase transition at $\rho_c \sim 5\rho_0$
- ✓ Studied in several ongoing and future experiments:

✓ collider experiments: maximum phase space, minimally biased acceptance, free of target parasitic effects

✓ fixed-target experiments: high rate of interactions, easily upgradeable, better vertex-finder for heavy flavor decays

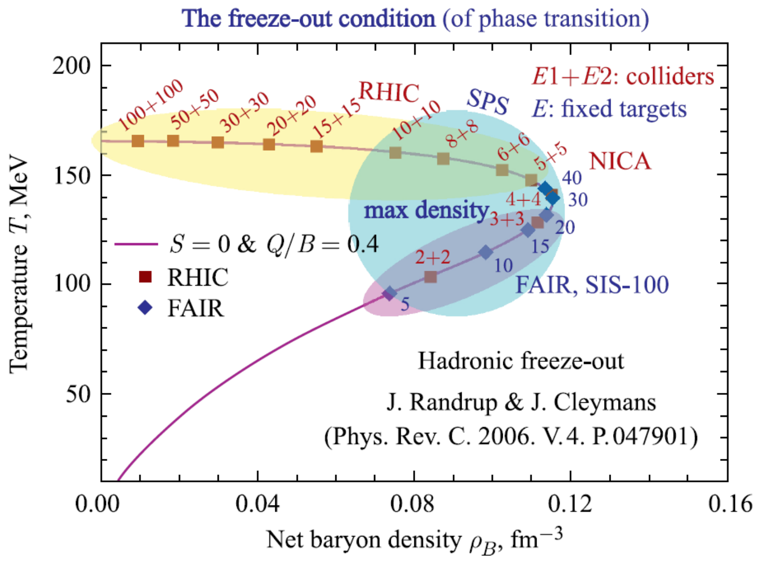

# NICA (Nuclotron-based Ion Colliding fAcility)


Can accelerate p+p, p+A, A+A

Maximal beam collision energy:
11 GeV for Au+Au
27 GeV for p+p

Energy region is well suited for precise study of the onset of deconfinement and QCD phase transitionin a variety of colliding systems (Bi+Bi, Au+Au, Cu+Cu, Ar+Ar, C+C)
Spin measurements on polarized proton and deuteron beams at SPD

| | |
|---|---|
| *Ring circumference, m* | **503,04** |
| *Number of bunches* | **22** |
| *r.m.s. bunch length, m* | **0,6** |
| *$\beta$, m* | **0,35** |
| *Energy in c.m., Gev/u* | **4-11** |
| *r.m.s. $\Delta p/p$, $10^{-3}$* | **1,6** |
| *IBS growth time, s* | **1800** |
| *Luminosity, $cm^{-2}$ $s^{-1}$* | **$1 \times 10^{27}$** |

# Overview of HIC experiments

Experimental programs at SPS, ALICE, RHIC, NICA, SIS, J-PARC

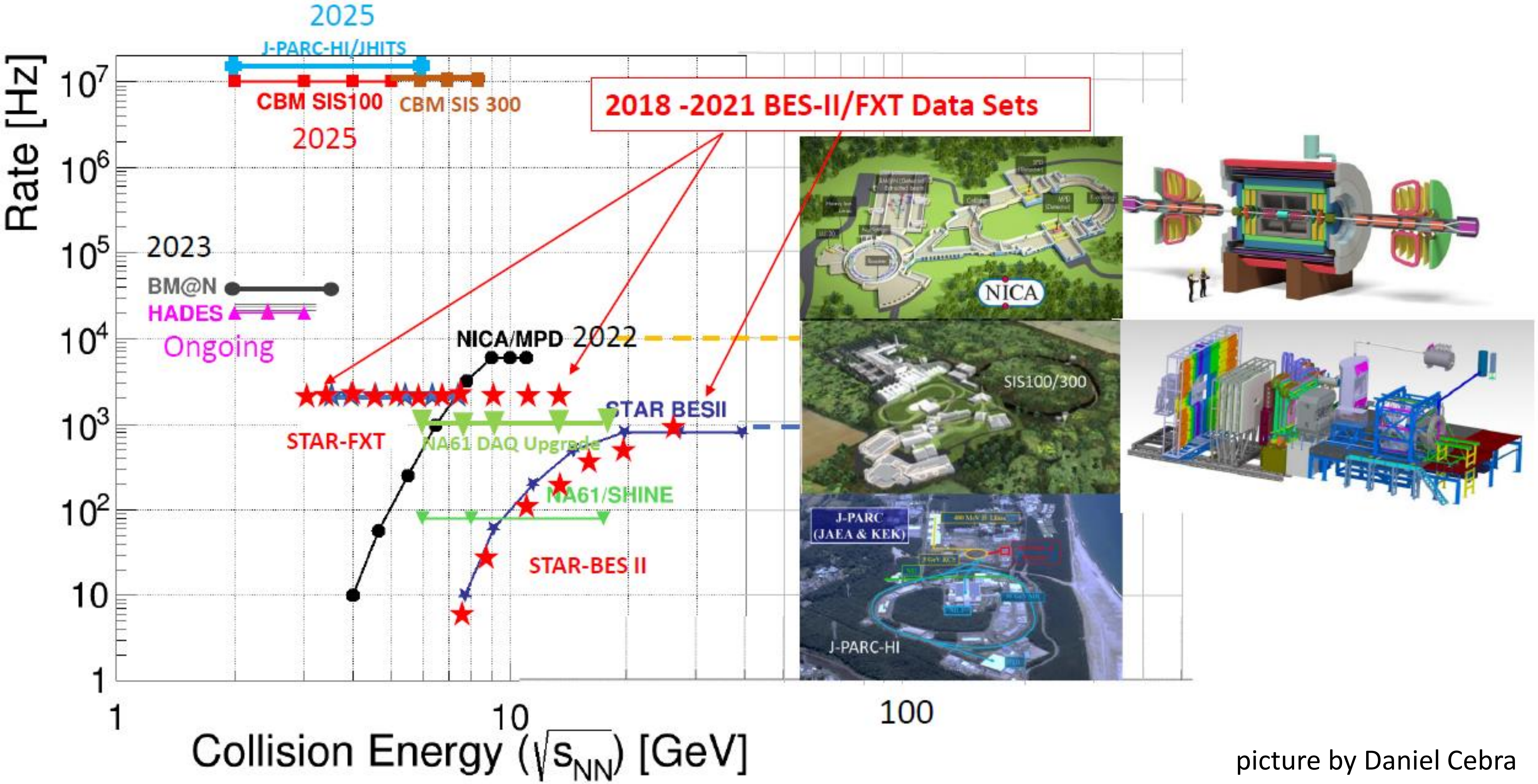


picture by Daniel Cebra

# Accelerator complexes for HIC

Relativistic Heavy Ion Collider (RHIC)

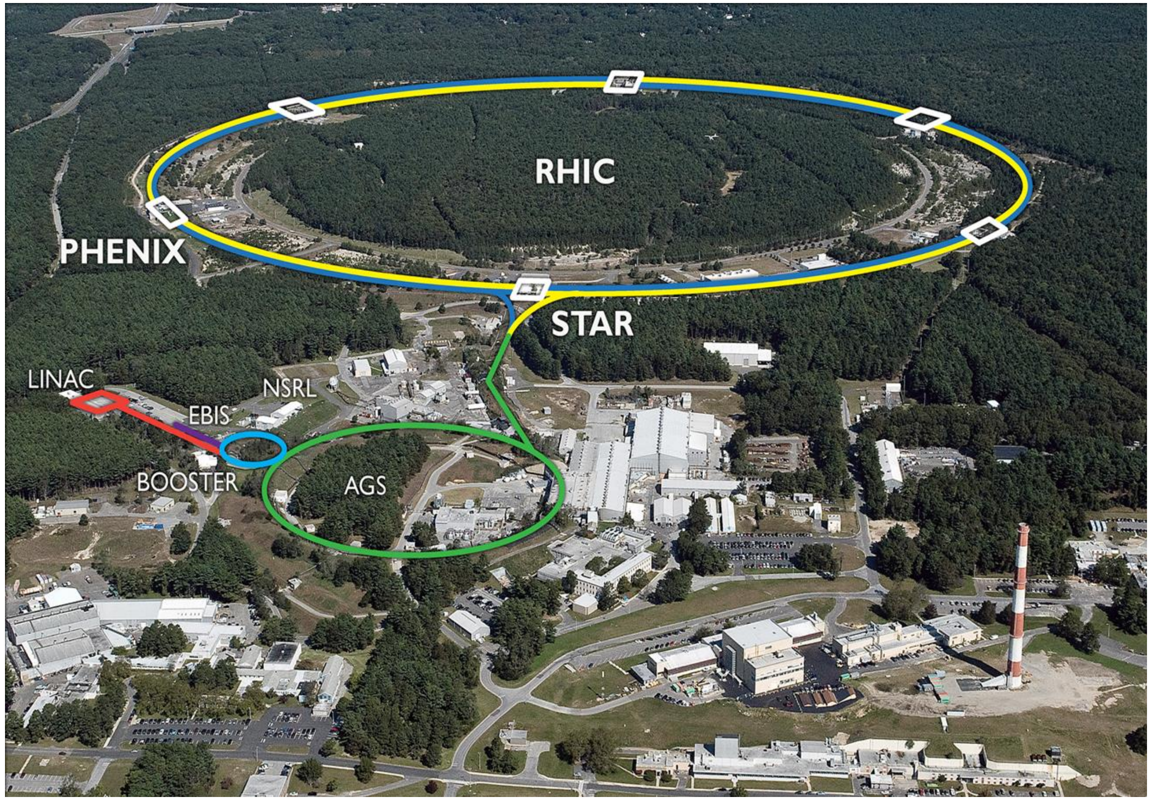


Large Hadron Collider (LHC)

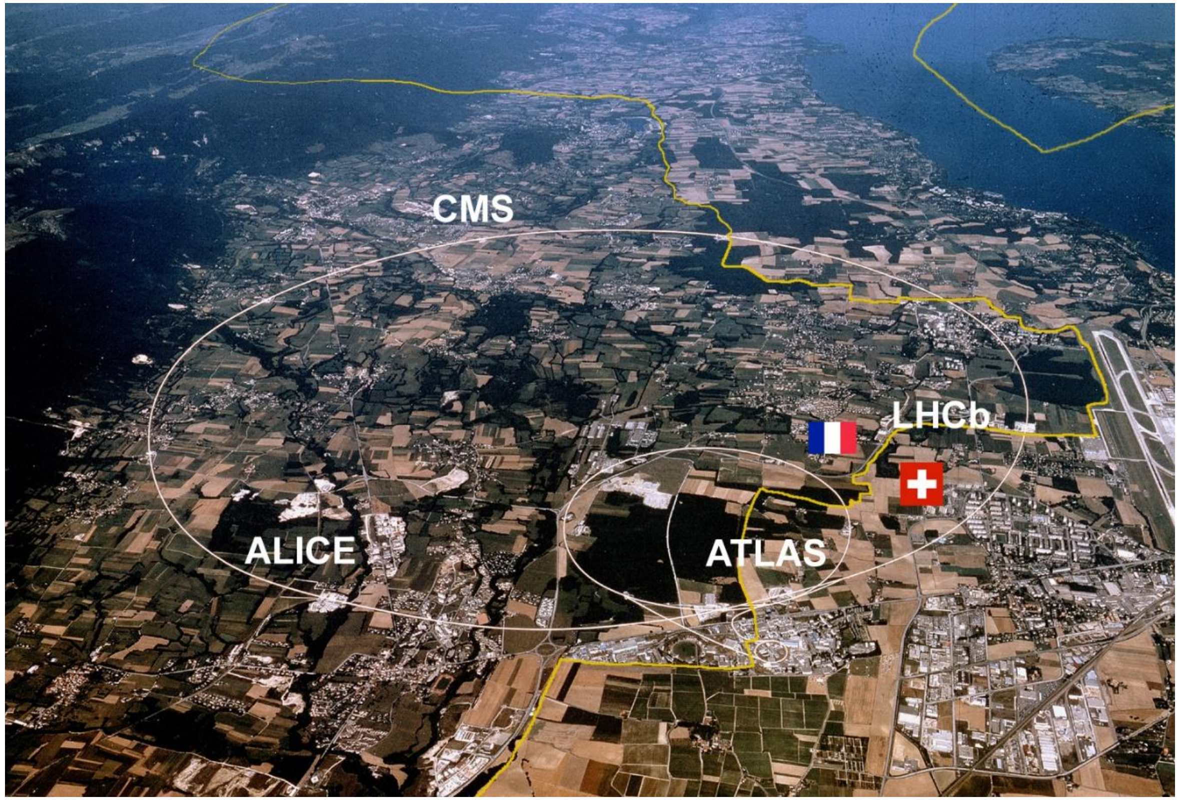


Brookhaven National Laboratory
In operation since 1999 Collider length 3,83 km
200 GeV Au+Au
510 GeV p+p

European Organization for Nuclear Research (CERN)
In operation since 2008 Collider length 27 km
5,02 TeV Pb+Pb
13 TeV p+p

# Data systems available at HIC experiments

NA61/SHINE

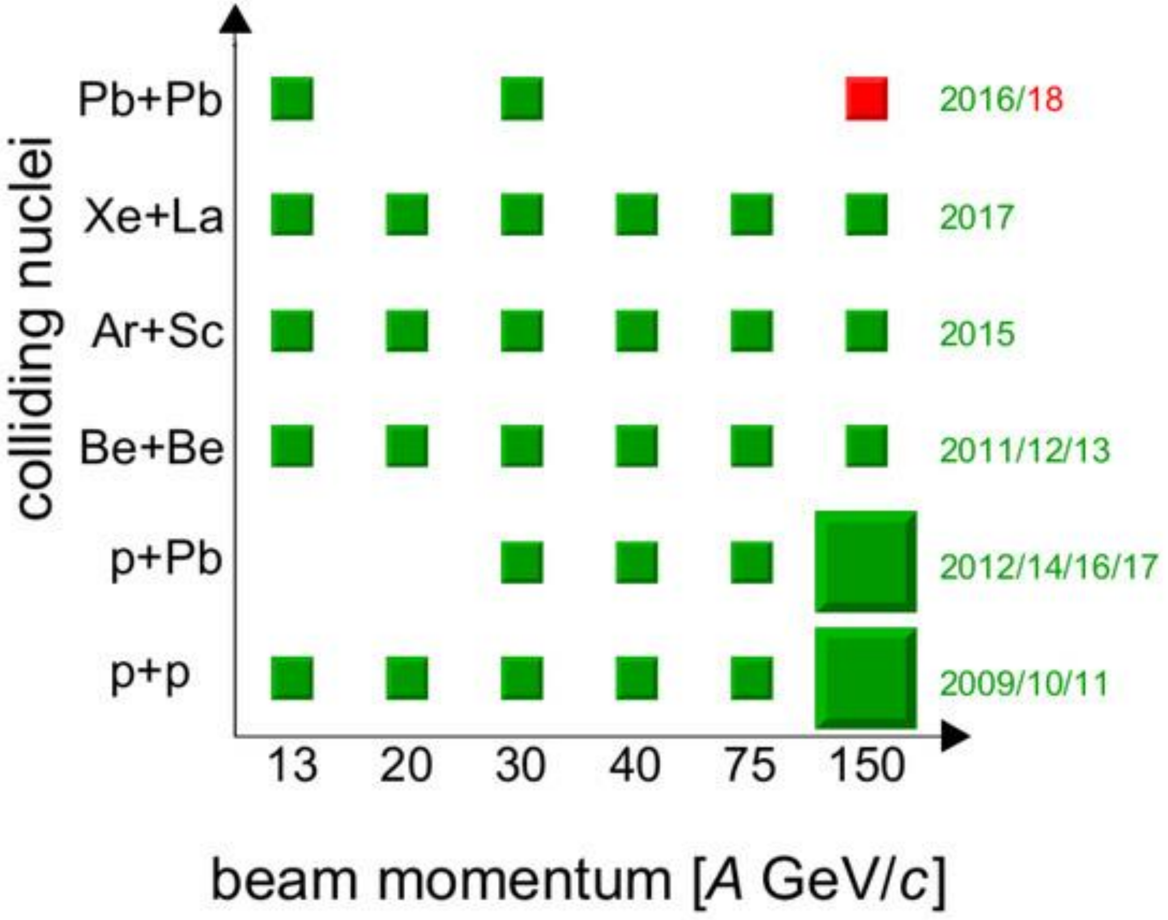


STAR

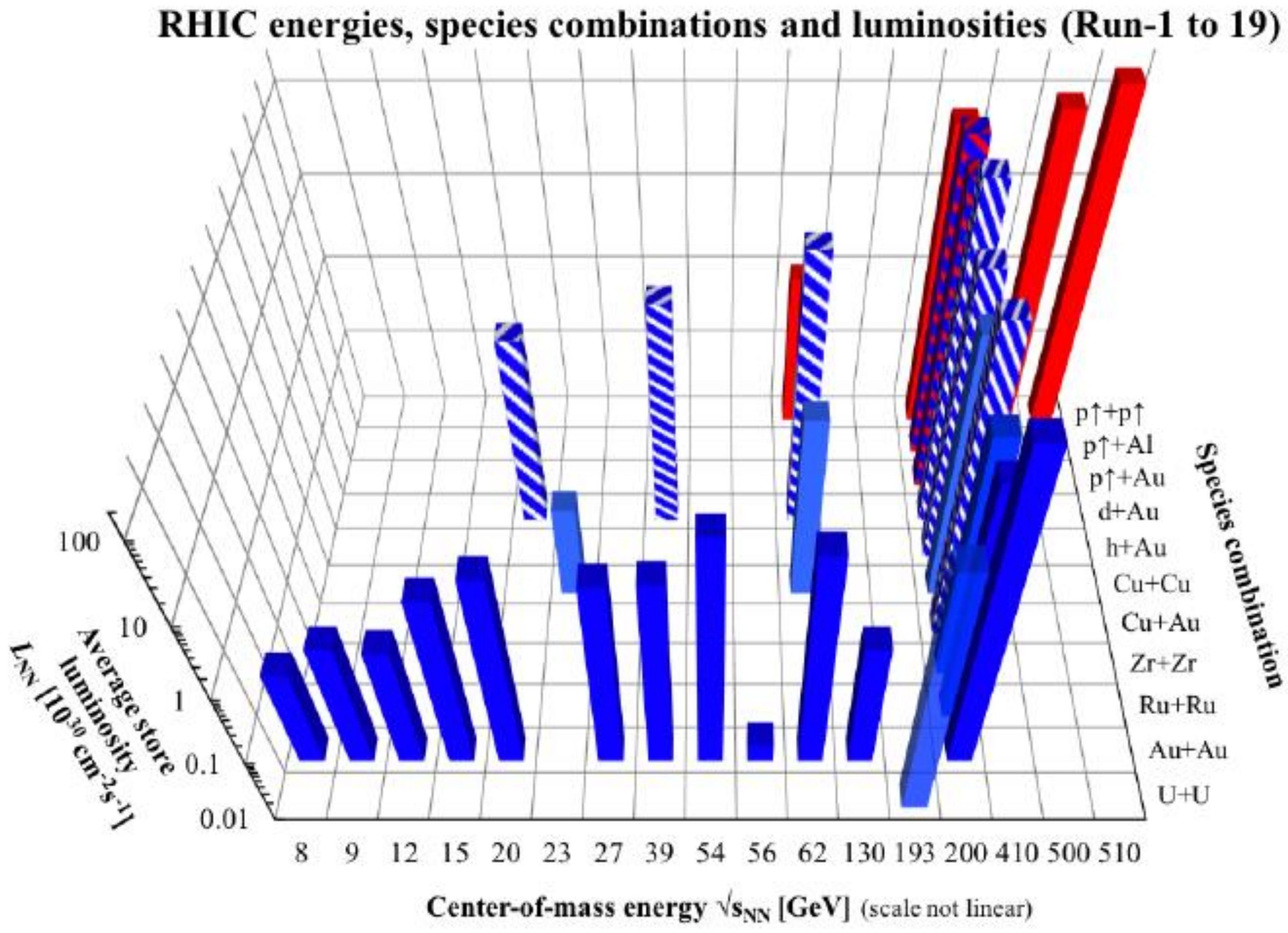

# Theory of QGP

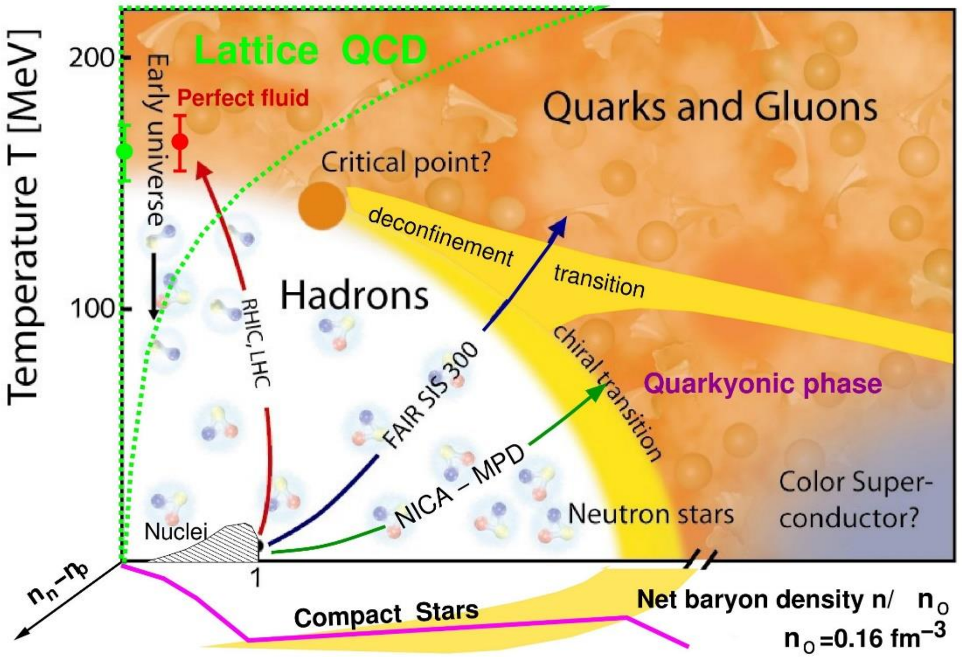


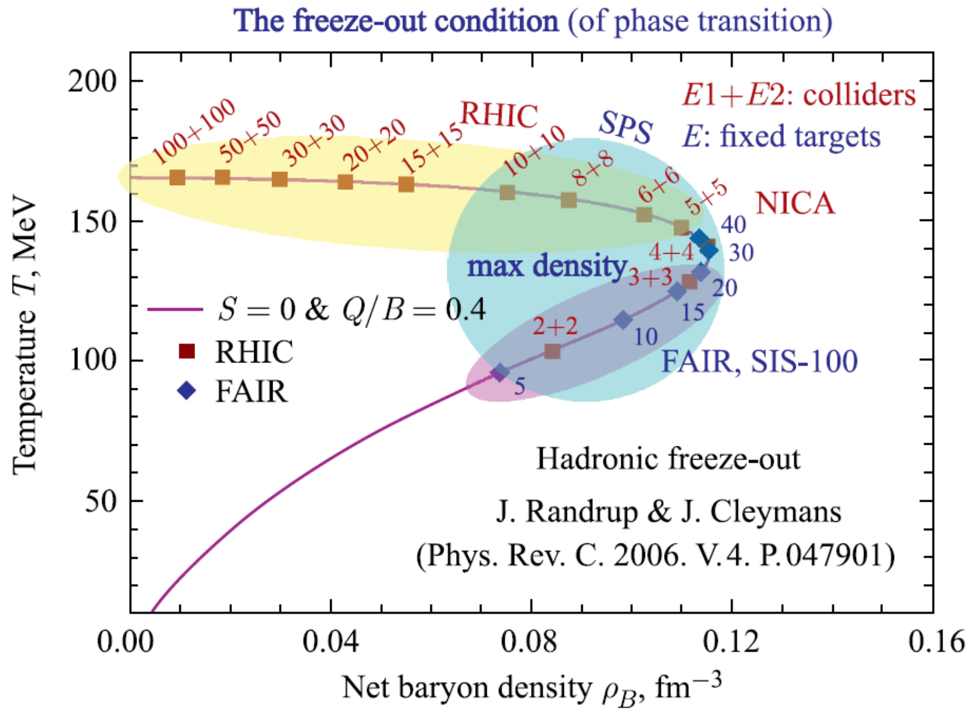


The energy scan covers the transition region from baryon to meson dominance in the chemical freeze-out regime. At the same time, this is the challenging domain of the transition from baryon stopping to nuclear transparency, where new experimental data would be very useful to progress in the theoretical understanding.

There is a minimum in the freeze-out volume related to the “softest point” in the EoS in the NICA energy window which is accessible to verification by femtoscopy measurements.

# Thermodynamic systems

Van-der-Waals Equation of State

$$(p + \frac{a \cdot n^2}{V^2})(V - n \cdot b) = n \cdot R \cdot T$$

| | | |
|---|---|---|
| $p$ | - | pressure |
| $V$ | - | volume |
| $T$ | - | temperature |
| $R$ | - | gas constant |
| $a$, $b$ | - | specific constants for each gas |

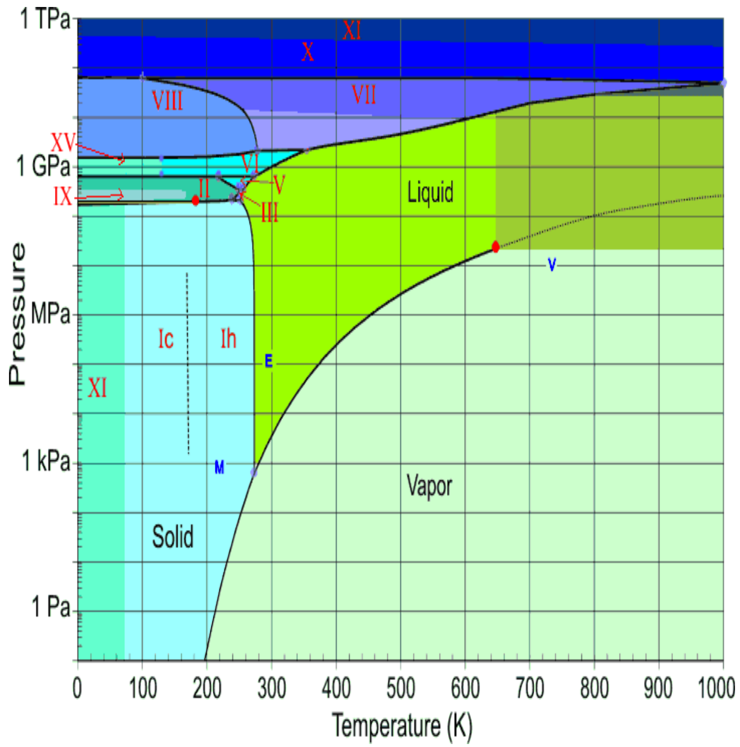


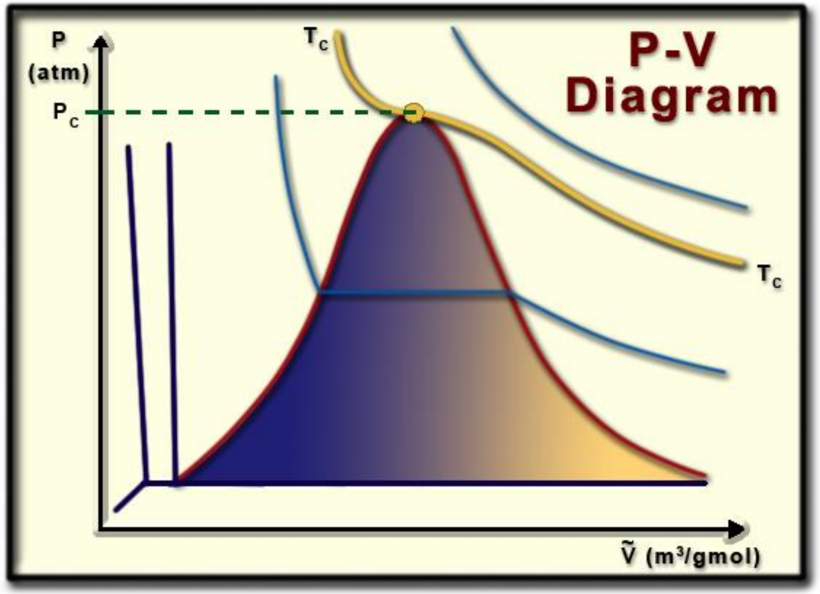


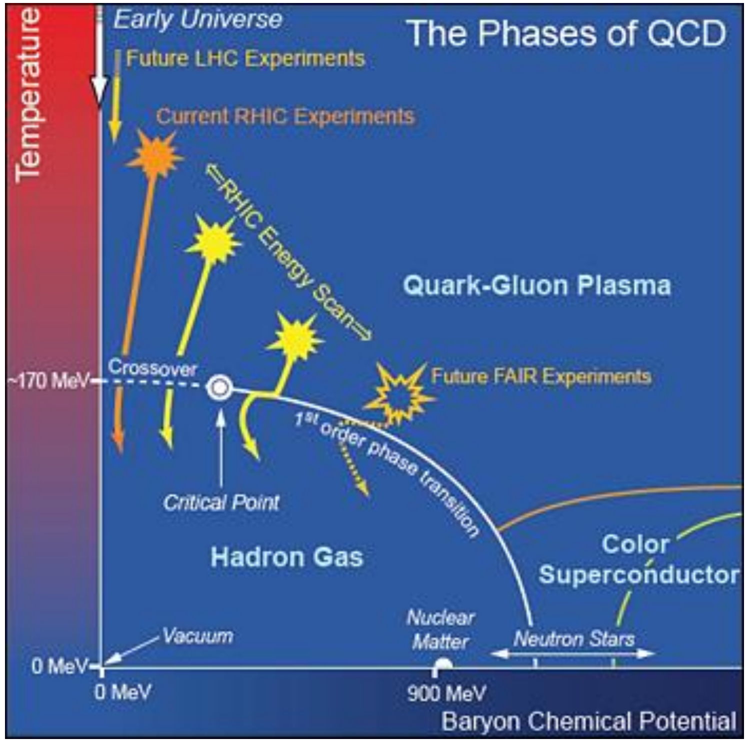


well studied

- Phases
- Phase boundaries
- Transition types
- Critical Point

under investigation

# Equation of State. Ideal gas

- In simple Bag model QGP is described as an ideal gas of massless quarks (zero chemical potential) and gluons
- Equations of State (Bag model):

$$\varepsilon = k\frac{\pi^2}{30}\frac{T^4}{(\hbar c)^3} + B \rightarrow energy \quad density$$

$$p = k\frac{\pi^2}{90}\frac{T^4}{(\hbar c)^3} - B \rightarrow pressure$$

$$s = \frac{\varepsilon + p}{T} = \frac{4}{3}k\frac{\pi^2}{30}T^3 \rightarrow entropy$$

**T** – gas temperature

**B** – pressure in the bag ~ 0.4 GeV/fm$^3$

***κ*** – number of degrees of freedom

# Equation of State. Ideal liquid

Relativistic hydrodynamic equation set for ideal liquid

$$\partial_\mu T^{\mu\nu} = 0$$

$$\partial_\mu N^{\mu} = 0$$

$$T^{\mu\nu} = (\varepsilon + \overline{p}) u^\mu u^\nu - p g^{\mu\nu}$$

$$N^\mu = n u^\mu$$

$T^{\mu\nu}$ – energy-momenta tensor
$N^\mu$ – number of particles flow through the liquid cell μ,
$u^\mu$ – local 4-speed of liquid cell μ,
ε – energy density
n – particle number density
p – pressure

If we know EoS p=p(ε) and initial conditions this system can be resolved (analytically or numerically)

5 equations for 5 independent variables

$$\varepsilon, n, u^\mu$$

# Equation of State. Viscous liquid

Relativistic hydrodynamic equation set for a viscous liquid

$$\partial_\mu T^{\mu\nu} = 0$$

$$\partial_\mu N^\mu = 0$$

$$T^{\mu\nu} = \varepsilon u^\mu u^\nu - pP^{\mu\nu}(p+\Pi) - P^{\mu\nu\alpha\beta}\pi_{\alpha\beta}$$

$$N^\mu = nu^\mu - P^{\mu\nu}v_\nu$$

$T^{\mu\nu}$ – energy-momenta tensor
$N^\mu$ – number of particles flow through the liquid cell μ,
$u^\mu$ – local 4-speed of liquid cell μ,
ε – energy density
n – particle number density
p – pressure
$g^{\mu\nu}$ – metric tensor

$$P^{\mu\nu} = \overline{p} - g^{\mu\nu}$$

9 additional variables, now it's not guaranteed to have a solution

$$\varepsilon, n, u^\mu, \Pi, \pi^{\mu\nu}, v^\mu$$

# Phase diagram of QCD matter

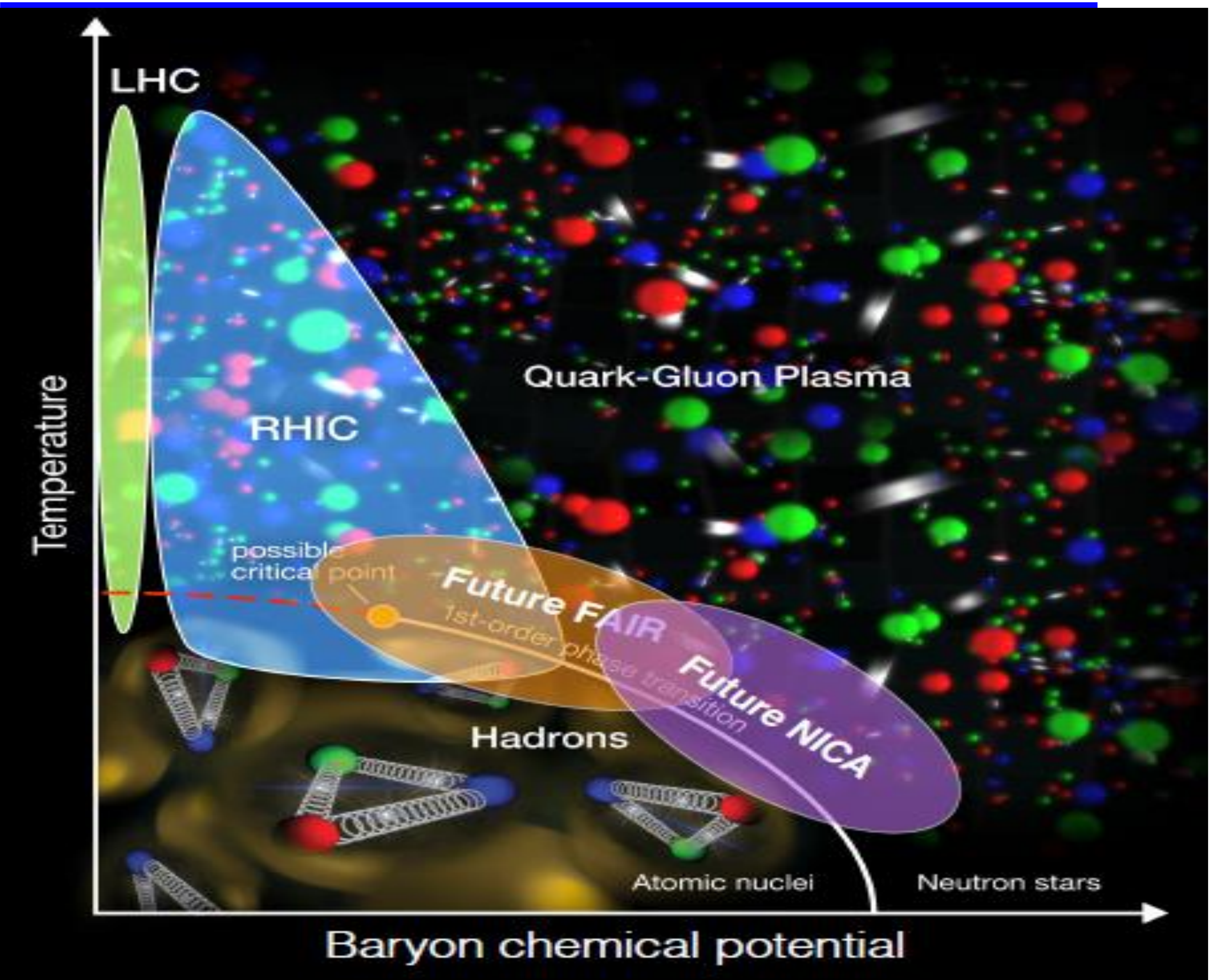


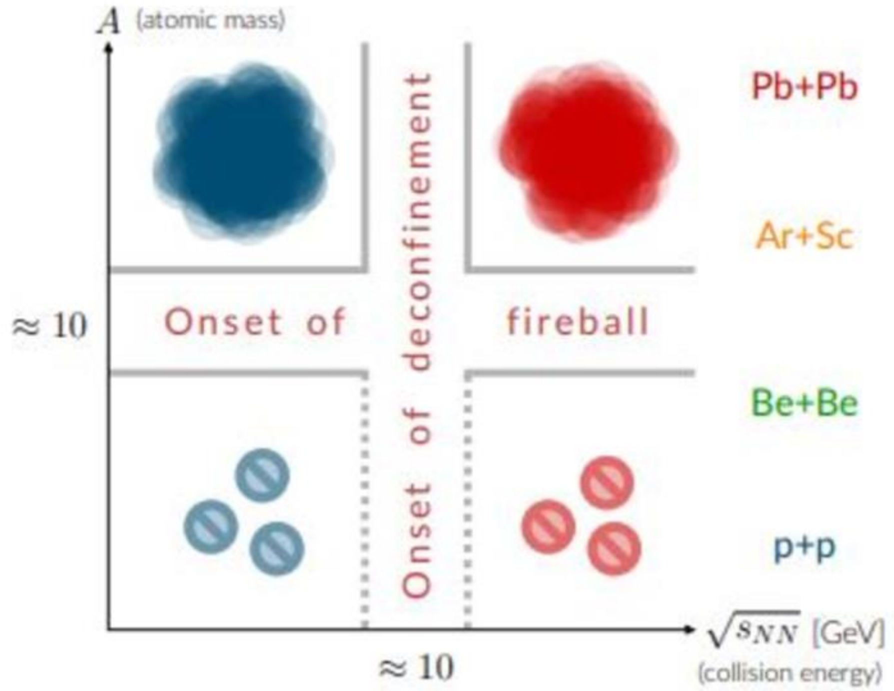


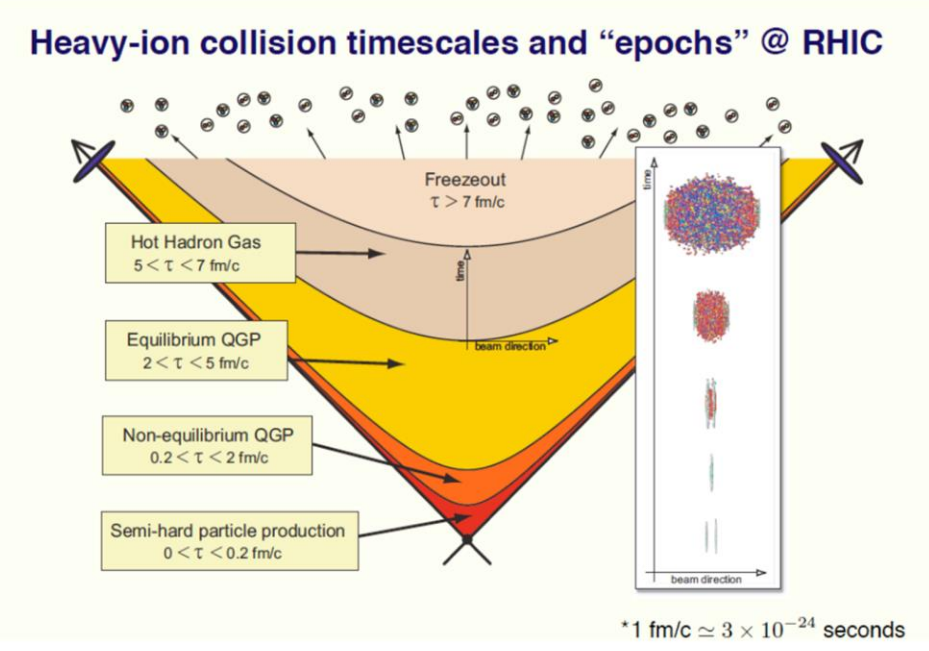

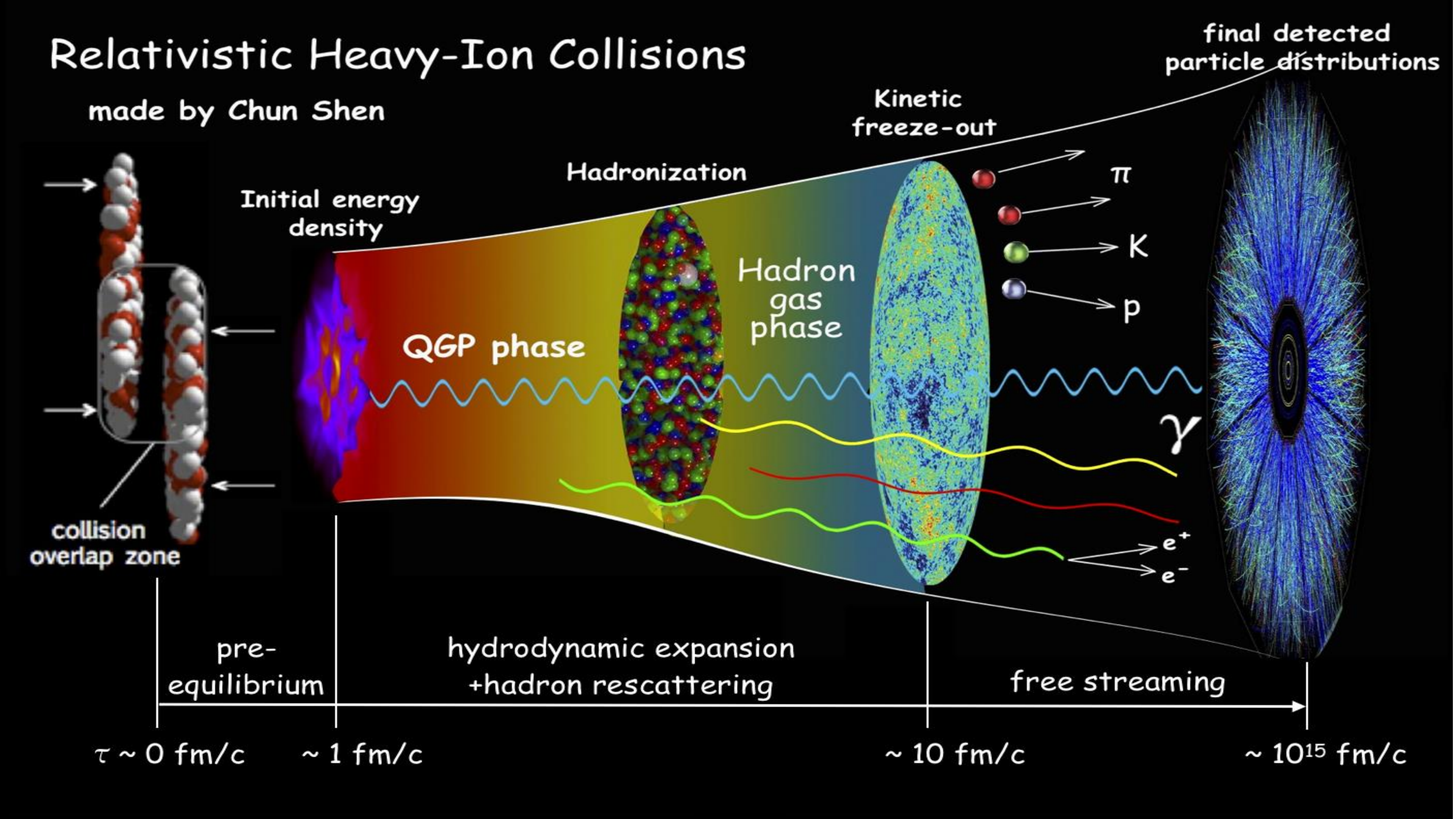
Relativistic Heavy-Ion Collisions
made by Chun Shen
final detected particle distributions
Kinetic freeze-out
Hadronization
Initial energy density
Hadron gas phase
QGP phase
π
K
p
γ
e+
e−
collision overlap zone
pre-equilibrium
hydrodynamic expansion +hadron rescattering
free streaming
τ ~ 0 fm/c
~ 1 fm/c
~ 10 fm/c
~ 10^15 fm/c

# HISTORY OF THE UNIVERSE

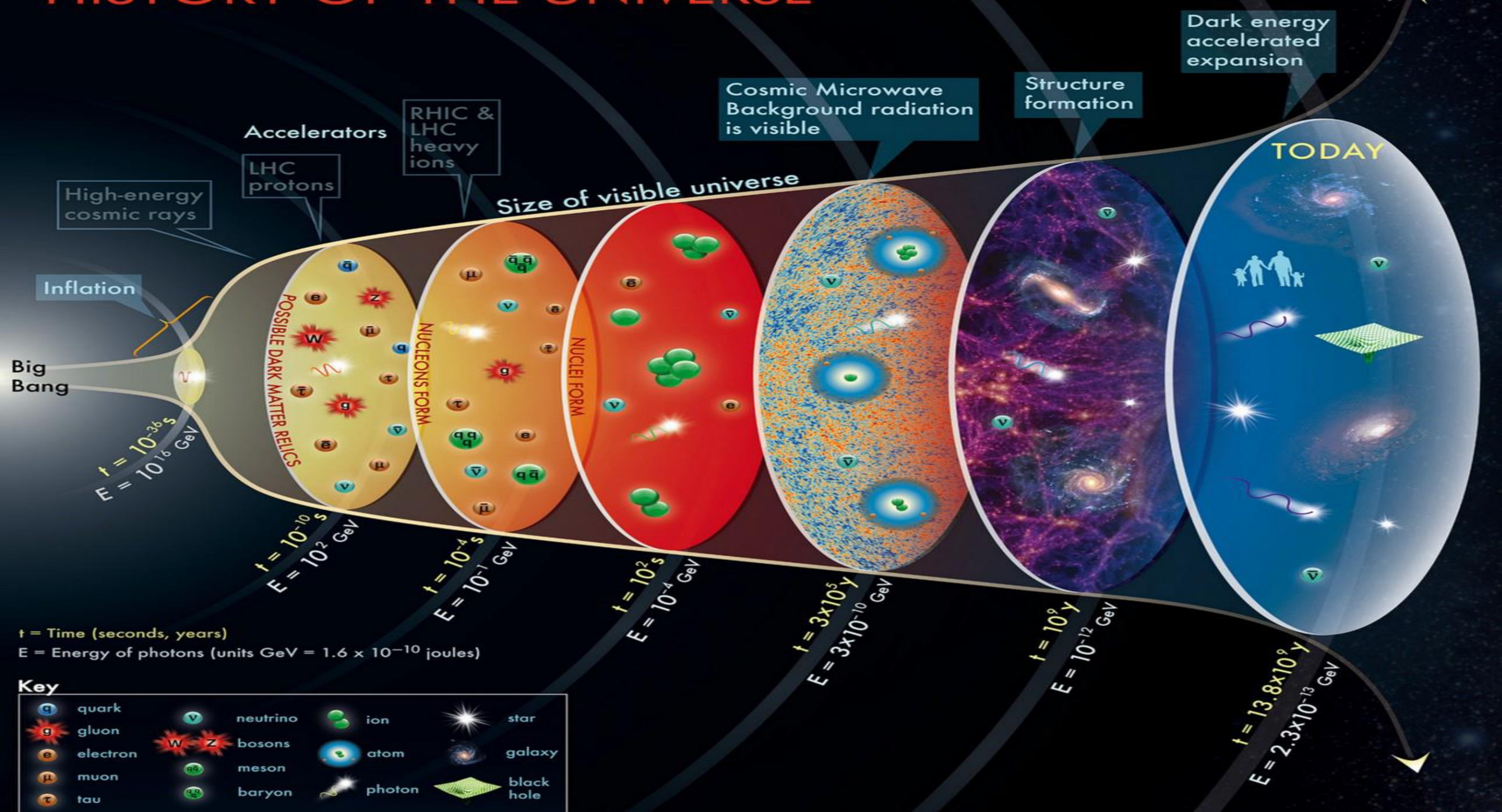

# MPD position in the physics landscape

Cover story for EPJ A

| | NA61/SHINE at SPS | CBM at FAIR | STAR BES+FXT at RHIC | MPD + BM@N at NICA |
|---|---|---|---|---|
| Coverage of region of transition from baryon to meson dominance („horn”) | only higher $\sqrt{s_{NN}}$ | only lower $\sqrt{s_{NN}}$ | Yes (mixing collider and fixed target) | Yes (consistent acceptance) |
| expected luminosity (w.r.t. MPD) | lower | higher | lower | reference |
| possibility for system size scan | yes | yes | yes (?) | yes |
| full centrality range | no | yes (?) | yes | yes |
| acceptance type | Fixed target | Fixed target | Collider + fixed target | Collider + fixed target |
| running plan (heavy-ions) | approved for 2021 (per-year decision) | beyond 2025 | running concluded in 2021 | 2023 and beyond |
| status at the facility (possible running time) | in competition with many projects (LHC) | CBM one of four main experiments | end of datataking (heavy-ion) in 2021 | flagship experiments several months/year |

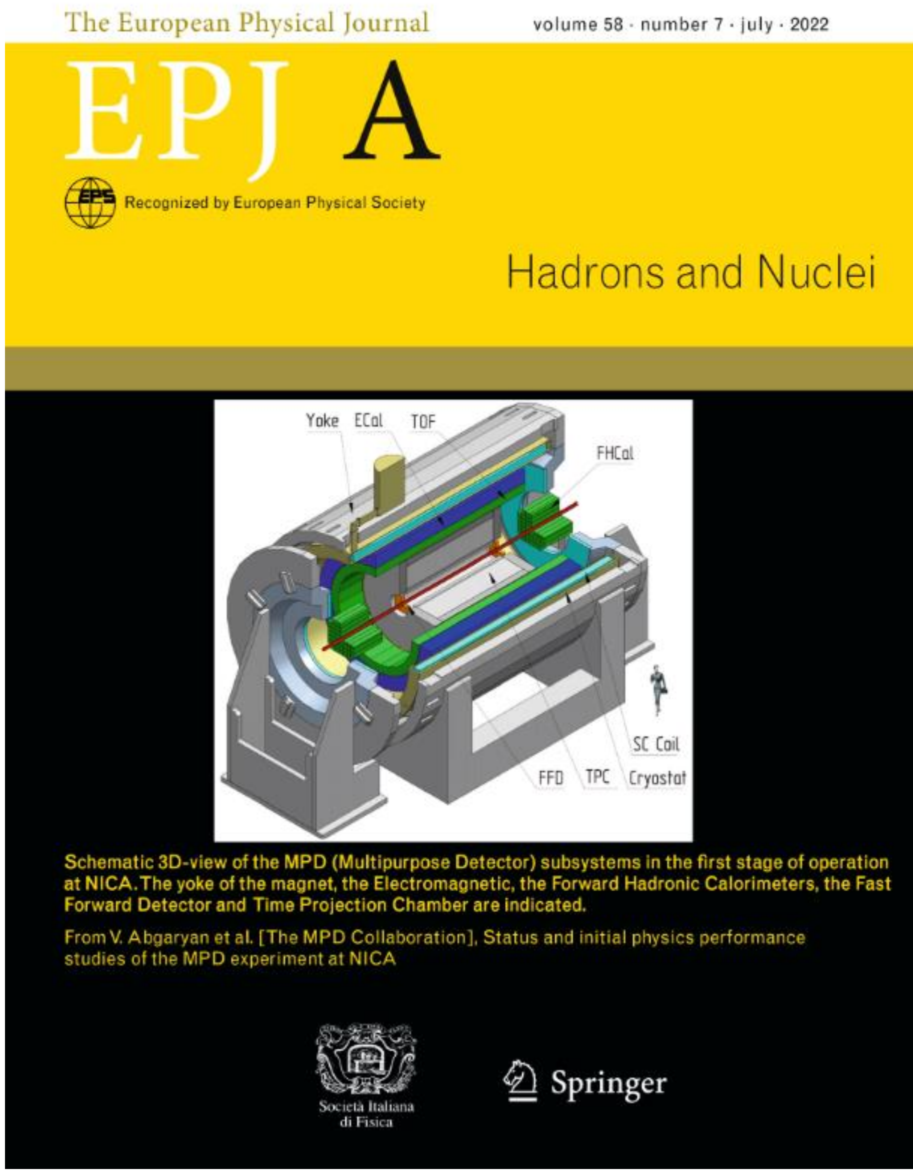


- ✓ The MPD strategy consists of performing a high-luminosity scan in energy and system size, looking for a wide variety of signals sensitive to the phase transition and presence of the critical point
- ✓ The scans are going to be performed using the same apparatus with all the advantages of collider experiments

*Eur.Phys.J. A 58 (2022) 7, 140*

# Multi-Purpose Detector

**Stage- I** → upgrade → **Stage- II**

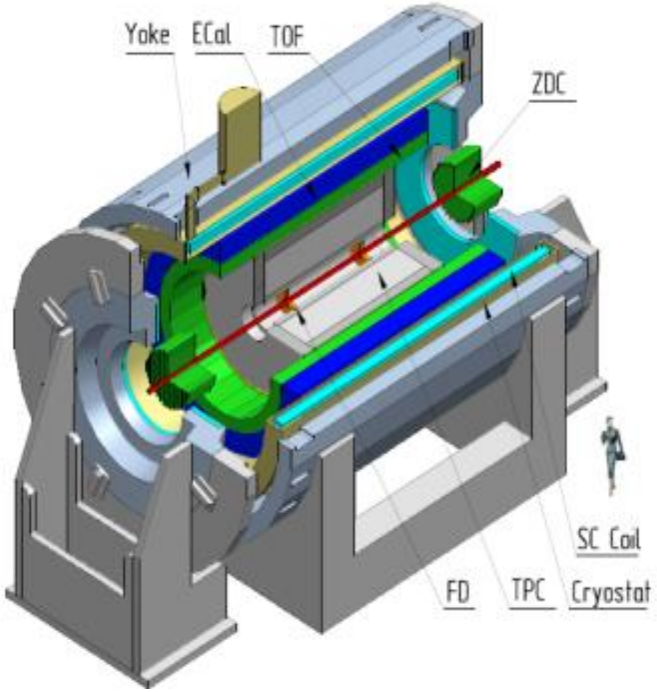


| | |
|---|---|
| Length | 340 cm |
| Vessel outer radius | 140 cm |
| Vessel inner radius | 27 cm |
| Default magnetic field | 0.5 T |
| Drift gas mixture | 90% Ar+10% $CH_4$ |
| Maximum event rate | 7 kHz ($L = 10^{27}$ $cm^{-2}s^{-1}$) |

**TPC**: $|\Delta\varphi| < 2\pi$, $|\eta| \leq 1.6$

**TOF, EMC**: $|\Delta\varphi| < 2\pi$, $|\eta| \leq 1.4$

**FFD**: $|\Delta\varphi| < 2\pi$, $2.9 < |\eta| < 3.3$

**FHCAL**: $|\Delta\varphi| < 2\pi$, $2 < |\eta| < 5$

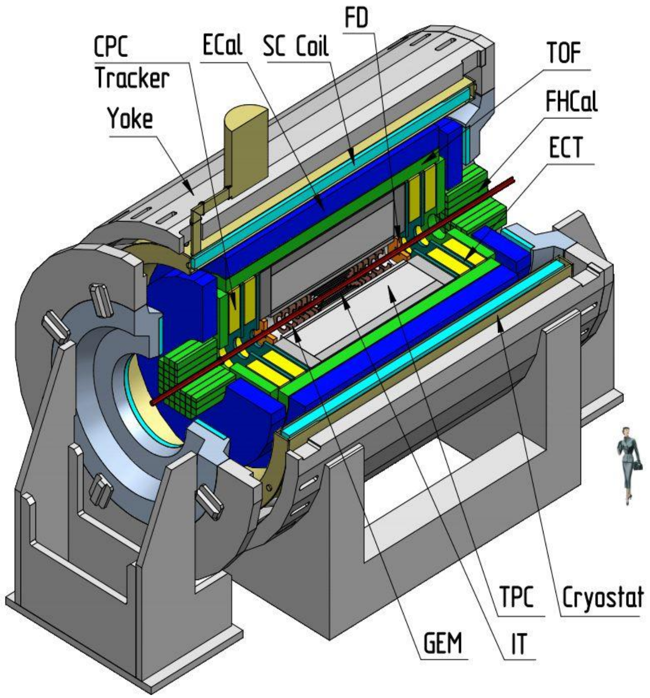


+ **ITS** (heavy-flavor measurements)

+ **forward spectrometers**

Au+Au @ 11 GeV (UrQMD + full chain reconstruction)

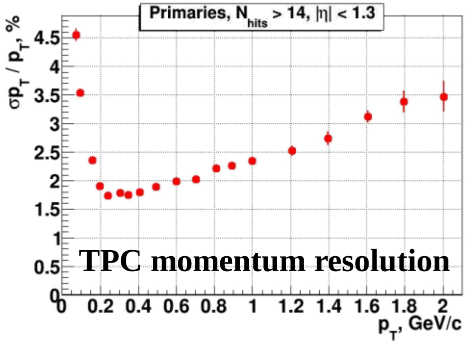


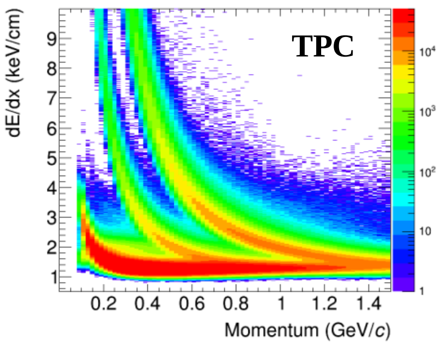


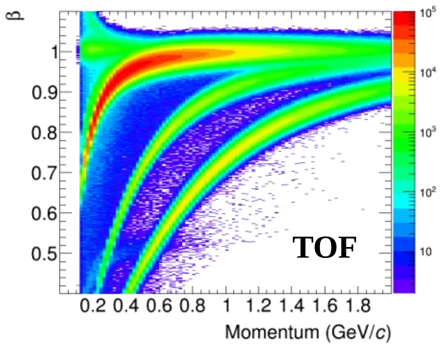


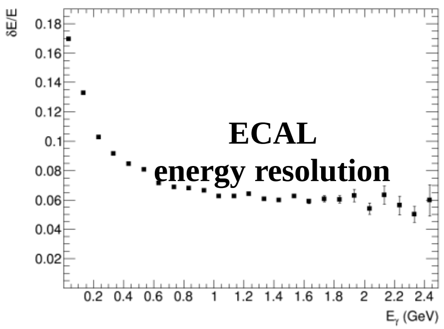

# MPD assembly

- ✓ MPD hall is available for detector activities
- ✓ Installation of the MPD superconducting coil inside the magnet yoke - 29 July, 2021, followed by alignment of cold mass, pressure test of thermal shield and cryostat cold mass, replacement of flanges, vacuum test of solenoid vessel, leak test of cryostat
- ✓ Ongoing: temperature probes cables, assembling magnet yoke, alignment, installation of top platform, chimney installation, cryogenic system with control systems, magnetic field measurement

# Cryogenic system assembly

- ✓ Barrel Magnet Yoke is completely assembled
- ✓ Cryogenic platform has been mounted, next step is mounting of the refrigerator, vacuum pumps, control electronics, etc.
- ✓ Assembling the refrigerator for installation on the platform
- ✓ Works on the magnet control system, cryogenics and power supplies
- ✓ Magnetic field mapper and magnetic field measurements

## Part 2 Signatures of QGP

Nuclear shape effects
Particle spectra and Yields
Collective flow
Femtoscopy
Global polarization

# Nuclear shape effects

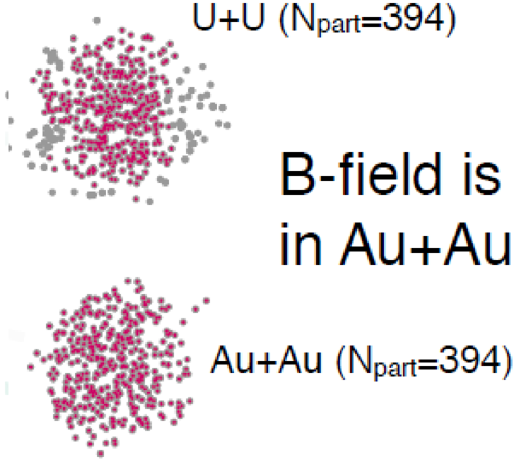


B-field is different
in Au+Au and U+U

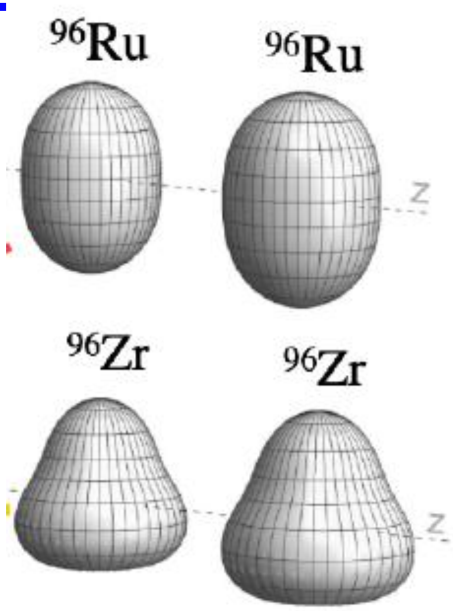


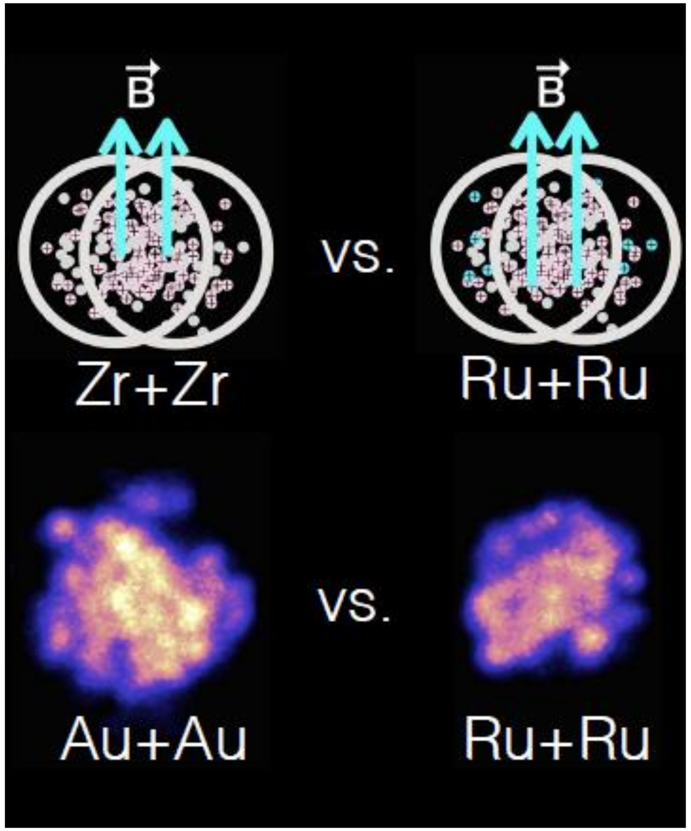


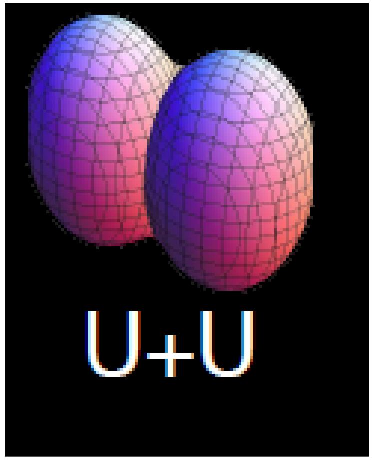


Gold nuclei is well shaped almost an ideal sphere, so is lead nuclei

Other nuclei has much more variable shapes, thus we need to carefully take into account trivial effects of interaction region geometry due to the shapes and exact conditions of the collision

# Chiral magnetic effect

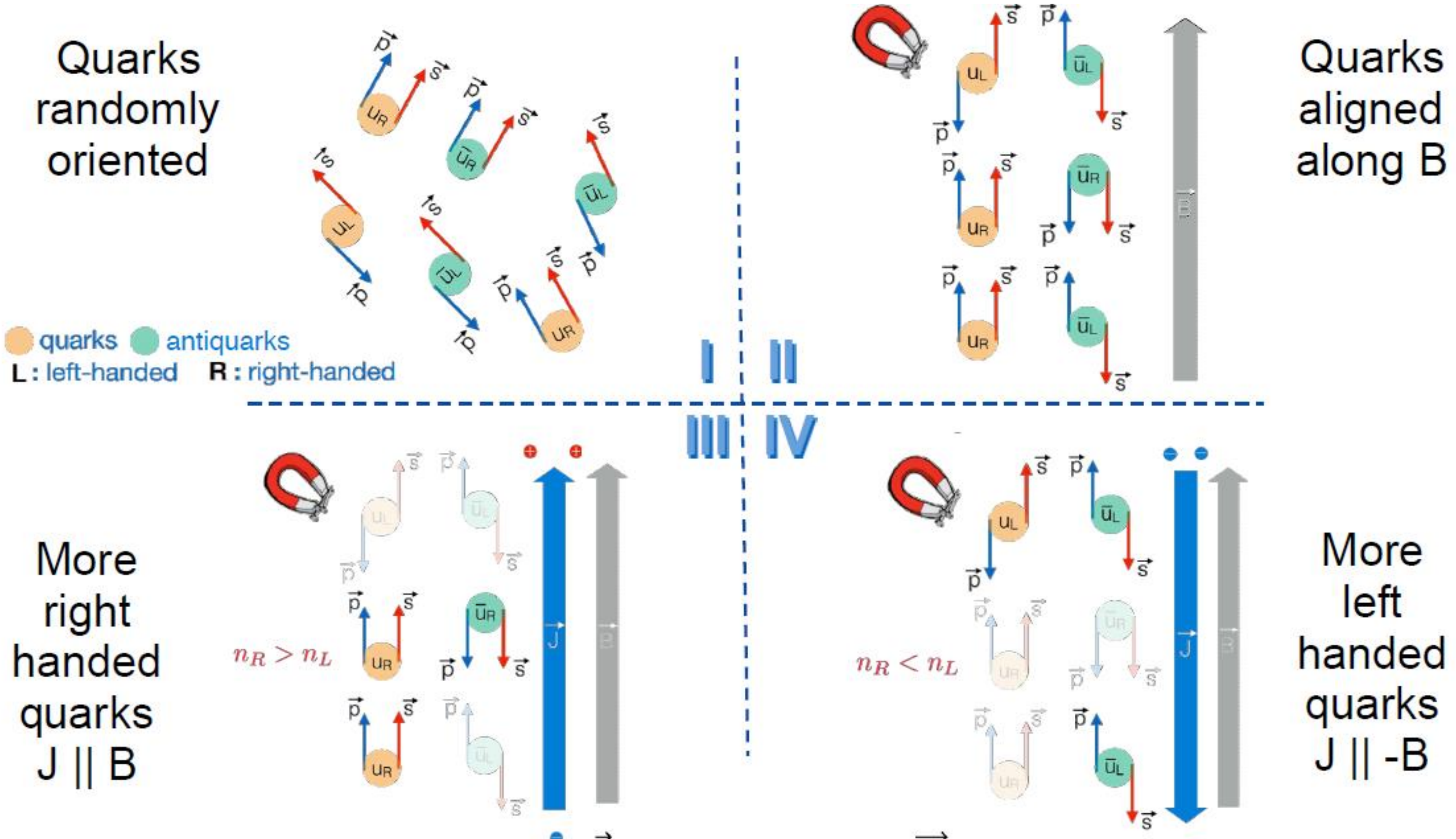


$$\vec{J} \propto \langle \vec{p} \rangle \propto (Qe)\mu_5 \vec{B}$$

# CME measurements

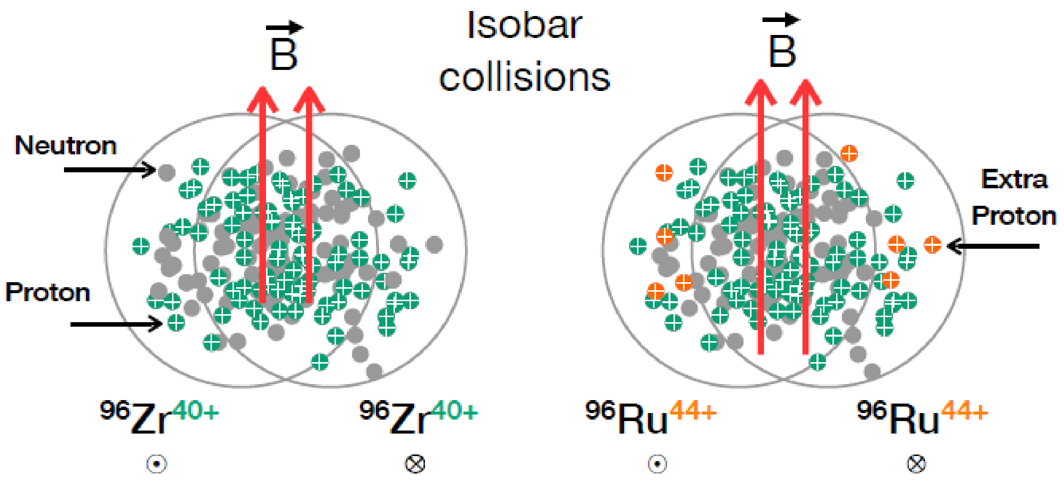


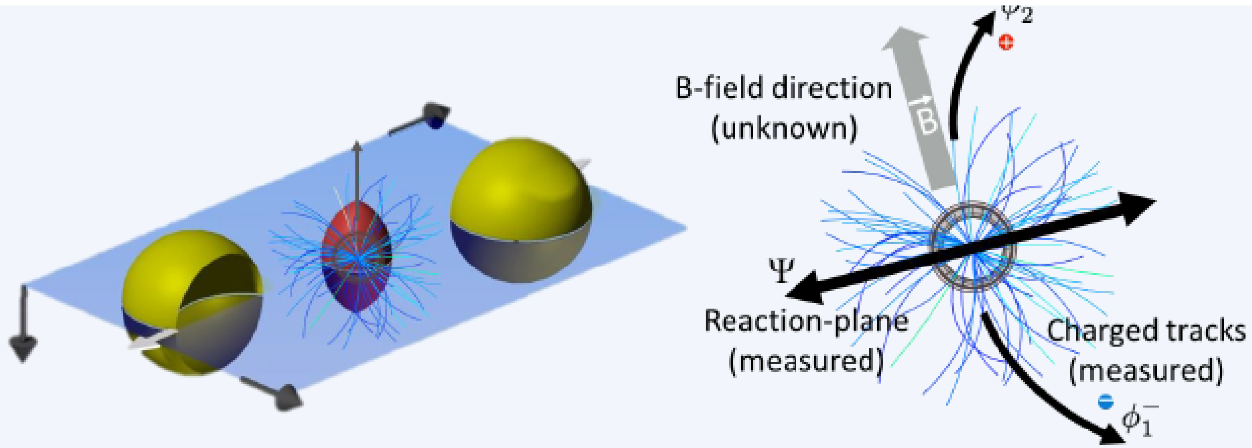


Use $\Delta\gamma$ as an example:

$$\gamma^{\alpha,\beta} \equiv \langle cos(\phi^{\alpha} + \phi^{\beta} - 2\psi_2)\rangle \qquad \Delta\gamma = \gamma^{OS} - \gamma^{SS}$$

$$\Delta\gamma = \Delta\gamma^{CME} + k\frac{v_2}{N} + \Delta\gamma^{non-flow}$$

Measurement — Signal — Background 1 — Background 2

$$\Delta\gamma^{Ru+Ru} = \Delta\gamma^{CME} + k\frac{v_2}{N} + \Delta\gamma^{non-flow}$$

$$\Delta\gamma^{Zr+Zr} = \Delta\gamma^{CME} + k\frac{v_2}{N} + \Delta\gamma^{non-flow}$$

$\boldsymbol{B}^2$ are ~15% different

Within 4%

# STAR results on un-blind CME analysis

*Chiral Separation Effect* $\mathbf{J}_5 \propto e\mu_V \mathbf{B}$

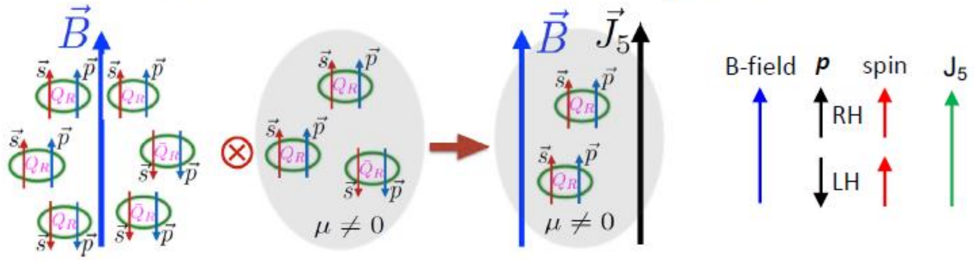


B-field + massless quarks + non-zero $\mu_V$ → axial current $J_5$

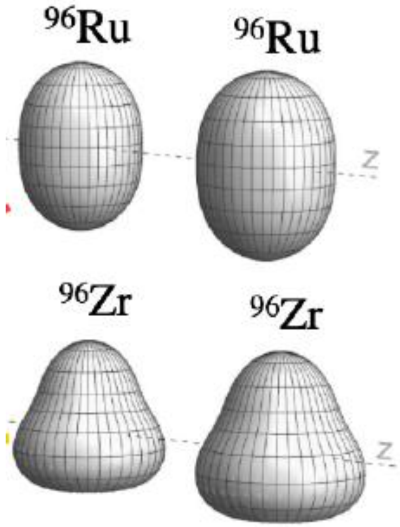


D. Kharzeev, PPNP88, 1 (2016)
STAR, PRC105, 014901 (2022)

**Chiral magnetic effect (CME)**

$$\mathbf{J}_{\mathbf{cme}} = \sigma_5 \mathbf{B} = \left(\frac{(Qe)^2}{2\pi^2}\mu_5\right)\mathbf{B},$$

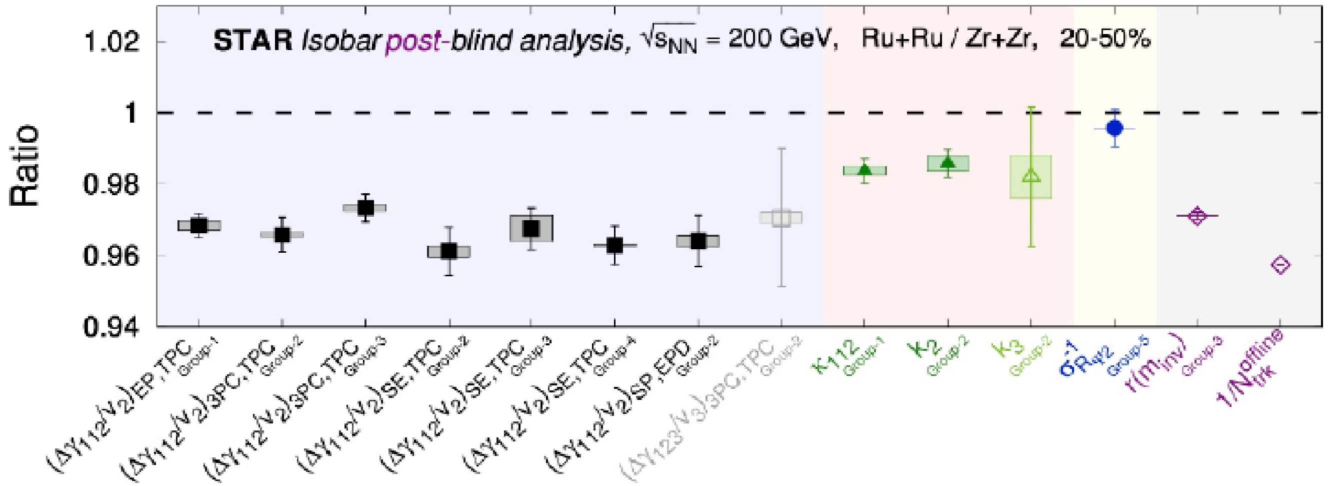


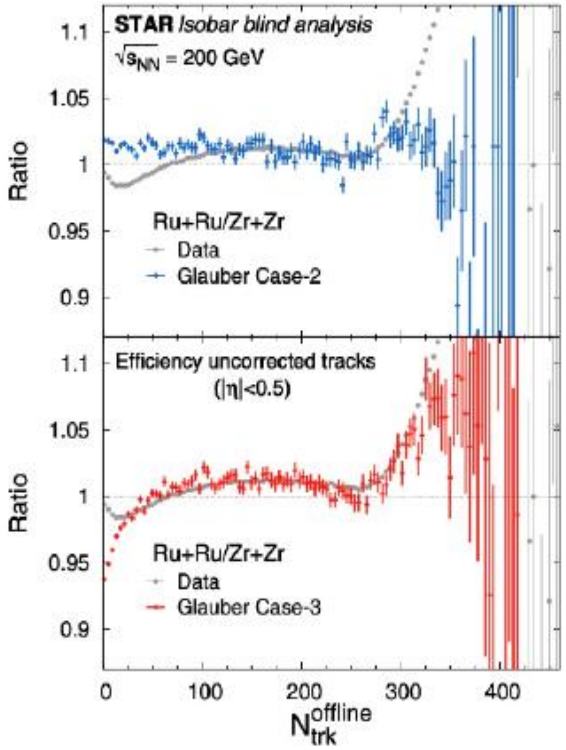


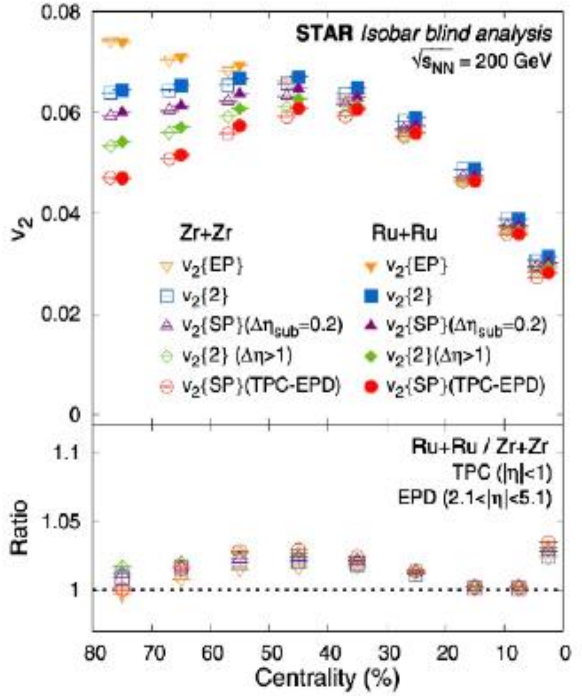

# Neutron skin effects

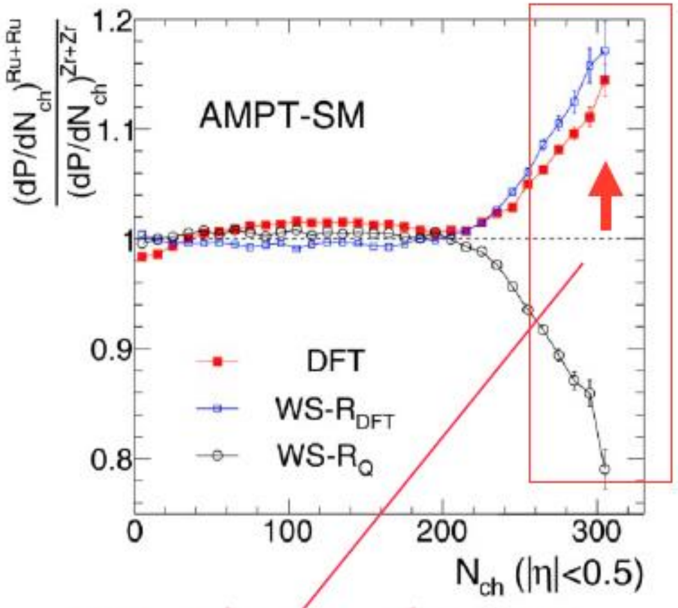


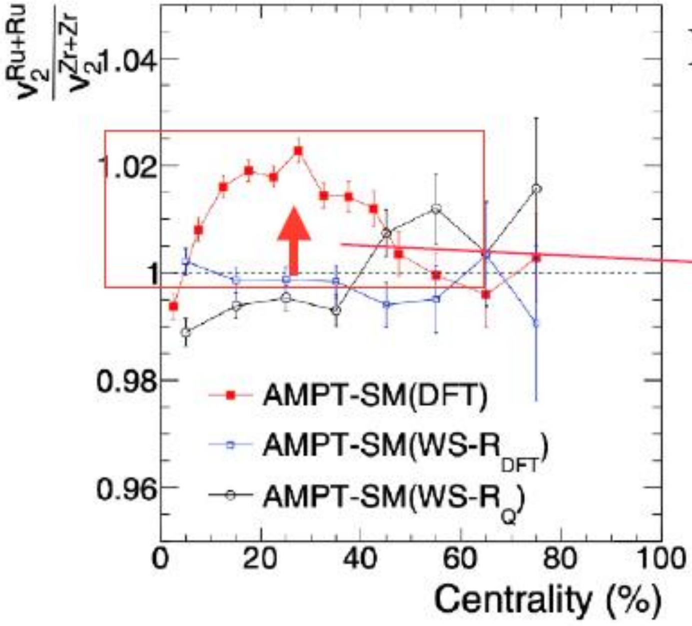


**Neutron skin thickness** $\Delta r_{np} \equiv \sqrt{\langle r_n^2 \rangle} - \sqrt{\langle r_p^2 \rangle}$

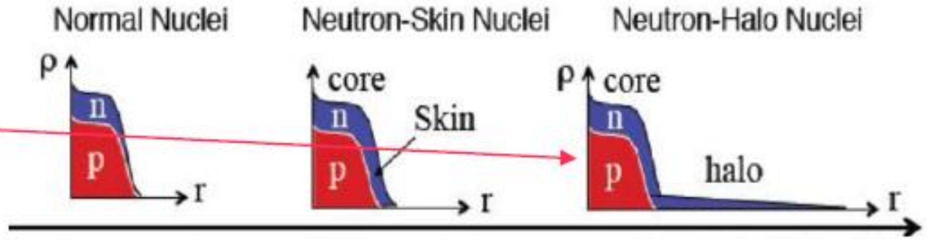


| Normal Nuclei | Neutron-Skin Nuclei | Neutron-Halo Nuclei |
|---|---|---|
| $R_n = R_p$ | $R_n > R_p$ | $R_n = R_p$ |
| $a_n = a_p$ | $a_n = a_p$ | $a_n > a_p$ |

$$\rho = \frac{\rho_0}{1 + \exp\left[\frac{r - R}{a}\right]}$$

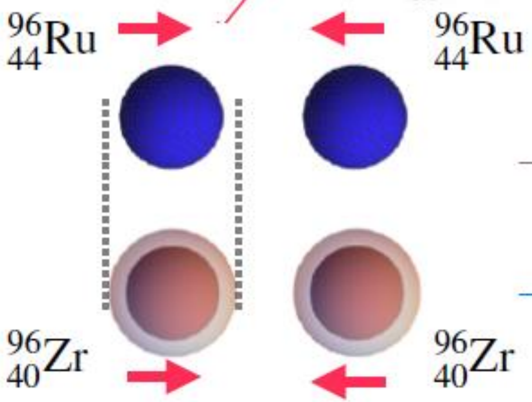


→ Smaller $r$, larger density → Larger $N_{ch}$ and $\langle p_T \rangle$

→ Larger $r$, smaller density → Smaller $N_{ch}$ and $\langle p_T \rangle$


HJX, et.al., PRL121, 022301 (2018)
H. Li, HJX, et.al., PRC98, 054907 (2018)
HJX, et.al., PLB819, 136453 (2021)

# Time evolution of the collision

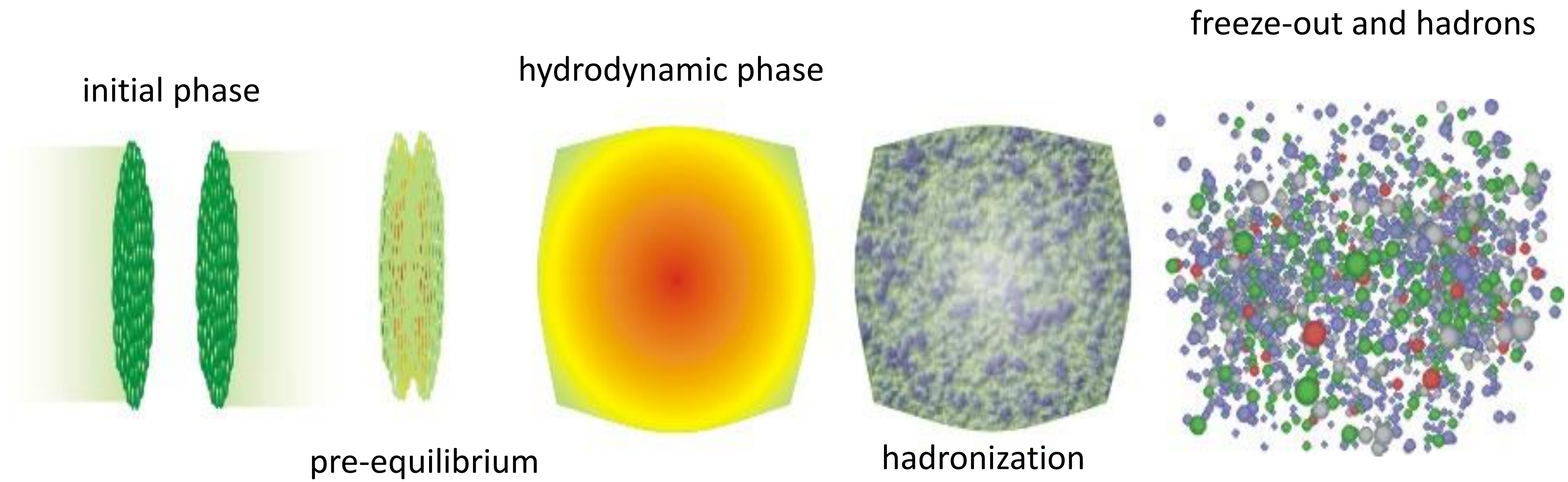


«Soft» probes ($p_T \sim T_{kin}$= 150 MeV)
- ✓ particle spectra at small transverse momenta $p_T$ and momentum correlations
- ✓ flow effect
- ✓ thermal photons and dileptons
- ✓ strange particle yields

"Hard" probes ($p_T >> T_{kin}$= 150 MeV)
- ✓ particle spectra at large transverse momenta $p_T$ and angle correlations
- ✓ hadron jets
- ✓ quarkonia
- ✓ heavy quark probes

# What we knew from early experiments

- Summary of AGS, SPS, and early RHIC Results
- Inclusive observables ➔ *onset of deconfinement* at 7-8 GeV.
- The observables suggest a change in the nature of the system.
- More discriminating studies were needed to understand the nature of the phase transition and to search for critical behavior.
- It is best to study regions above and below the possible onset energy.

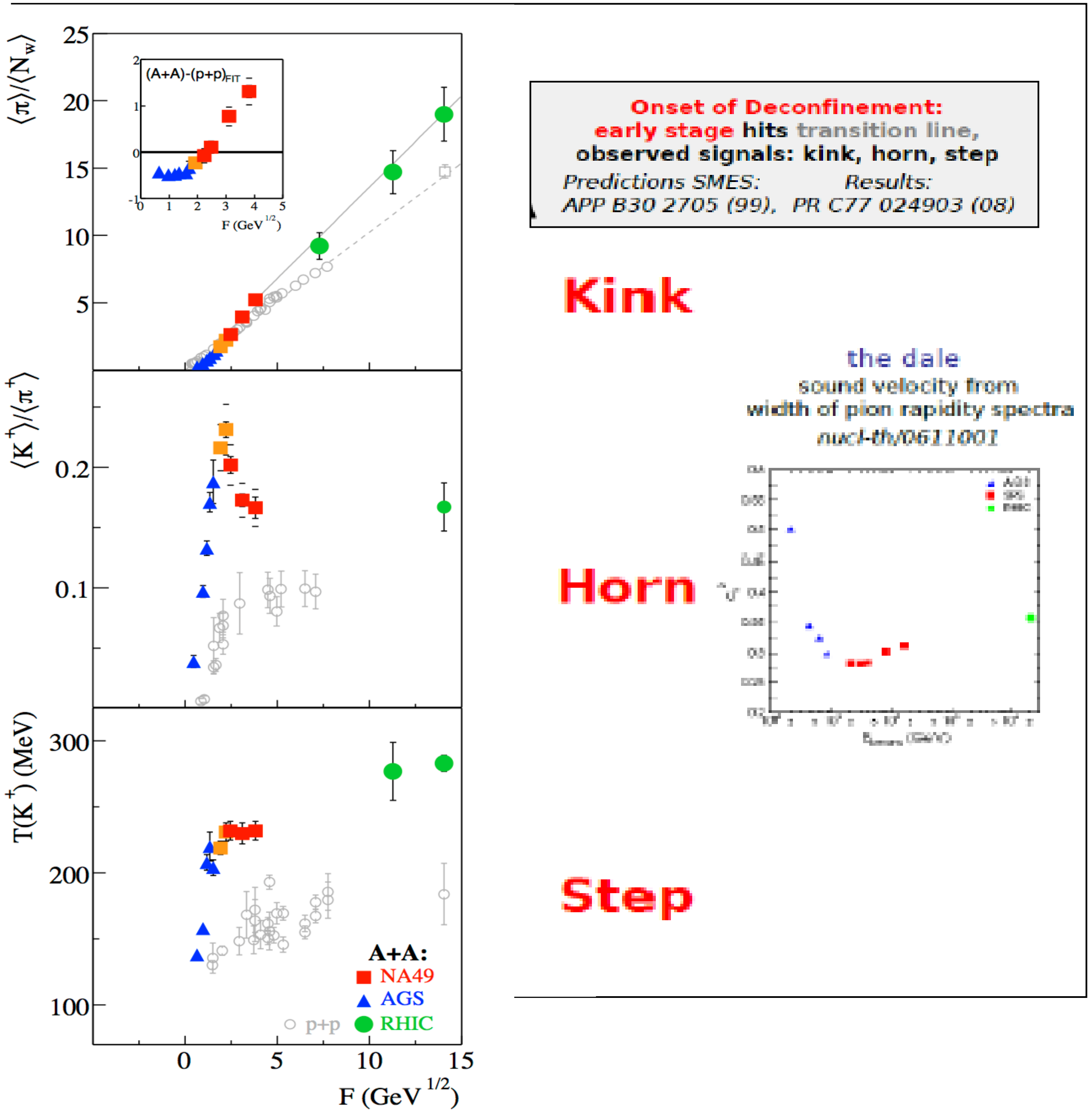

# Blast-Wave model and chemical freeze-out

Elastic collisions among the particles cease and the momentum distribution gets fixed

## Blast-Wave (BW) Model:

$$\frac{dN}{p_T dp_T} \propto \int_0^R r dr m_T I_0\left(\frac{p_T \sinh\rho(r)}{T_{kin}}\right) \times K_1\left(\frac{m_T \cosh\rho(r)}{T_{kin}}\right)$$

E. Schnedermann, J. Sollfrank, and U. W. Heinz, Phys. Rev. C **48**, 2462 (1993).

$I_0$, $K_1$: Modified Bessel functions

$\rho(r) = \tanh^{-1}\beta$, r/R: relative radial position; R: radius of fireball

$\beta$: transverse radial flow velocity, $T_{kin}$: Kinetic freeze-out temperature

**Model Features:**

- Hydrodynamic based model
- Assumes particles are locally thermal at a kinetic freeze-out temperature and moving with a common radial flow velocity

# Momentum spectra of strange particles

Phys. Rev. C **102** (2020) 34909

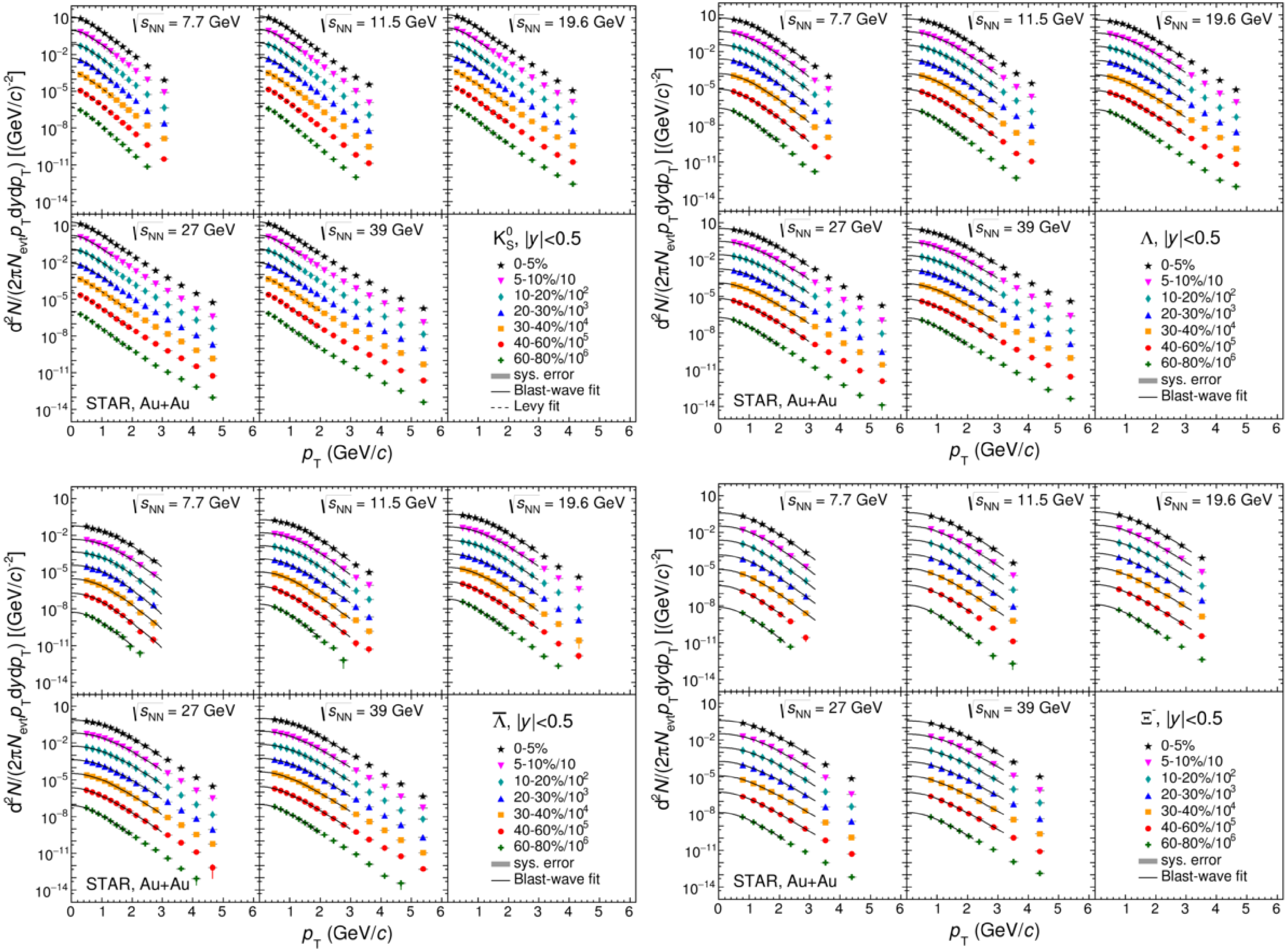


$K^0_s$, Λ, anti-Λ, $\Xi^-$ transverse momentum spectra at midrapidity |y| < 0.5

Levy fit

$$\frac{d^2N}{2\pi p_T dp_T dy} \propto \left(1+\frac{m_T-m_0}{nT}\right)^{-n}$$

Blast-wave fit

$$\frac{d^2N}{2\pi p_T dp_T dy} \propto \int_0^R r dr m_T I_0\left(\frac{p_T \sinh\rho(r)}{T}\right) \times K_1\left(\frac{m_T \cosh\rho(r)}{T}\right)$$

# Particle production differential and integral

$$y = \frac{1}{2}\ln\frac{E+p_z}{E-p_z}$$

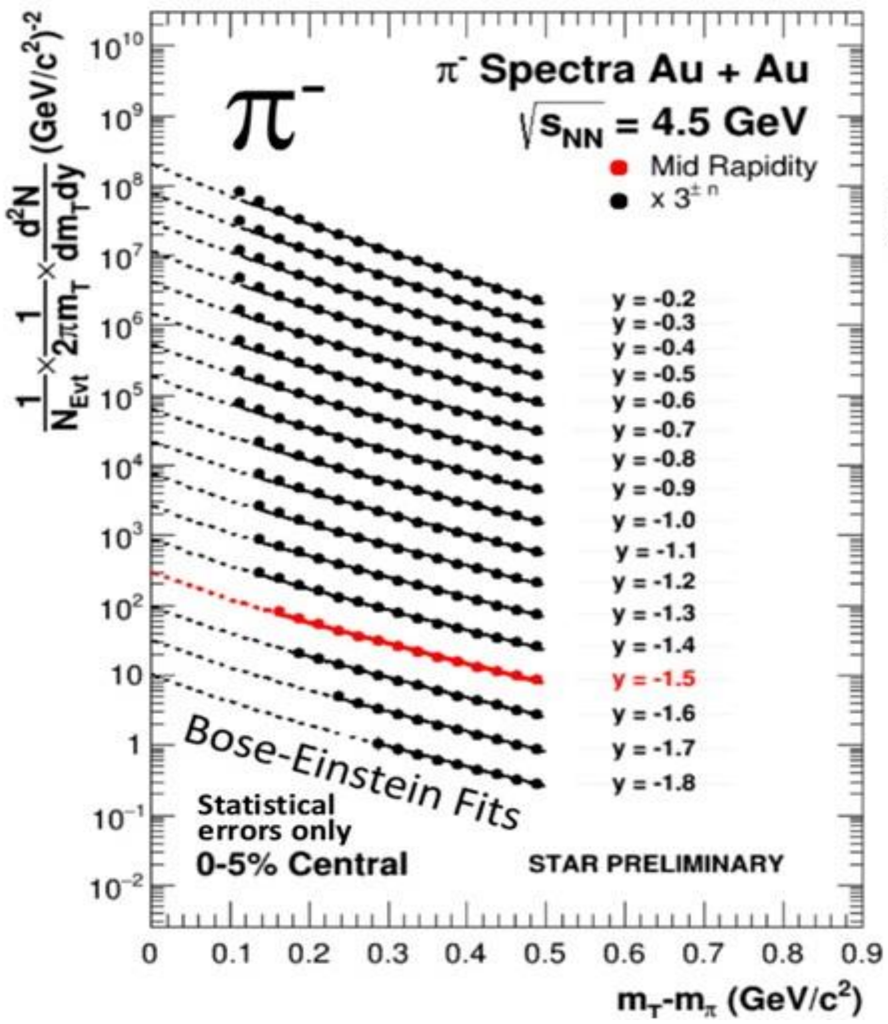


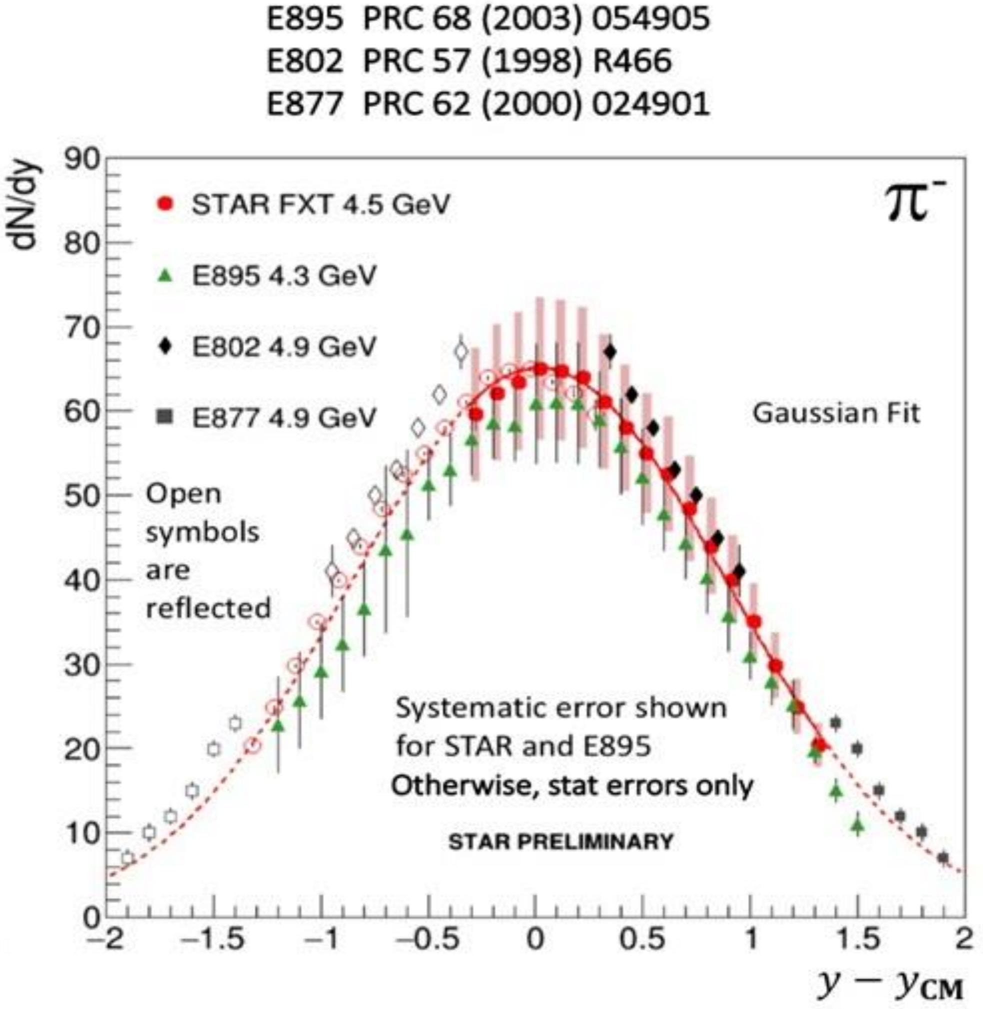

# Thermal model and kinematic freeze-out

Inelastic collisions among the particles cease; the particle yields and ratios gets fixed

Statistical thermal model: J. Cleymans et al., Comp. Phys. Comm. **180**, 84 (2009)

$$n = \frac{1}{V}\frac{\partial(T\ln Z)}{\partial\mu} = \frac{VTm_i^2 g_i}{2\pi^2}\sum_{k=1}^{\infty}\frac{(\pm1)^{k+1}}{k}\left(e^{\beta k\mu_i}\right)K_2\left(\frac{km_i}{T}\right)$$

(Grand canonical ensemble)

$\beta \cong 1/T$; -1(+1) for fermions (bosons),
Z - partition function;
$m_i$ - mass of hadron species i;

V - volume; T - Temperature;
$K_2$ - 2nd-order Bessel function;
$g_i$ - degeneracy; $\mu_i$ - chemical potential

**Model Features: Assumes**

- ❑ Non-interacting hadrons and resonances
- ❑ Thermodynamically equilibrium system

# Energy dependence of yields

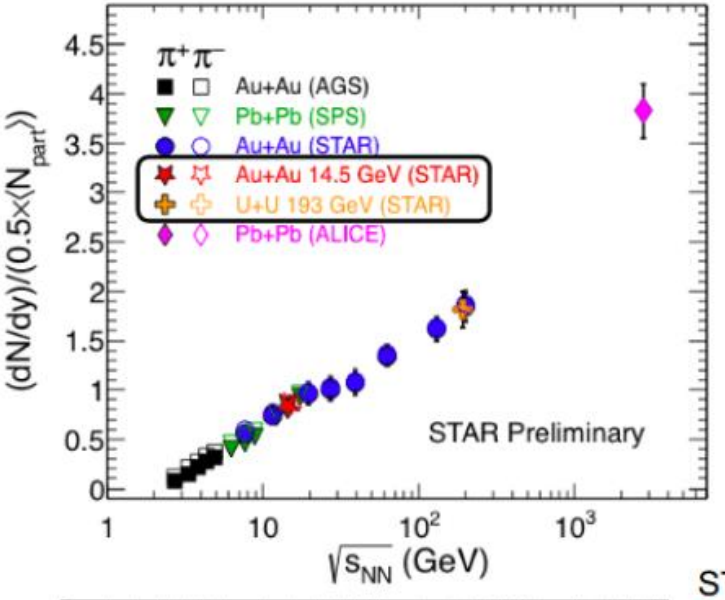


STAR: PRC **96**, 044904 (2017)

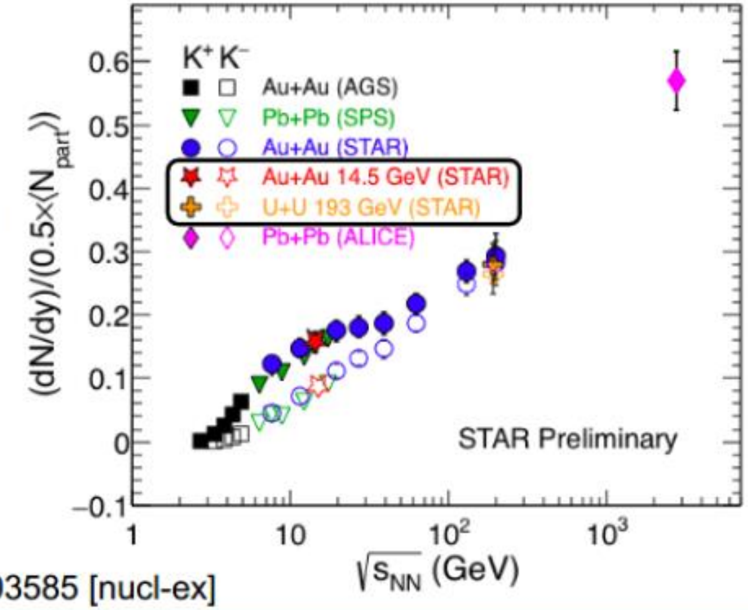


STAR: arXiv:1908.03585 [nucl-ex]

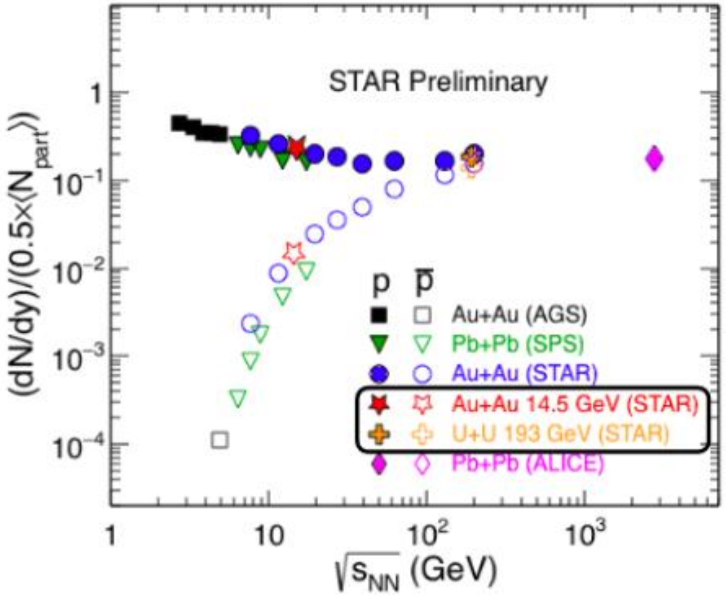


- Yields increase as a function of collision energy except for protons
- *Au+Au 14.5 GeV and U+U 193 GeV fit well in the trend*
- **Higher energies:** Similar (pair) production of particle and anti-particle

**Lower energies:** $\pi^- > \pi^+$, $K^+ > K^-$, $p > \bar{p}$

# Energy dependence of particle ratios

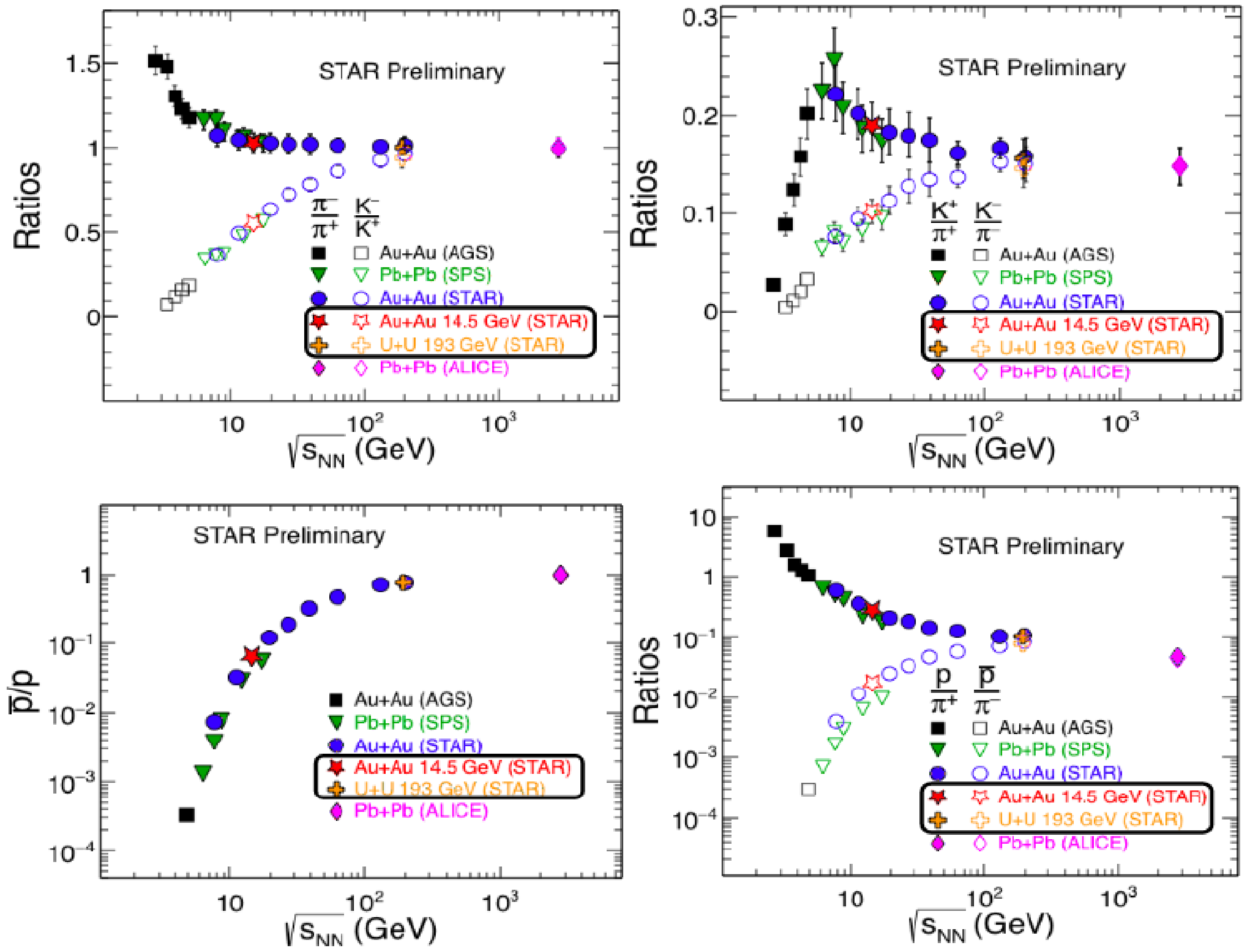


STAR: PRC **96**, 044904 (2017) STAR: arXiv: 1908.03585 [nucl-ex]

Ratios shows interesting trends for energy dependence

Au+Au 14.5 and U+U 193 fit well in established trend

Almost no barion asymmetry at high energies

At lower energies

$$\pi^- > \pi^+, K^+ > K^-, p > \bar{p}$$

# Thermal model particle production

$$\frac{p}{T^4} = \frac{1}{T^3}\frac{\partial \ln Z(V,T,\mu)}{\partial V}$$

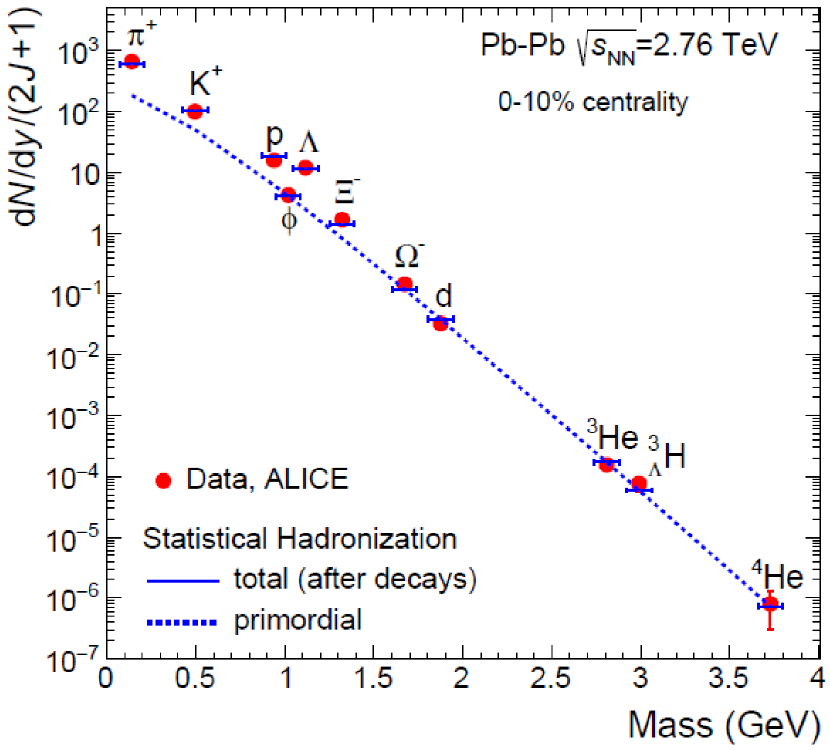


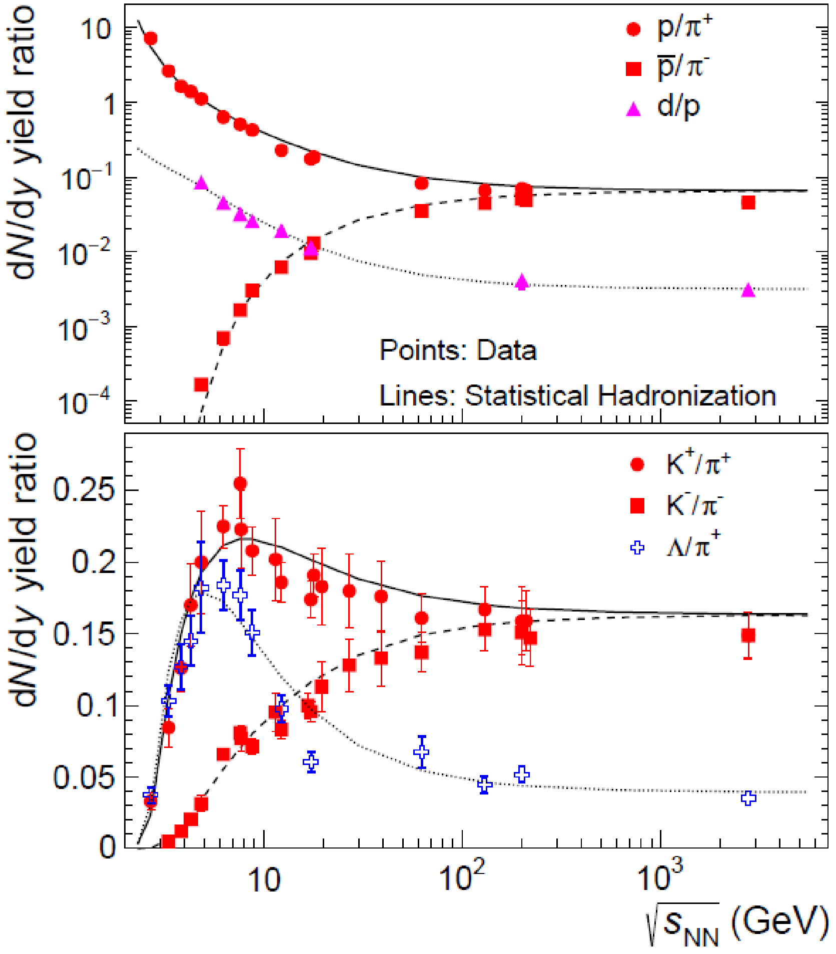

# Phase diagram scan

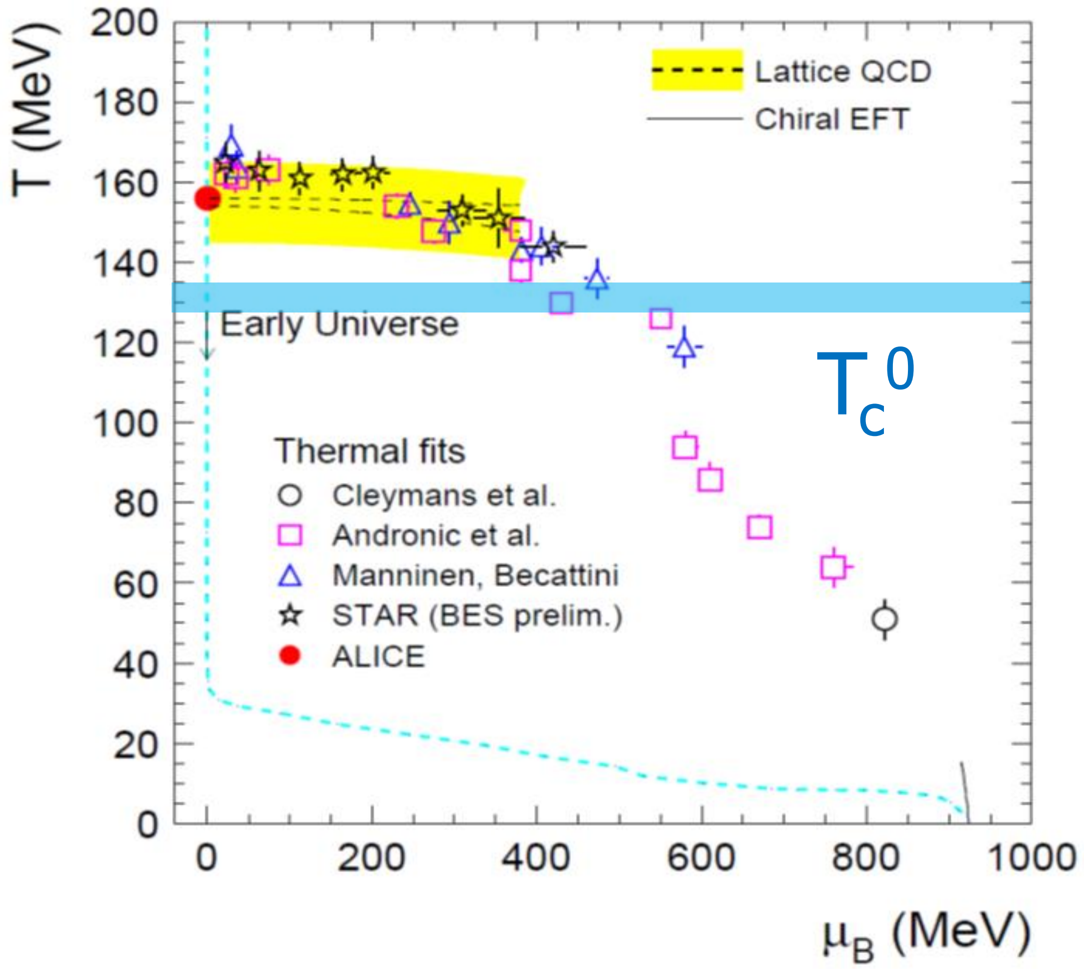


A. Andronic et al., Jour. Phys. G38 (2011)

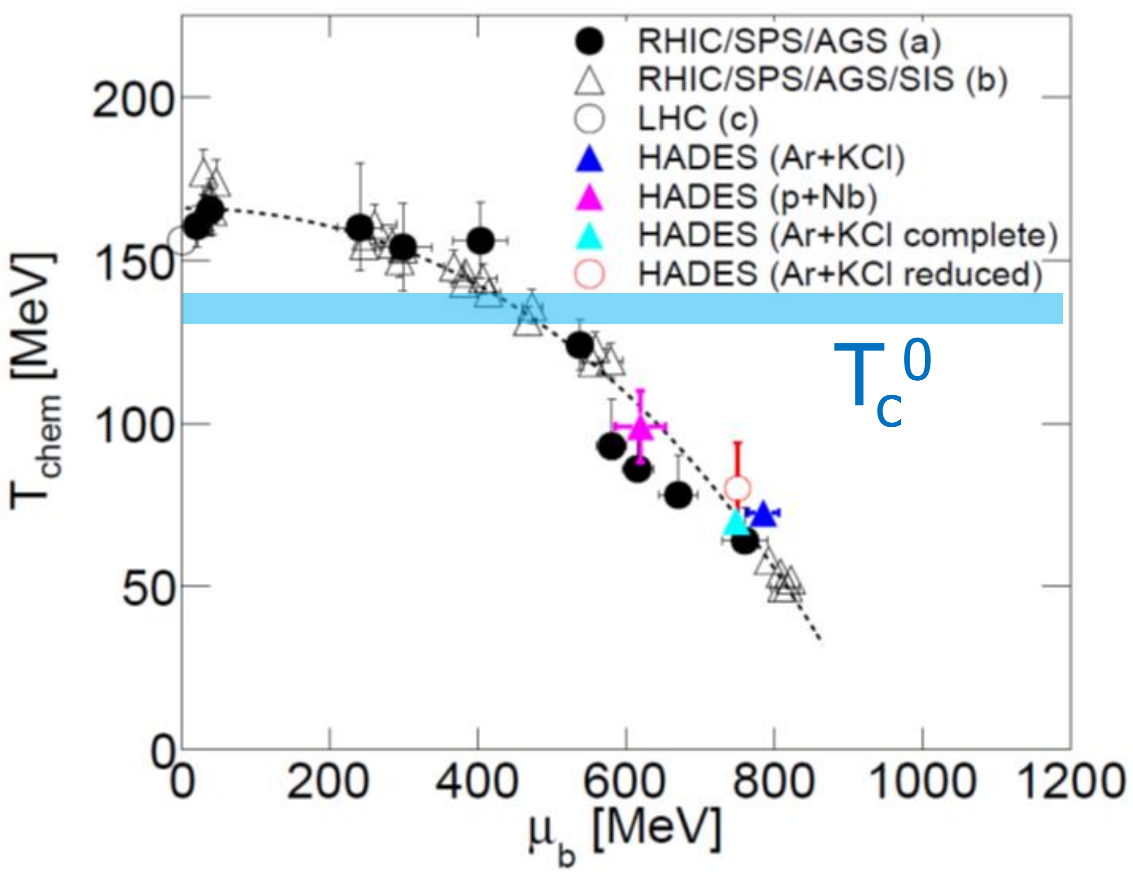


G. Agakishiev et al., arXiv:1512.07070

# Phase diagram scan

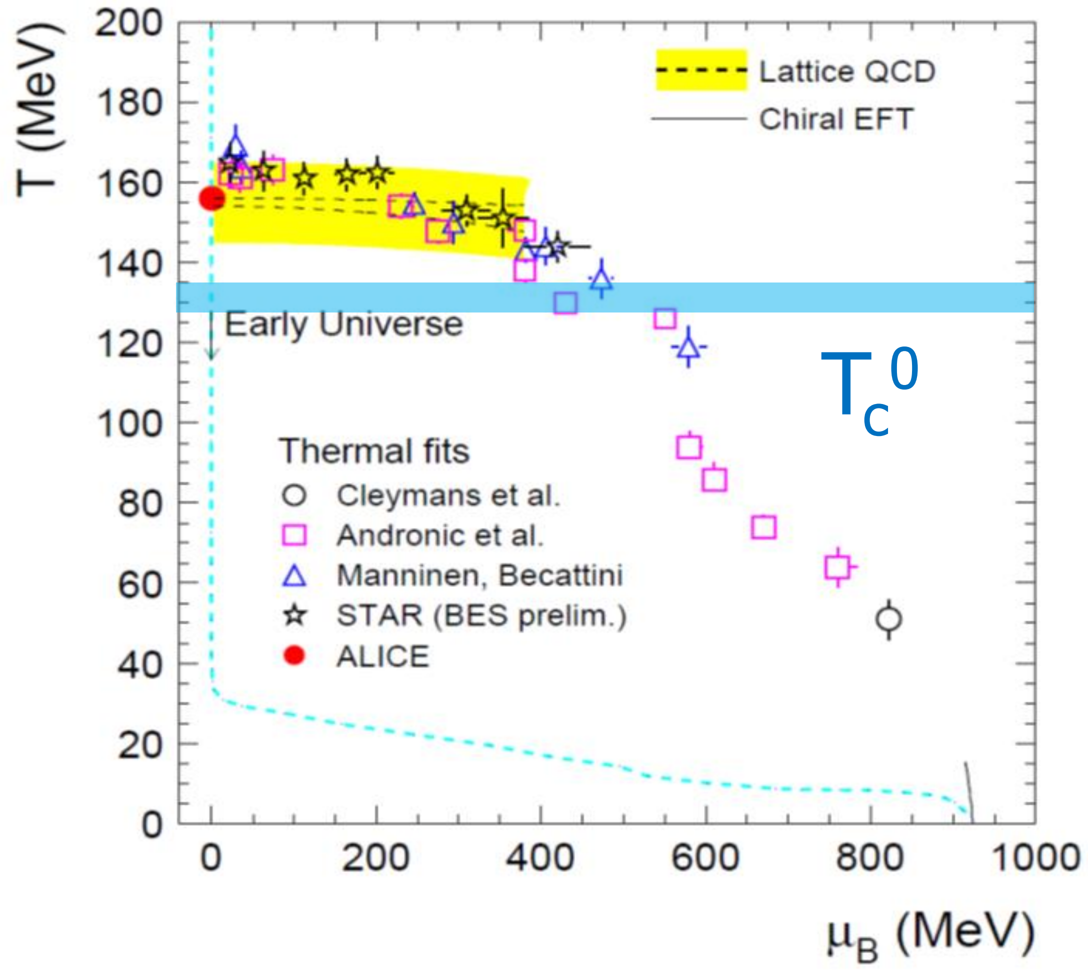


$T_{chem}$ and $T_{kin}$ diverge at around 7 GeV.

$T_{kin}$ and <β> flatten

Softening of the EoS?

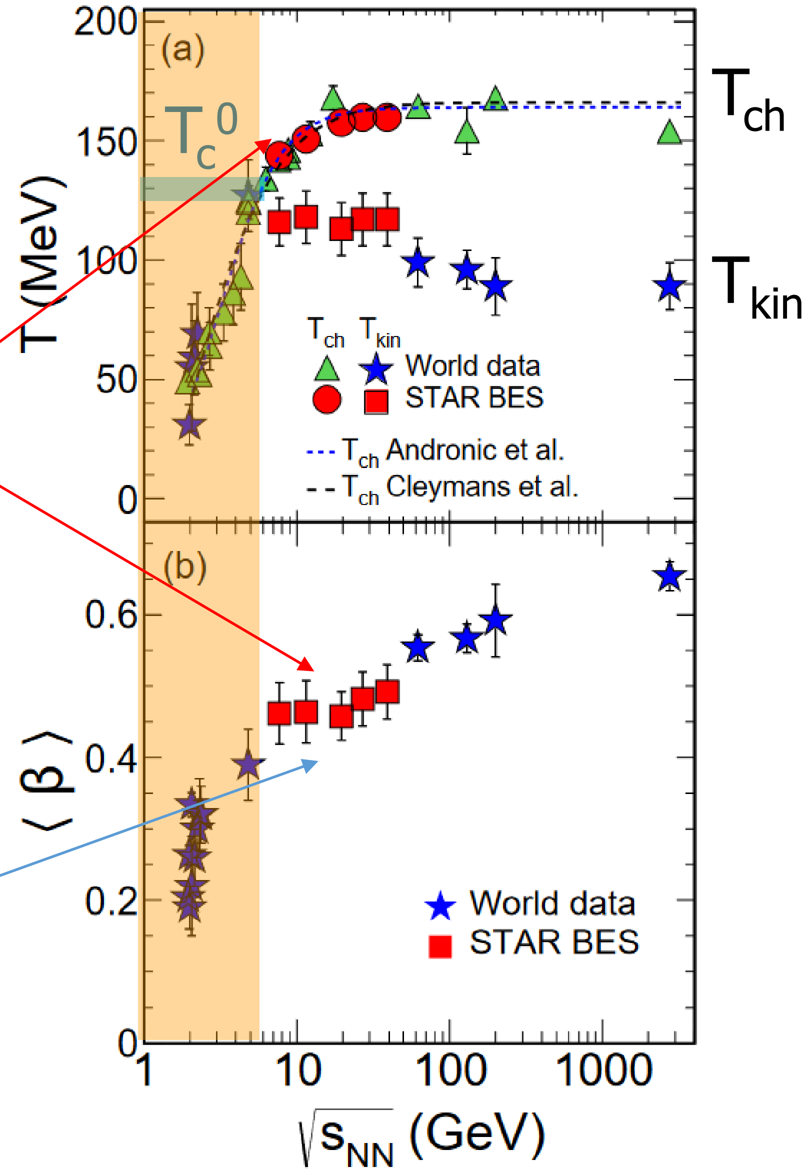


L. Adamczyk, et al. STAR Collaboration Phys. Rev. C96 (2017) 044904

# Strange particle production

Pike is observed in particle ratios for strange/non-strange particles for HIC and not observed for light collision systems

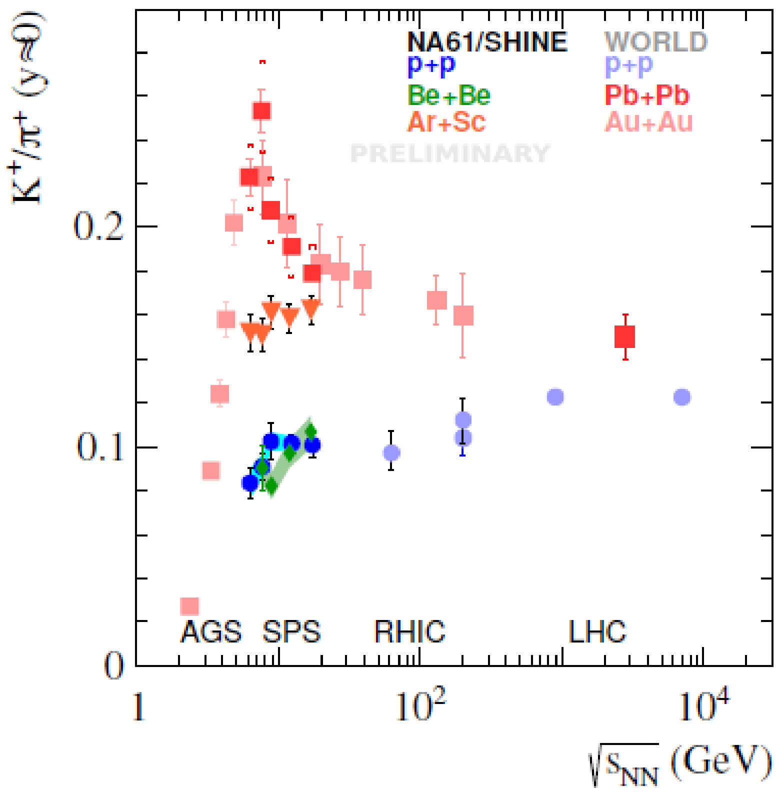


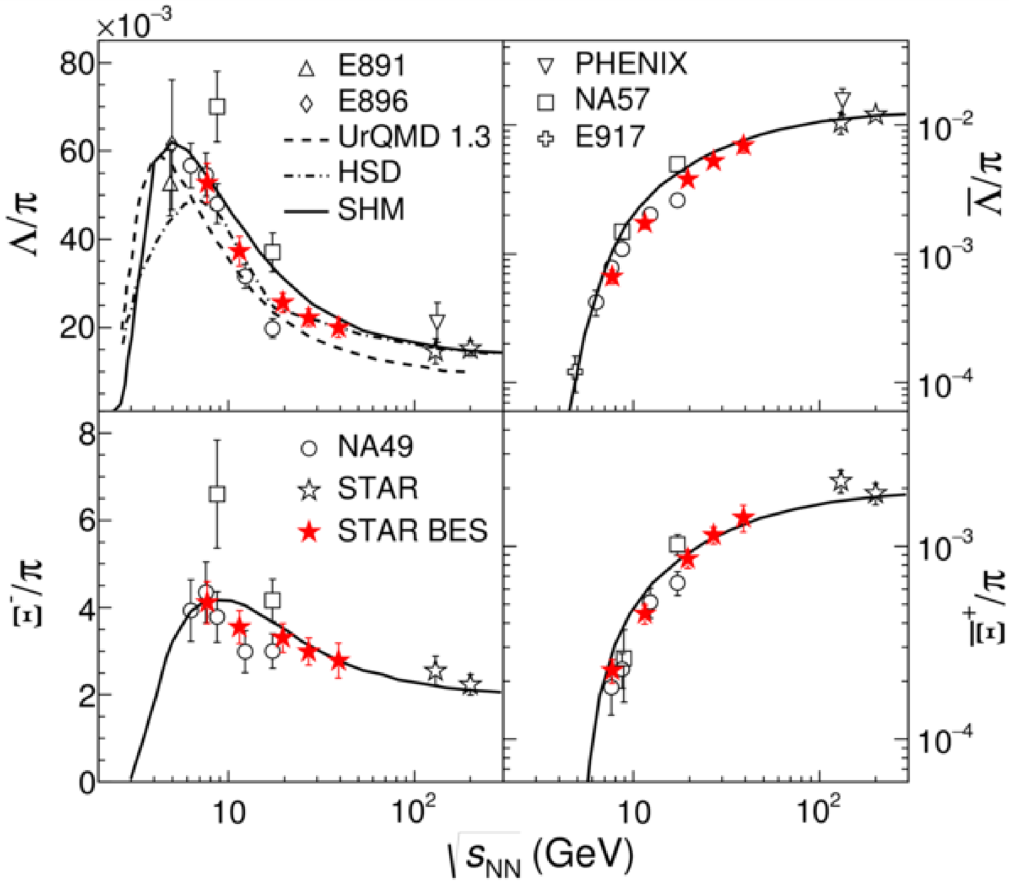

# Collective flow

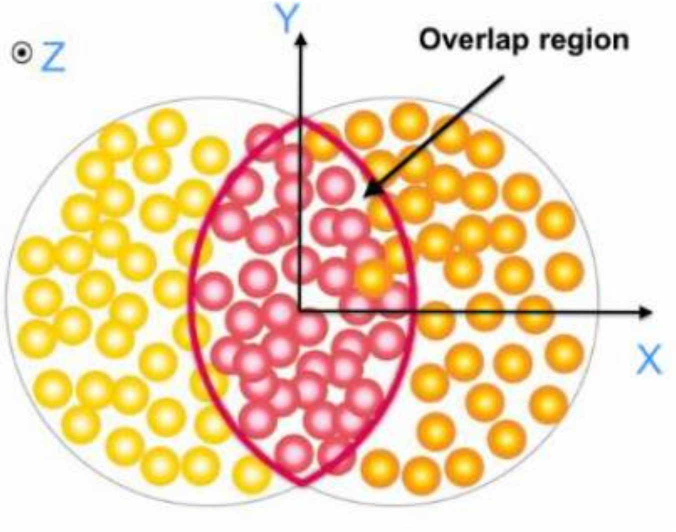


Interactions
↓
Pressure(P)

$$y > x \rightarrow \frac{\partial P}{\partial x} > \frac{\partial P}{\partial y}$$

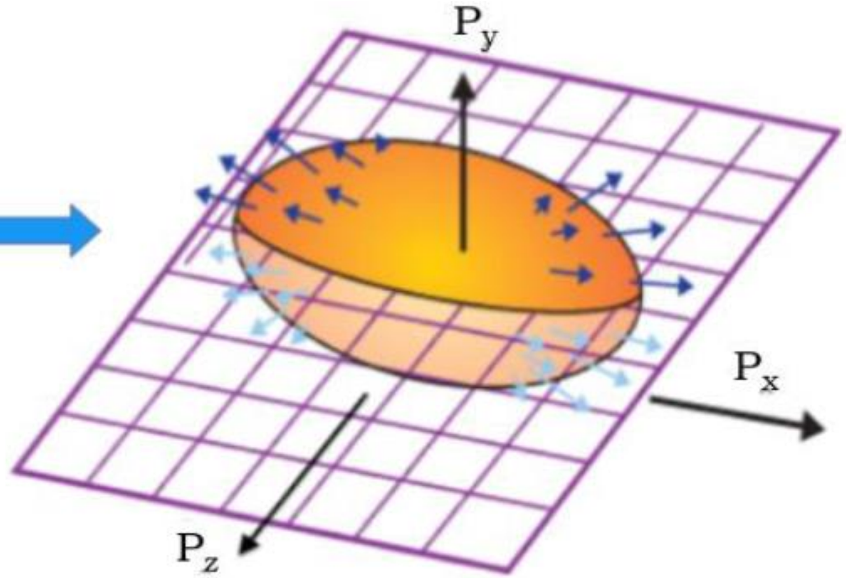


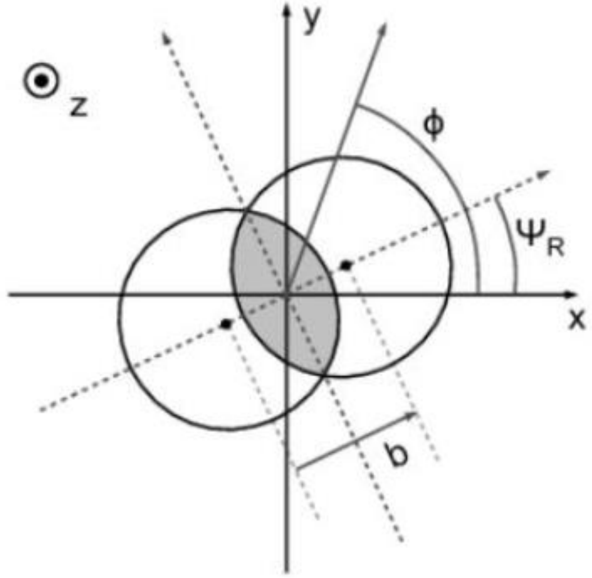


$$\frac{dN}{d\phi} \propto \frac{1}{2\pi}\left[1 + \sum_{n=1}^{\infty} 2v_n \cos\left(n(\phi - \psi_{rp})\right)\right]$$

$$v_n = \langle \cos\left(n(\phi - \psi_{rp})\right)\rangle$$

- ✓ Sensitive to early times in the evolution of the system
- ✓ Sensitive to the equation of state

**Probe of the early (partonic) stage of the collision**

# Collective flow

$$\frac{dN}{d(\phi-\psi_n)} = \frac{1}{2\pi}\left(1 + 2\sum_{n=1}^{+\infty} v_n cos\ [n(\phi-\psi_n)]\right)$$

Initial spatial asymmetry is transferred to the final momentum asymmetry

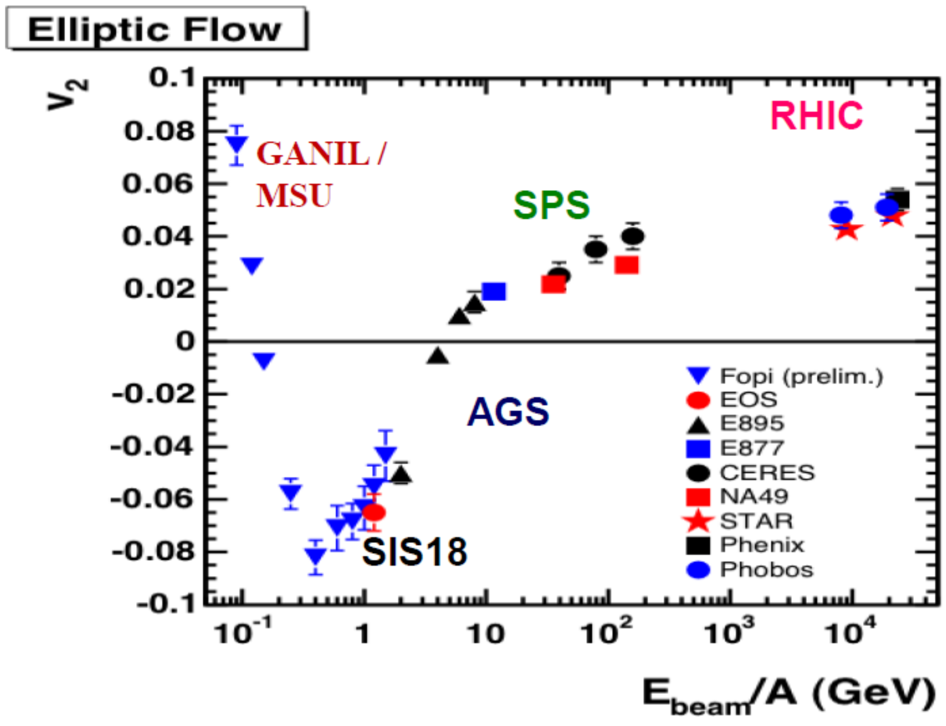


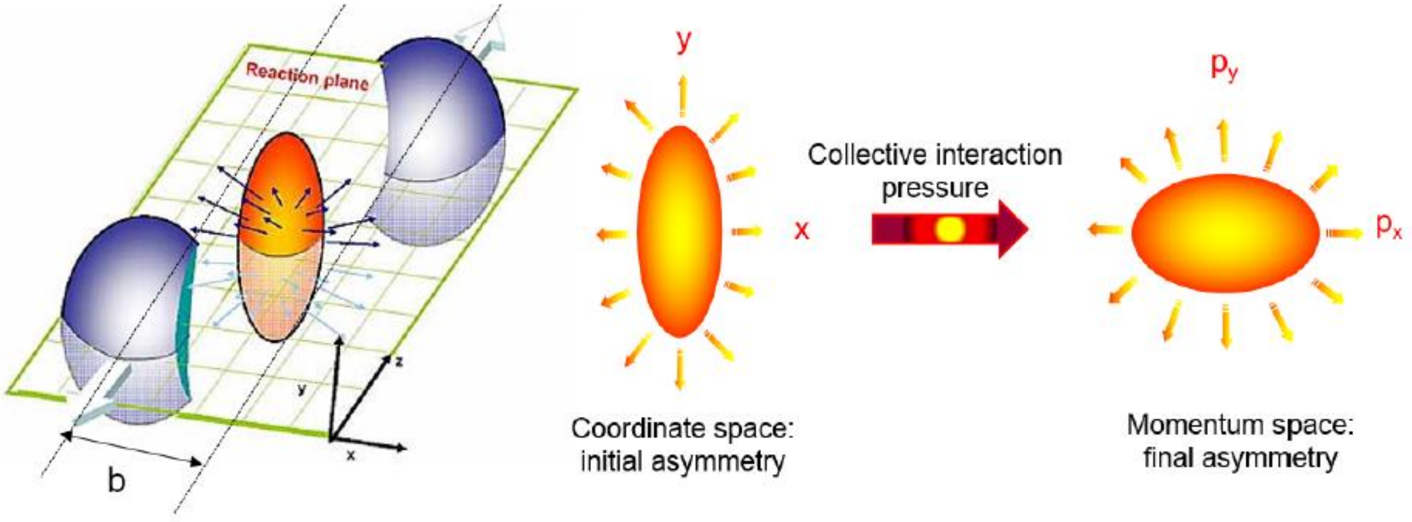


$$E\frac{d^3N}{dp^3} = \frac{1}{2\pi}\frac{d^2N}{p_t dp_t dy}\left(1 + \sum_{n=1}^{\infty} 2v_n \cos[n(\varphi - \Psi_r)]\right)$$

# Kinematic effects in flow

Squeeze-out: due to large passage time of the spectators results in the particles being predominantly emitted in the out-of-plane directions

$v_2 > 0$

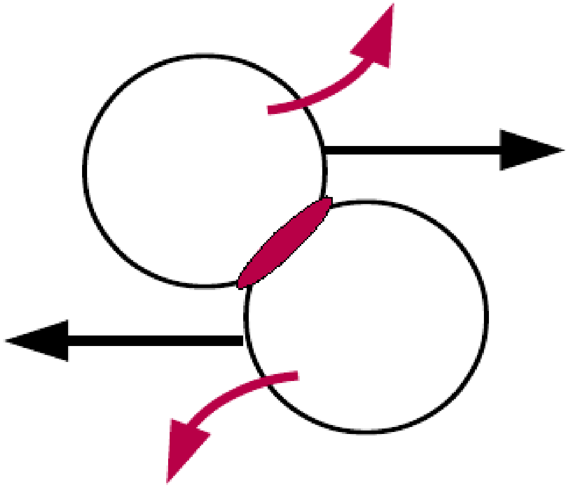

$v_2 < 0$

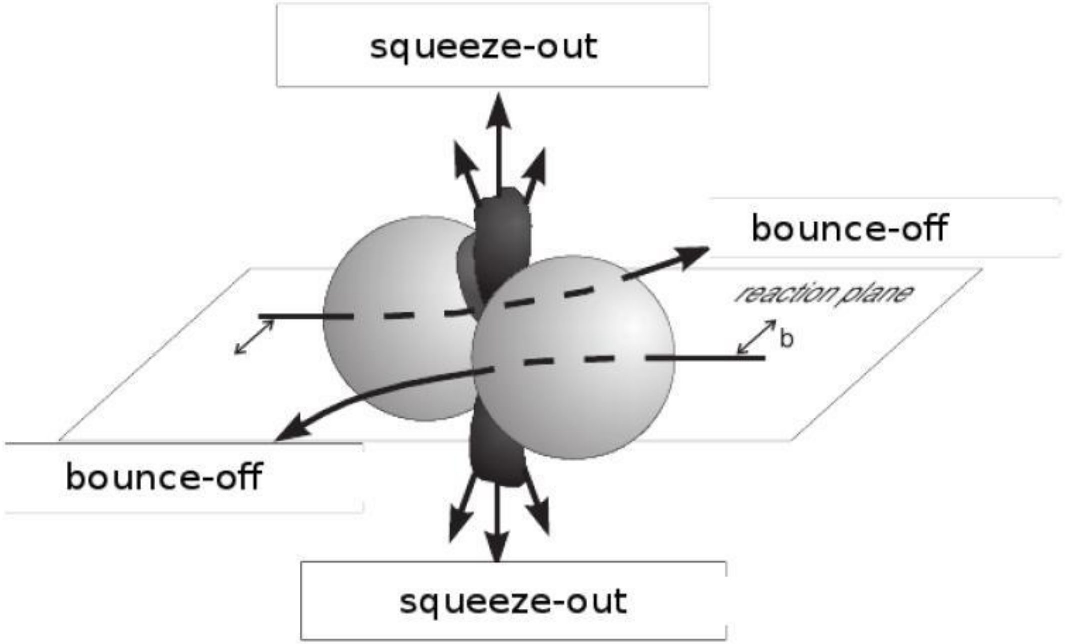

# Elliptic flow, NCQ-scaling

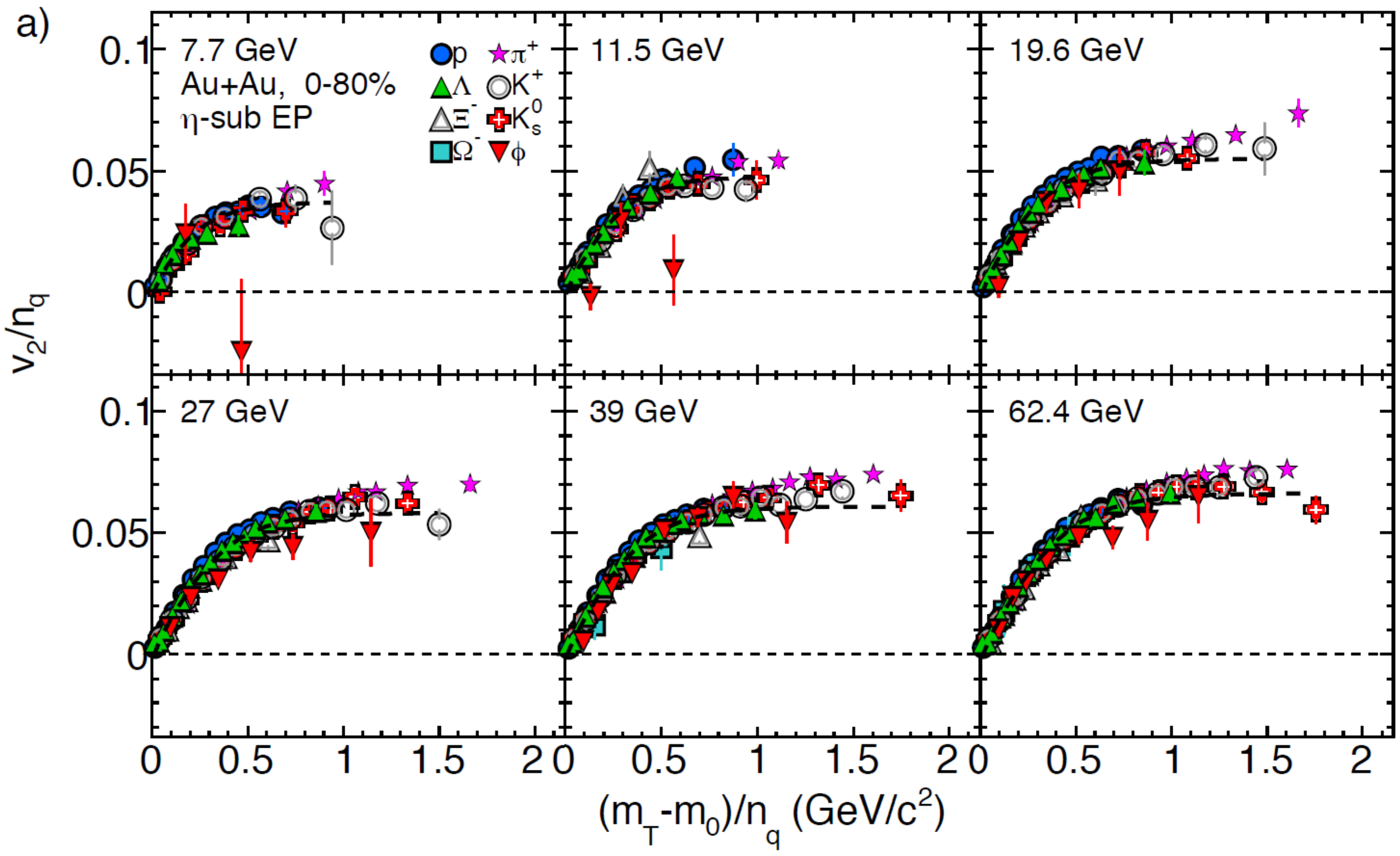


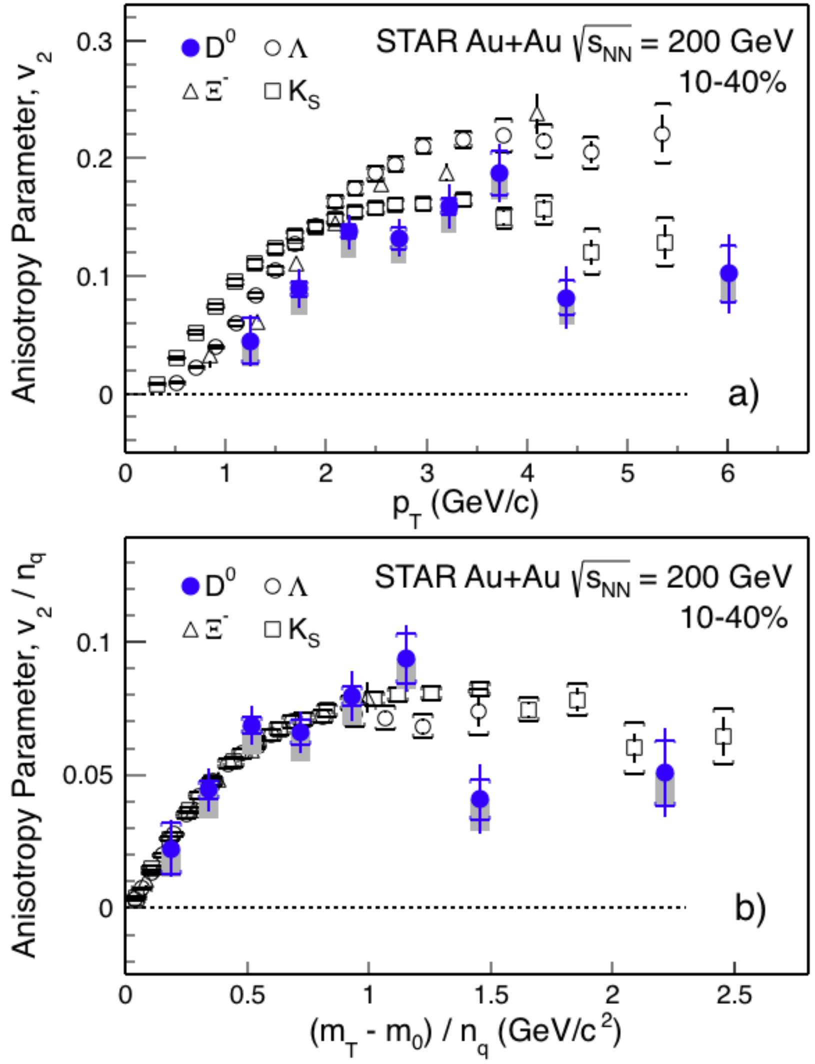

# Elliptic flow, NCQ-scaling

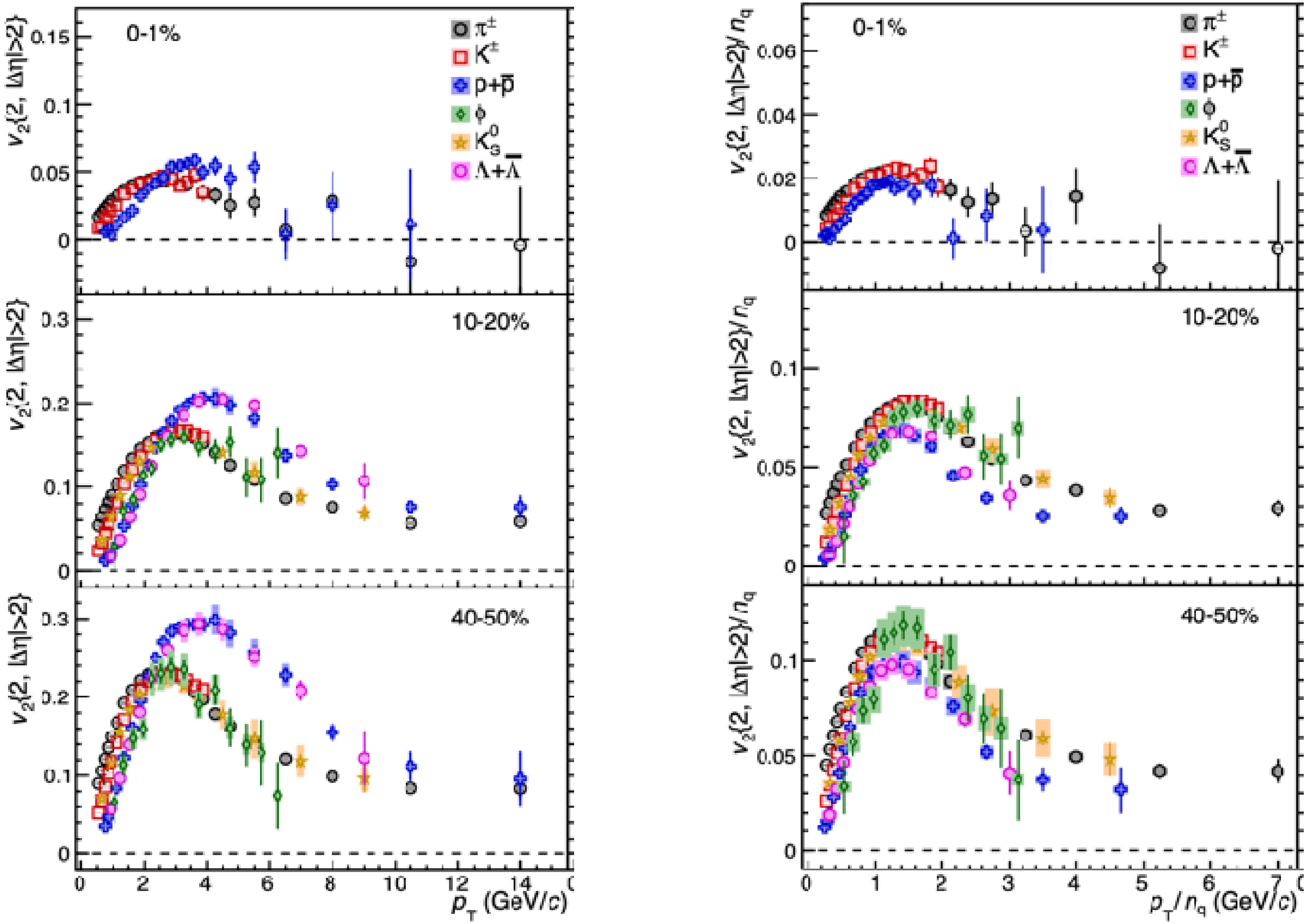


All data from RHIC and LHC are consistent with the interpretation that collective flow is established at the quark level and imprinted on the flow pattern of hadrons.

Valence quark scaling laws of flow observables are our most direct evidence that light quarks are unconfined in the QGP

# Directed and elliptic flow

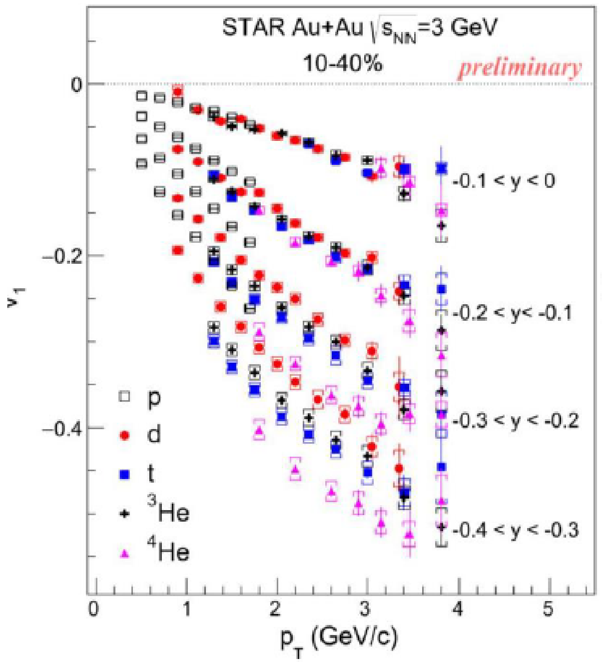


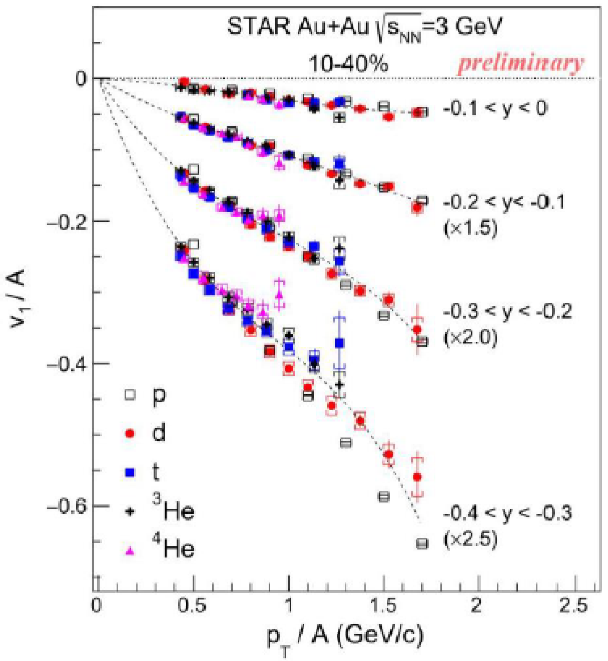


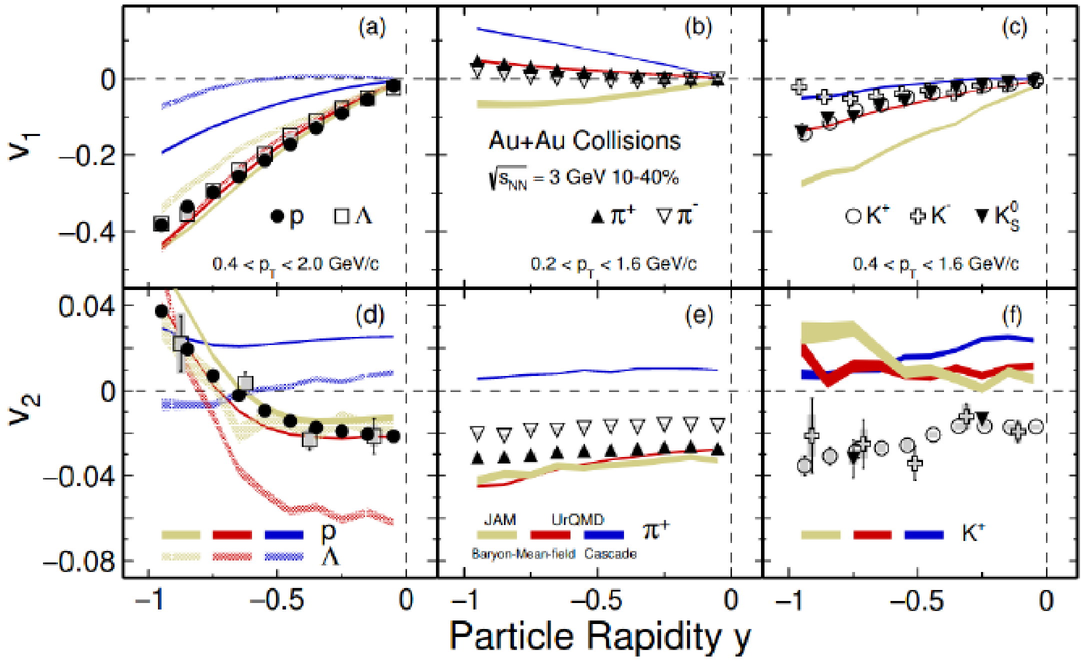


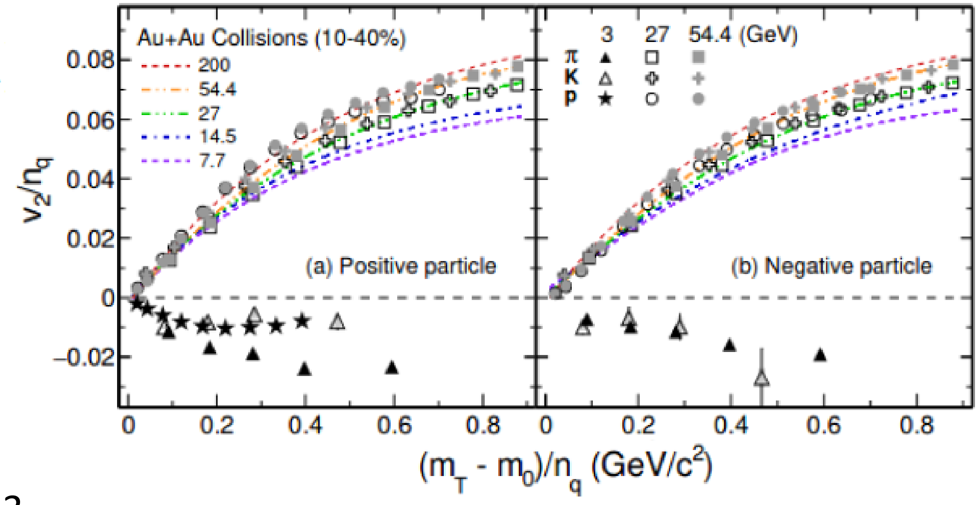


- Light nucleus $v_1(p_T)$ follows atomic-mass-number (A scaling at different rapidity bins
- Particles and antiparticles are no longer consistent with the single-particle NCQ scaling due to the mixture of the transported and produced quarks

# Search for the first order phase transition

- Softening of the EoS
  - Could be observed in the $dv_1/dy$ slope
  - Strong softening: consistent with the $1^{st}$-order phase transition
  - Weaker softening: likely due to crossover

$$E\frac{d^3N}{d^3p}=\frac{1}{2\pi}\frac{d^2N}{p_t dp_t dy}\left(1+\sum_{n=1}^{\infty}2v_n\cos[n(\phi-\Psi_r)]\right) \qquad v_1=\langle p_x/p_t\rangle$$

$\phi$ is the azimuthal angle of a produced particle

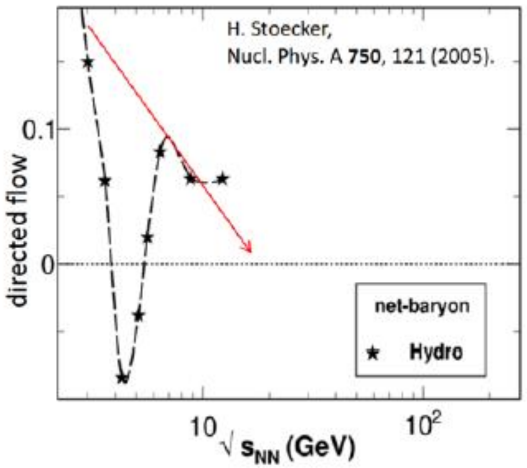


STAR. PRL 120, 062301(2018)

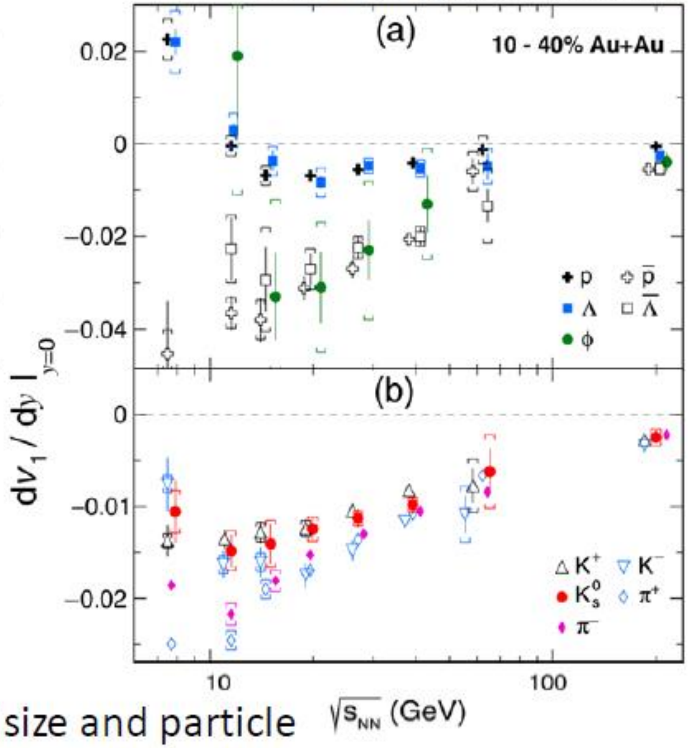


- Time delays of the particle emission
  - Could be observed using femtoscopy technique (via $R_{out}/R_{side}$ or $R_{out}^2$-$R_{side}^2$)

D.H. Rischke, M. Gyulassy. NPA 608 (1996) 479

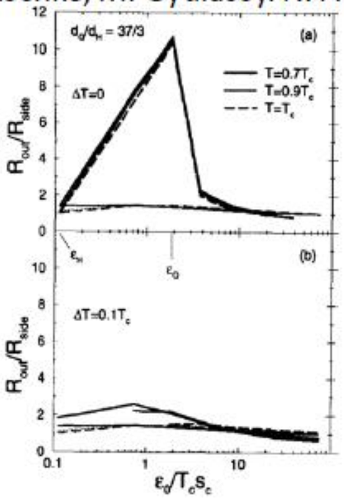


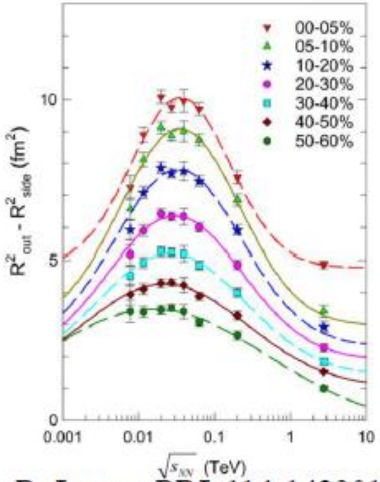


R. Lacey. PRL 114 142301(2015)

$R_{side}$ – geometrical size

$R_{out}$ – sensitive to geometrical size and particle emission duration

$R_{long}$ – sensitive to the time of maximum emission

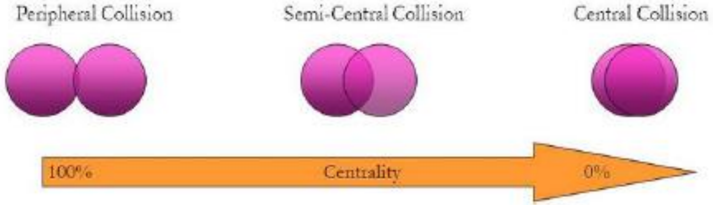

# HBT and femtoscopy

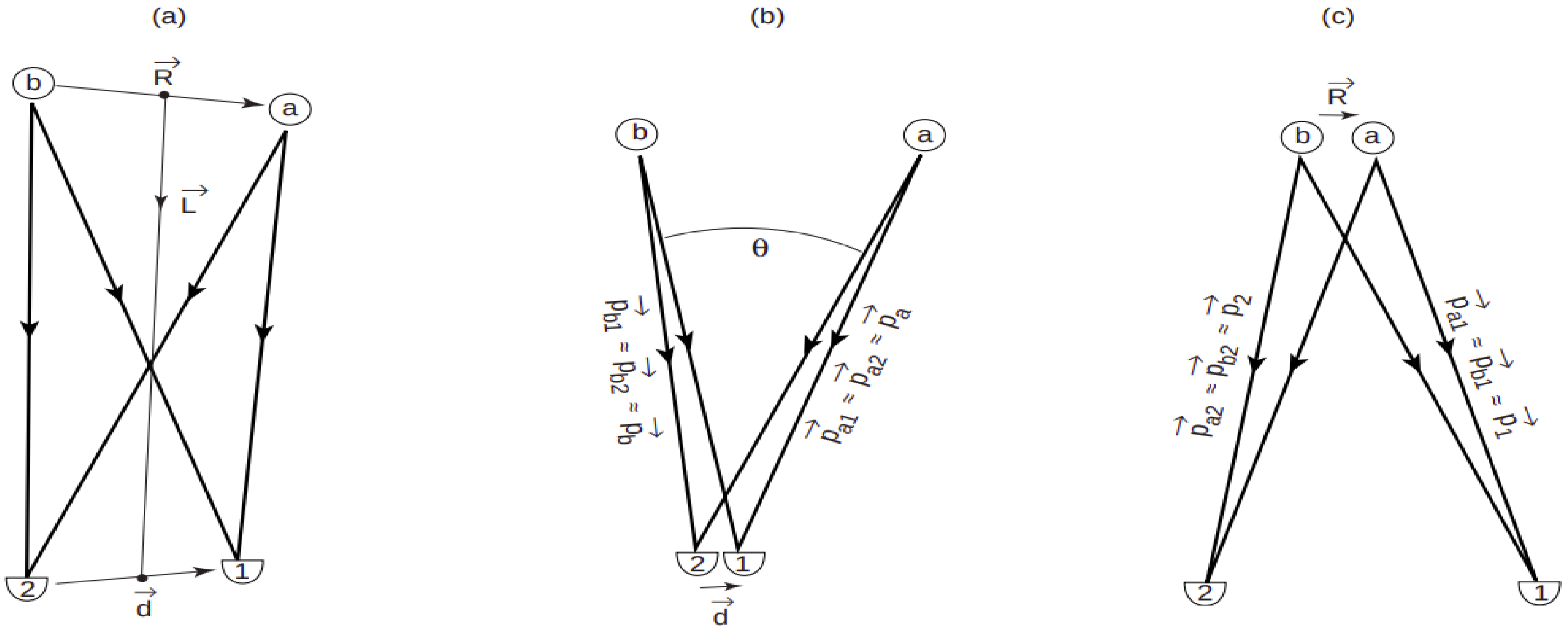


1,2 — detectors; a,b — sources
(a) — general idea
(b) — astronomy R>>d
(c) — nuclear physics R<<d

Similar to the astrophysics, HBT correlations

*Sov.J.Nucl.Phys.* 35 (1982) 770
*Phys.Lett.B* 373 (1996) 30-34

# Correlation function effects

$$C(\vec{k}^*) = \int S(\vec{r}^*)\,|\psi(\vec{k}^*, \vec{r}^*)|^2\, d^3r^*$$

➡ Relative wave function sensitive to interaction potential

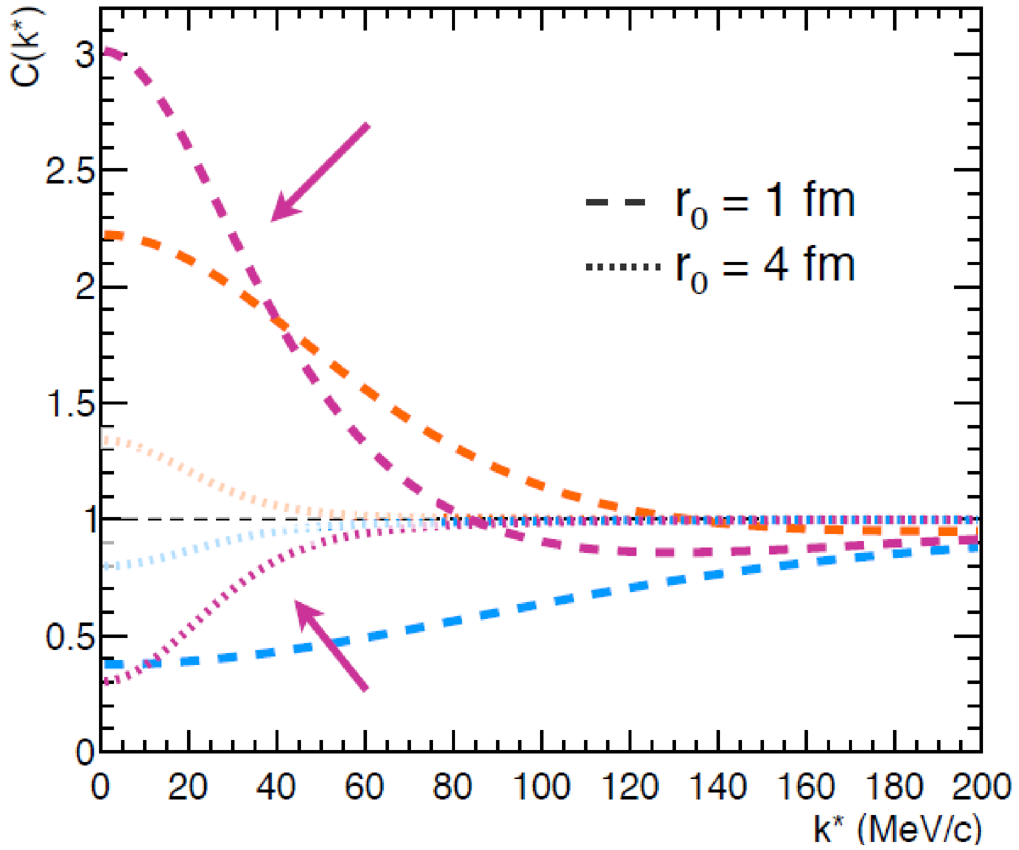


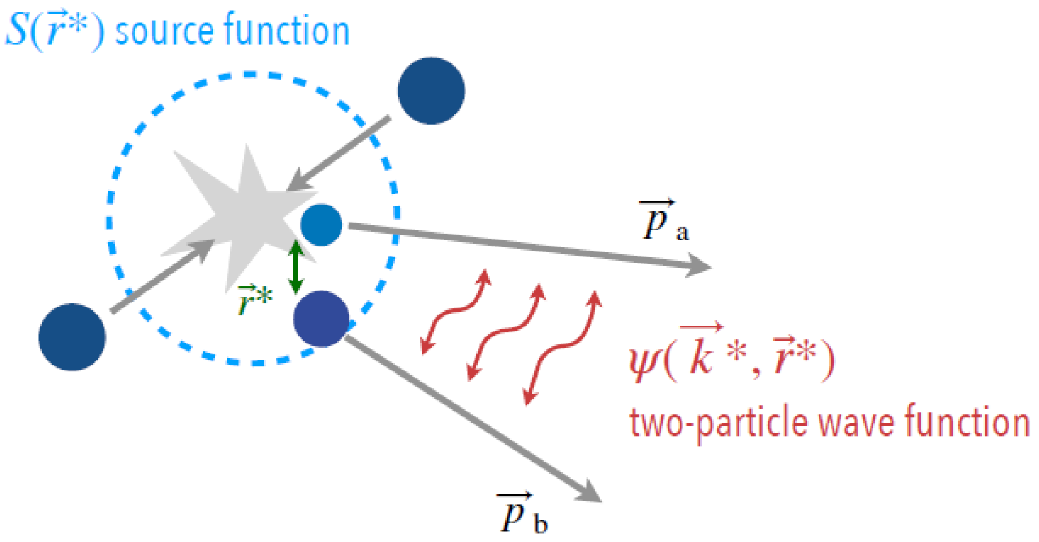


➡ Absence of interaction $C(k^*) = 1$

➡ Attractive potential $C(k^*) > 1$

➡ Repulsive potential $C(k^*) < 1$

➡ Bound-state formation $C(k^*) <> 1$

# Two particle correlation analysis

General case

$$C(p_1,p_2)=\frac{P_2(p_1,p_2)}{P_1(p_1)P_1(p_2)}$$

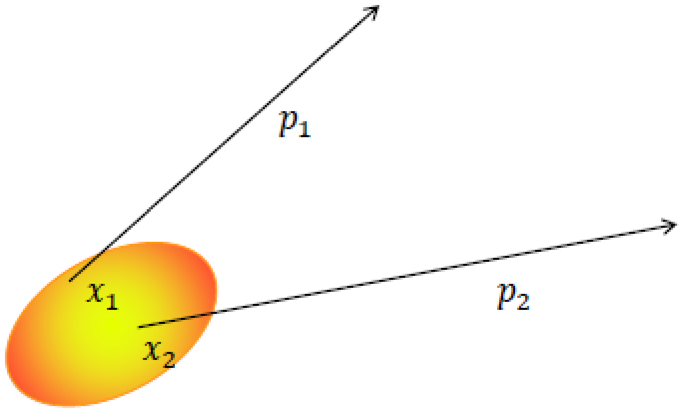


$$P_1(p)=E\frac{dN}{d^3p}=\int d^4xS(x,p)$$

S – is the source parameter

$$P_2(p_1,p_2)=E_1E_2\frac{dN}{d^3p_1d^3p_2}$$

for non-point source

$$C(\boldsymbol{p}_1-\boldsymbol{p}_2)-1\sim\int d^3R\,\rho(\boldsymbol{R})\,\cos(\boldsymbol{R}\cdot(\boldsymbol{p}_1-\boldsymbol{p}_2))$$

For the assumption of Gaussian shaped emittance source the correlation function C(q,K)

$$C(q,K)=1\pm\exp\left[-R_s^2q_s^2-R_o^2q_o^2-R_l^2q_l^2-2R_{ol}^2q_oq_l\right]$$

$$R_s^2=\langle\tilde{x}_s^2\rangle\,,\qquad R_o^2=\langle(\tilde{x}_o-\beta_\perp\tilde{t})^2\rangle\,,$$
$$R_l^2=\langle(\tilde{x}_l-\beta_l\tilde{t})^2\rangle\,,\qquad R_{ol}^2=\langle(\tilde{x}_o-\beta_\perp\tilde{t})(\tilde{x}_l-\beta_l\tilde{t})\rangle$$

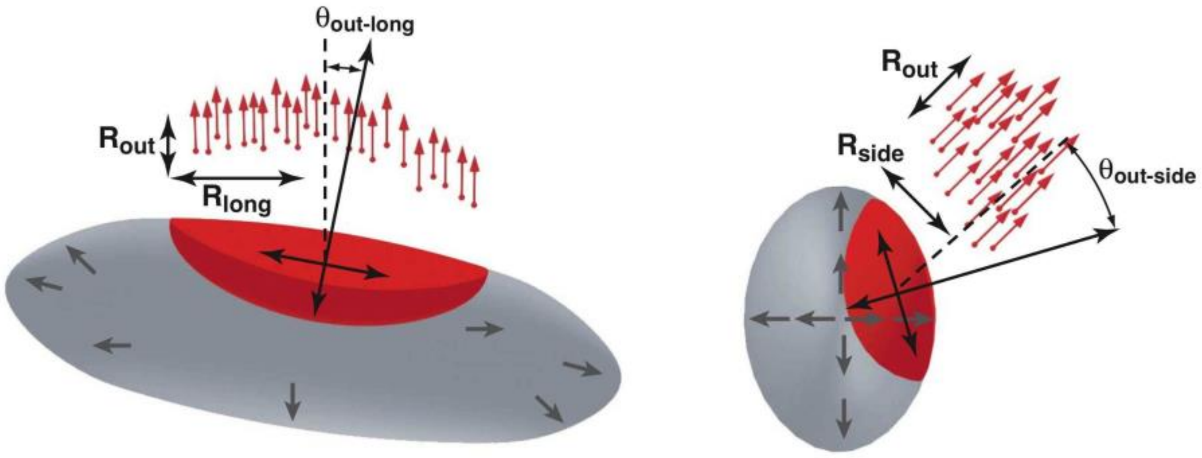

# Femtoscopy results at low energies

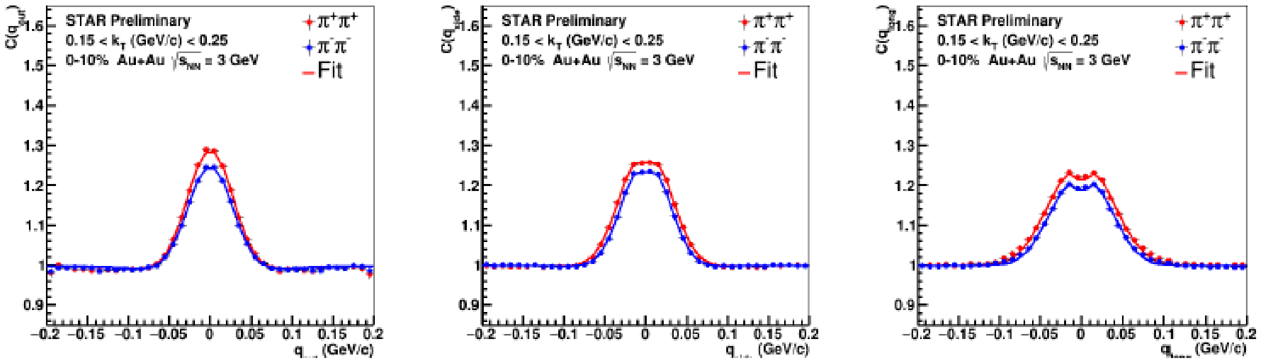


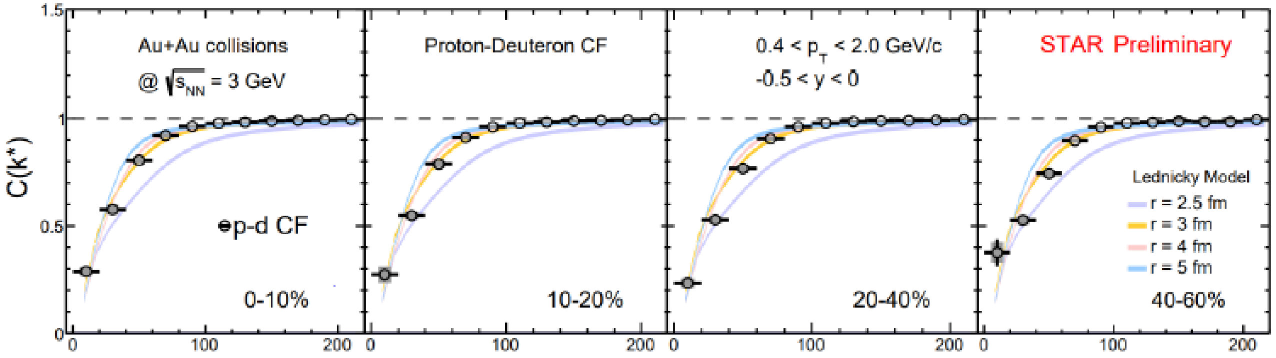


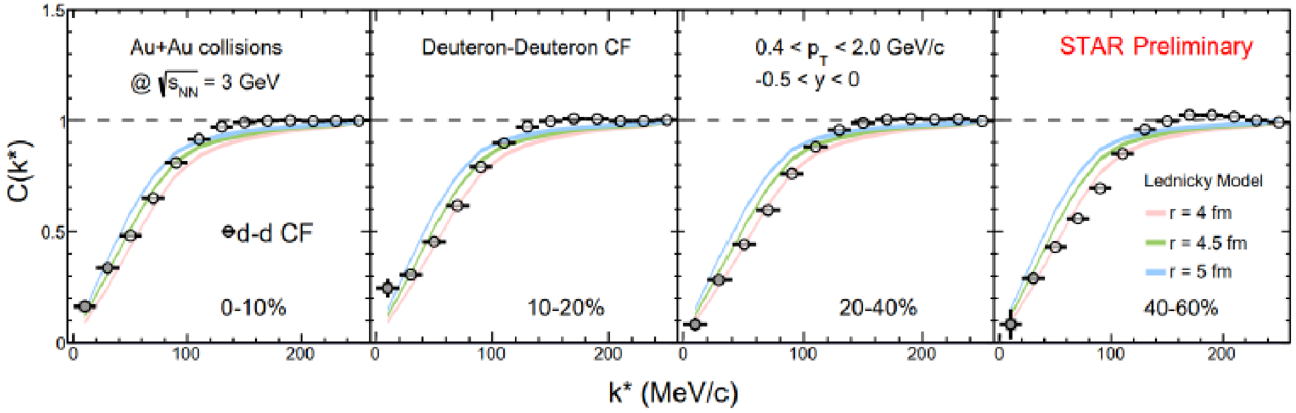


- Many interesting results from low-energy nuclear collisions: $\pi\pi$, pp, pd, dd, and others
- Provide information about particle interactions
- The source shape evolves from oblate to prolate, as energy increases

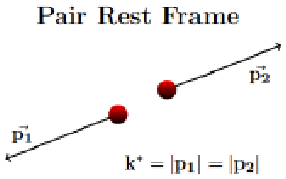


STAR. PRC 103, 034908(2021)

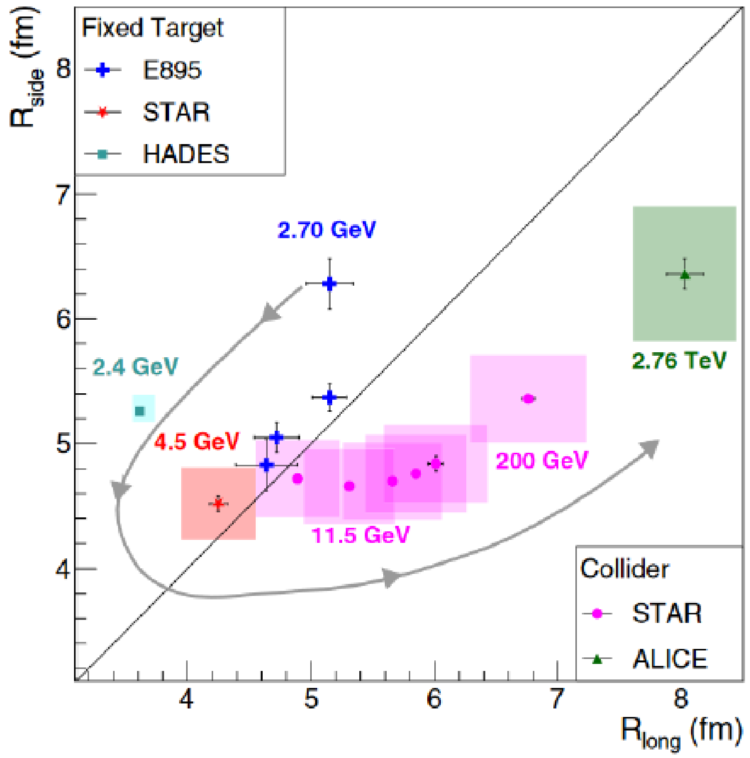

# The most vortical fluid

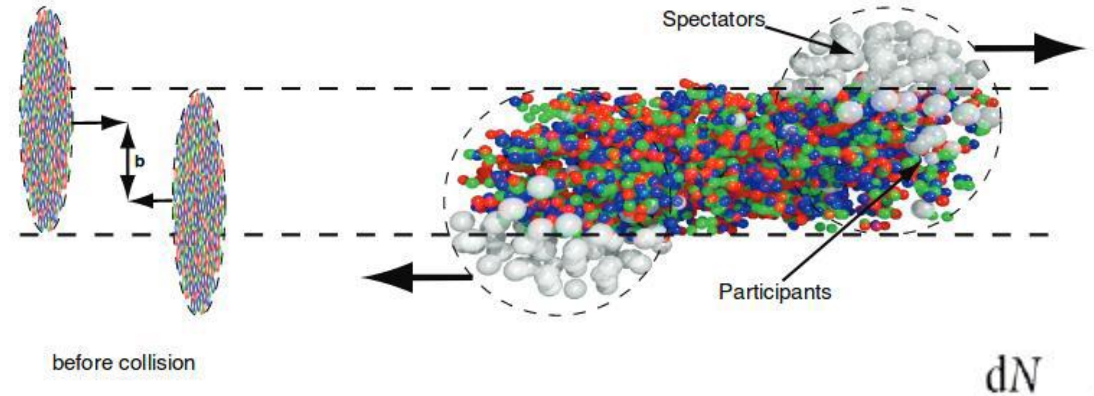


$$\frac{dN}{d\cos\theta^*} = \frac{1}{2}\left(1 + \alpha_H |\mathcal{P}_H| \cos\theta^*\right)$$

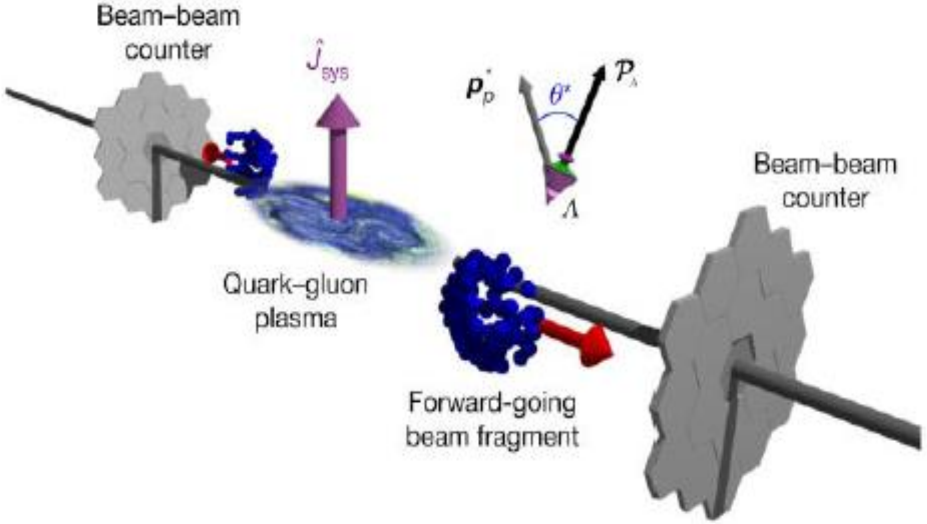



The most vortical fluid

$$\omega = k_B T(\overline{P}_{\Lambda} + \overline{P}_{\overline{\Lambda}})/\hbar = 10^{22} s^{-1}$$

STAR, Nature, 2017, 1701.06657
Phys. Rev. C 98 (2018) 014910

# Global polarization of particles

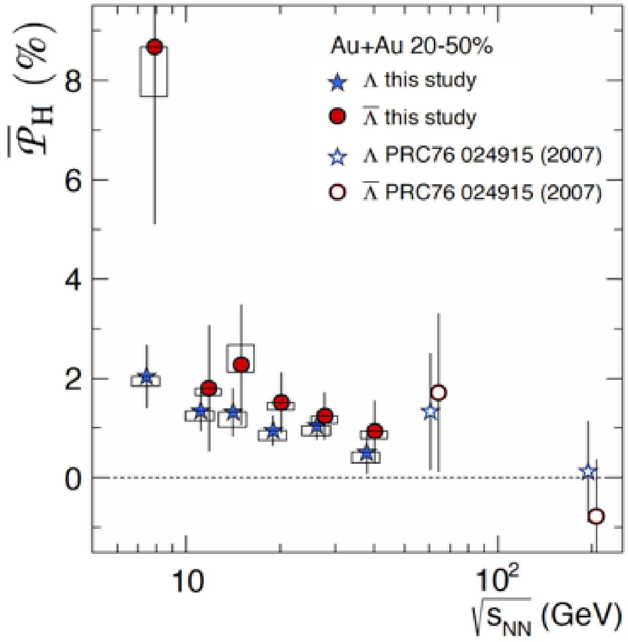


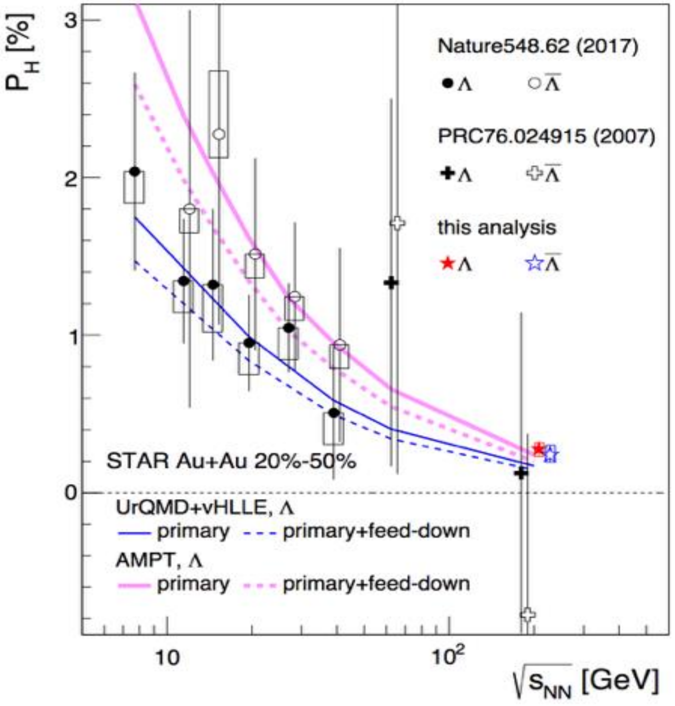


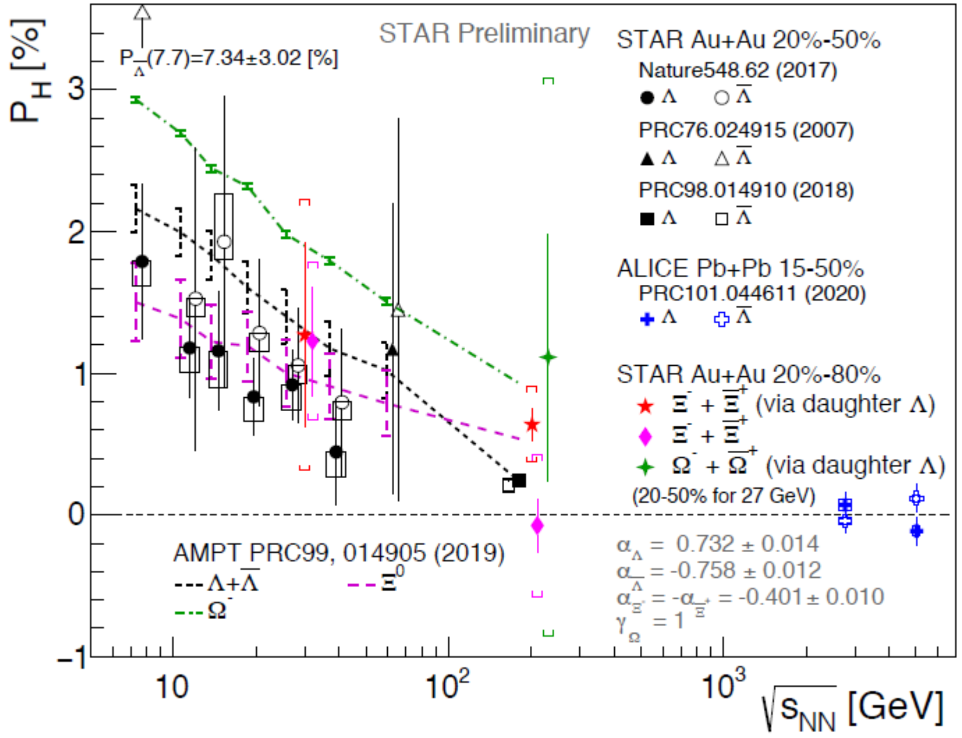


* published results are rescaled by $\alpha_{old}/\alpha_{new}$~0.87

Becattini, Karpenko, Lisa, Upsal, and Voloshin, PRC95.054902 (2017)

$$P_\Lambda \simeq \frac{1}{2}\frac{\omega}{T} + \frac{\mu_\Lambda B}{T}$$

$$P_{\bar{\Lambda}} \simeq \frac{1}{2}\frac{\omega}{T} - \frac{\mu_\Lambda B}{T}$$

$\mu_\Lambda$: Λ magnetic moment
T: temperature at thermal equilibrium

$$\omega = (P_\Lambda + P_{\bar{\Lambda}})k_B T/\hbar$$
$$\sim 0.02\text{-}0.09\ \text{fm}^{-1}$$
$$\sim 0.6\text{-}2.7 \times 10^{22}\text{s}^{-1}$$

(T=160 MeV)

Thank you!

&

Ready for questions

# QGP – was it really discovered?

The press conference at BNL on 24 April 2005



Evidence for a **new type of nuclear matter**:

At the Relativistic Heavy Ion Collider (RHIC) at Brookhaven National Lab (BNL), two beams of gold atoms are smashed together, the goal being to recreate the conditions thought to have prevailed in the universe only a few microseconds after the big bang, so that novel forms of nuclear matter can be studied. At this press conference, RHIC scientists will sum up all they have learned from several years of observing the world's most energetic collisions of atomic nuclei. The four experimental groups operating at RHIC will present a consolidated, surprising, exciting new interpretation of their data…

# QGP – was it really discovered?

At the RHIC Users' Meeting June 9-12, 2015 a 10 year anniversary session “The Perfect Liquid at RHIC: 10 Years of Discovery" was held, the press release of June 26, 2015 says:

*“RHIC lets us look back at matter as it existed throughout our universe at the dawn of time, before QGP cooled and formed matter as we know it,”* said Berndt Mueller, Brookhaven's Associate Laboratory Director for Nuclear and Particle Physics. “*The discovery of the perfect liquid was a turning point in physics, and now, 10 years later, RHIC has revealed a wealth of information about this remarkable substance, which we now know to be a QGP, and is more capable than ever of measuring its most subtle and fundamental properties.”*

# QGP – was it really discovered?

CERN special seminar 10 February 2000

At the seminar spokespersons from the experiments on CERN's Heavy Ion programm presented compelling evidence for the existence of a new state of matter in which quarks, instead of being bound up into more complex particles such as protons and neutrons, are liberated to roam freely.

Professor Luciano Maiani, CERN Director General, said:
*"The combined data coming from the seven experiments on CERN's Heavy Ion program have given a clear picture of a new state of matter. This result verifies an important prediction of the present theory of fundamental forces between quarks. It is also an important step forward in the understanding of the early evolution of the universe. We now have evidence of a new state of matter where quarks and gluons are not confined. There is still an entirely new territory to be explored concerning the physical properties of quark-gluon matter. The challenge now passes to the Relativistic Heavy Ion Collider at the Brookhaven National Laboratory and later to CERN's Large Hadron Collider."*

In an interview in January 2017 with Luciano Maiani, Director General of CERN from 1999 to 2003 we read:

Luciano Maiani: *I think that the announcement was quite clear. I have the text of it with me, it reads: "The data provide evidence for color deconfinement in the early collision stage and for a collective explosion of the collision fireball in its late stages. The new state of matter exhibits many of the characteristic features of the theoretically predicted Quark-Gluon Plasma." The key word is "evidence", not discovery, and the evidence was there, indeed*

# QGP – was it really discovered?

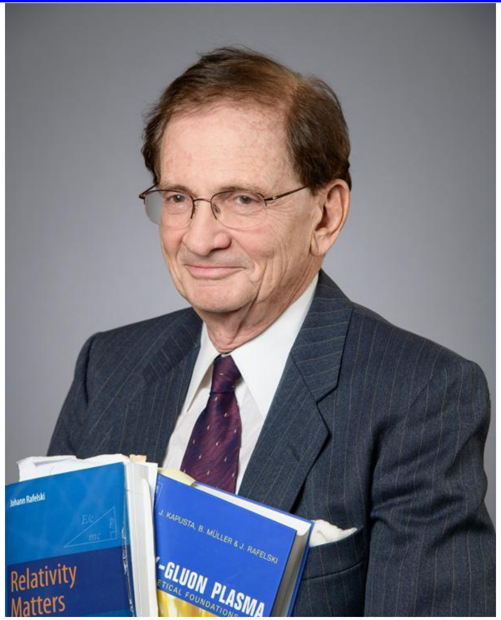


In the book "**Quark-Gluon Plasma: Theoretical Foundations An Annotated Reprint Collection**" prepared in 2002 by Berndt Muller, Joseph Kapusta and Johann Rafelski.

This book introduces the theoretical roots of QGP with a time cut off in 1992. The rationale of the authors was to look more than 10 years back in 2002/3, since in 1992 QGP was already discovered but recognized only by a small subset of researchers.

**Looking back at the Universe the Size of a Melon**

*Already in the mid-90s there was some indication for quark-gluon plasma in heavy ion experiments at CERN and at Brookhaven National Laboratory. However, I was at that time due to fragmentary data very cautious. In hindsight I know my position was too cautious…*

*Actually, I hoped that this procedure would switch off the quark-gluon plasma in a controlled manner, but this attempt failed. Also at SPS energies there are in the now much more extensive data records unmistakable signatures.*

# How do we see the ion collisions

https://online.star.bnl.gov/aggregator/livedisplay/

Au+Au @ STAR 200 GeV

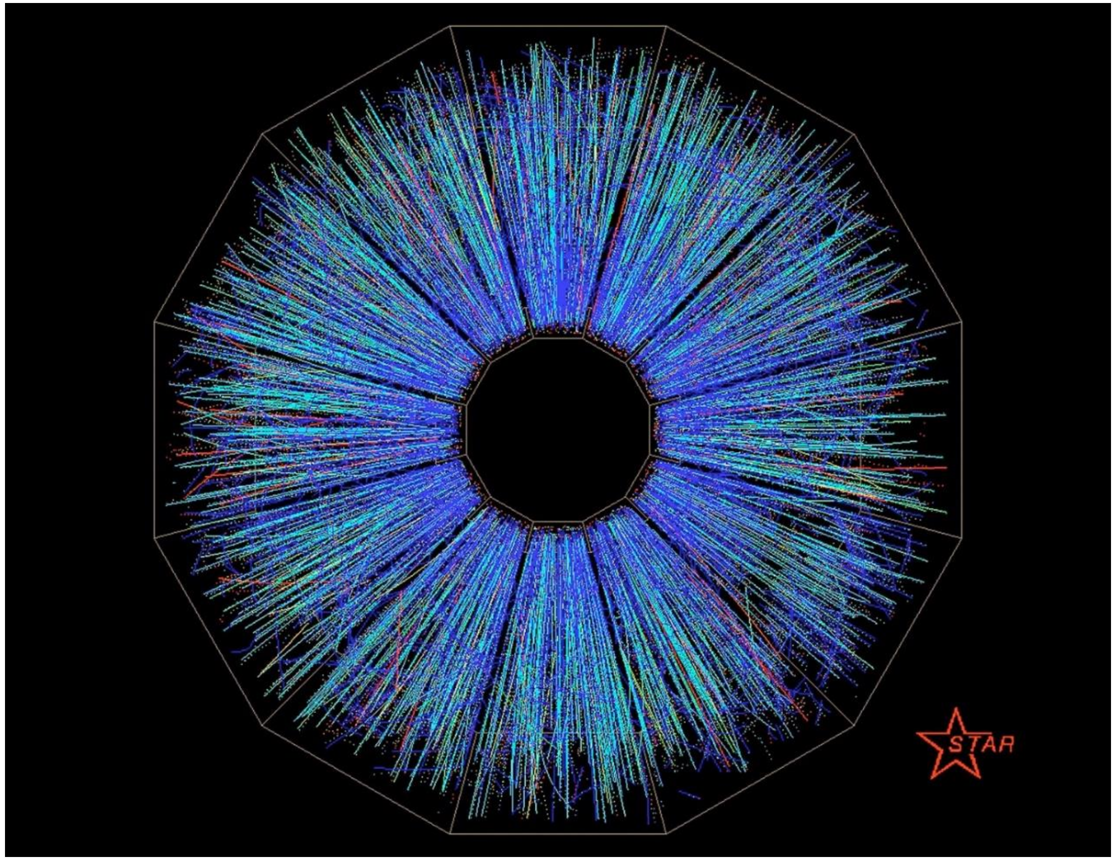


Pb+Pb @ ALICE 2,76 TeV

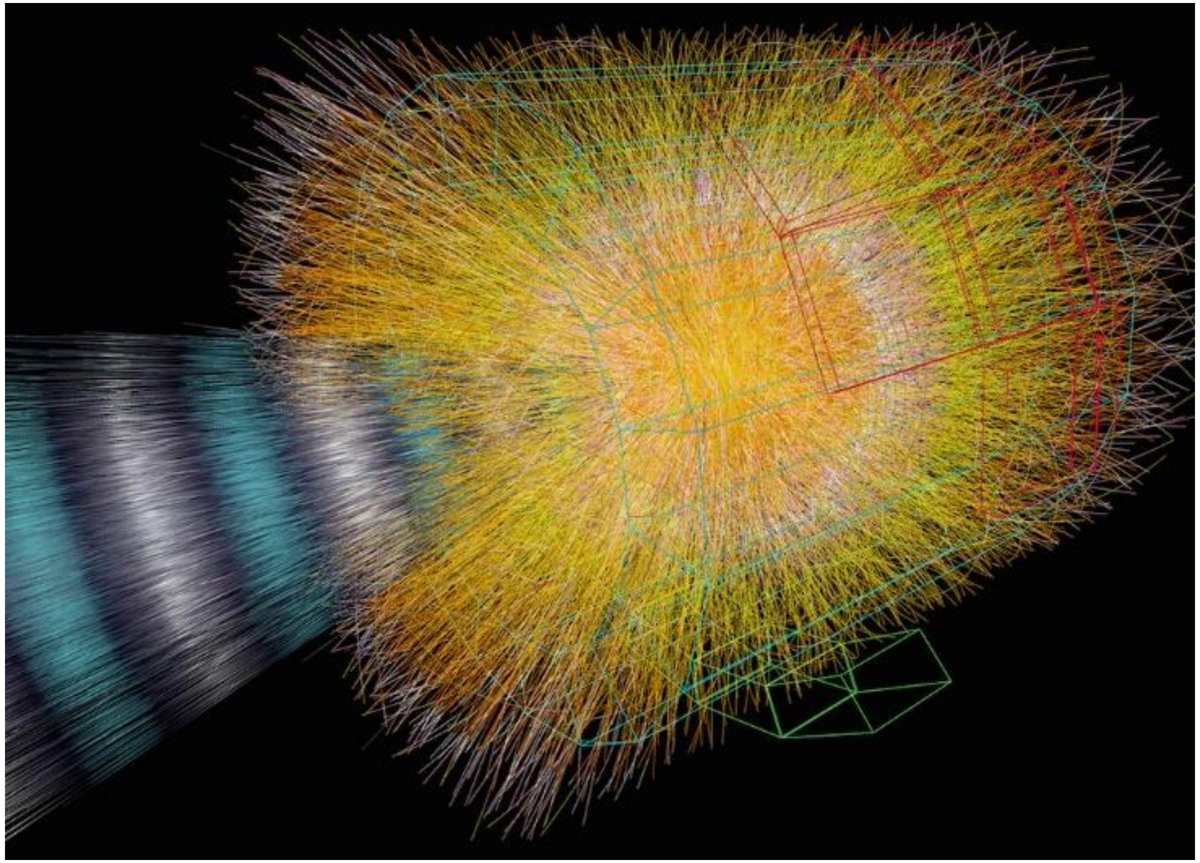

Heavy ion collisions provide a huge number of produced particles. We detect hundreds and thousands charged particles after each collision.
At 200 GeV ~ 1 000 charged particles are produced and at 2,76 GeV ~ 8 000 to 10k

# Kinematic coverage

**Snapshots where 0 < x < 1 is the shutter exposure time**

| **$x \approx 10^{-4}$** | **$x \approx 10^{-2}$** | **$x \approx 0.3$** |
|---|---|---|
| **Probe non-linear dynamics short exposure time** | **Probe rad. dominated medium exposure time** | **Probe valence quarks long exposure time** |

$Q^2$ is the Lorentz invariant four-momentum transfer and
$x = Q^2/(2m(E-E'))$

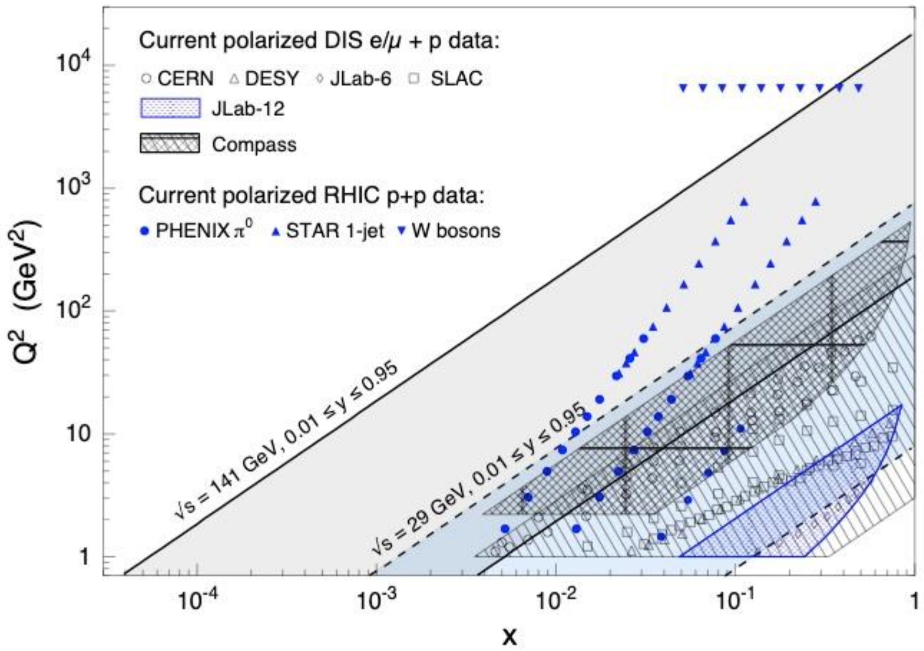


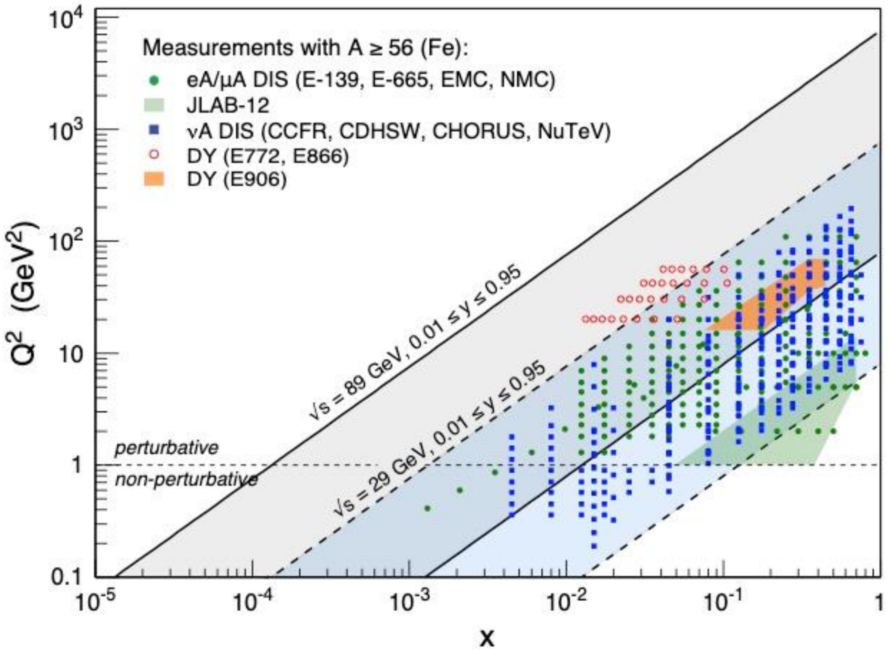


Alexey Aparin

# HIC experiments

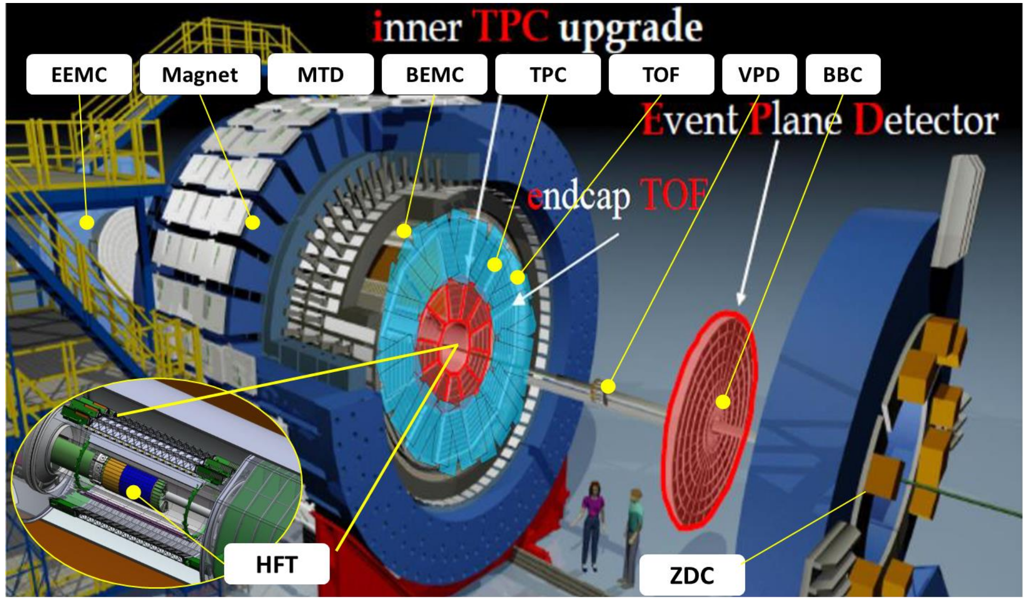


STAR

NA61

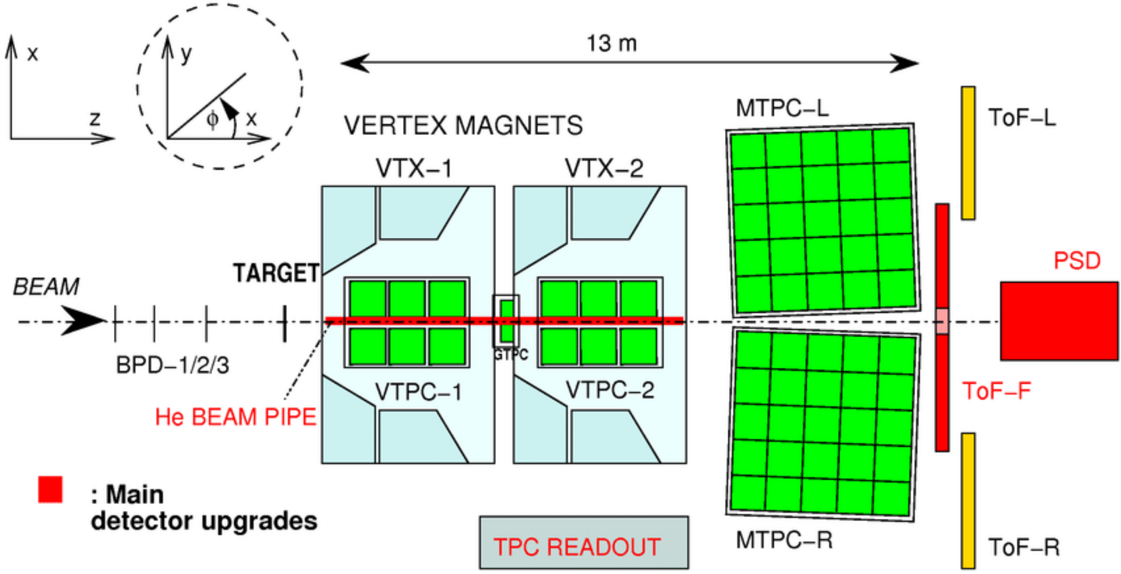


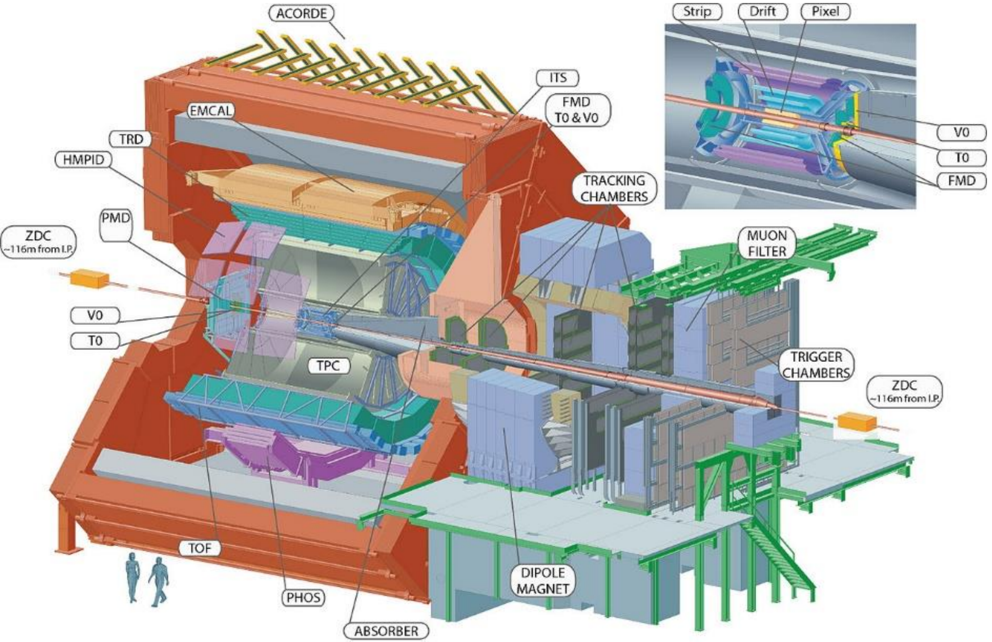


ALICE

CBM

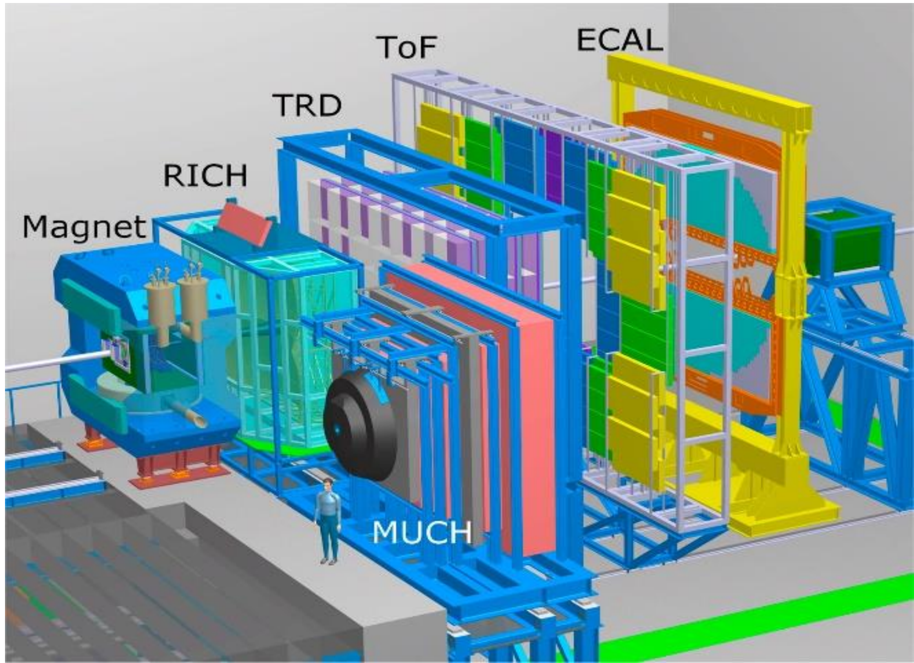

# MPD detector

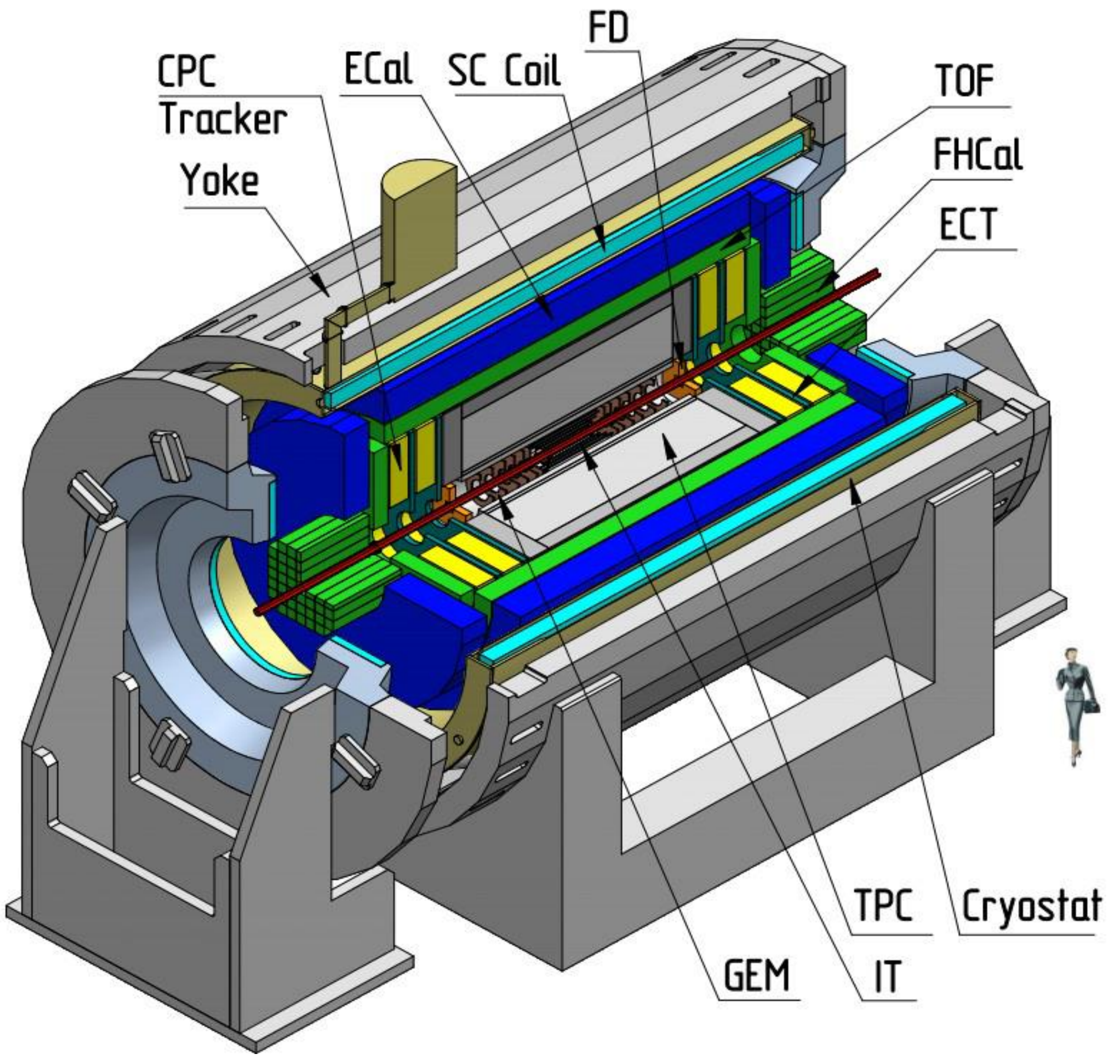


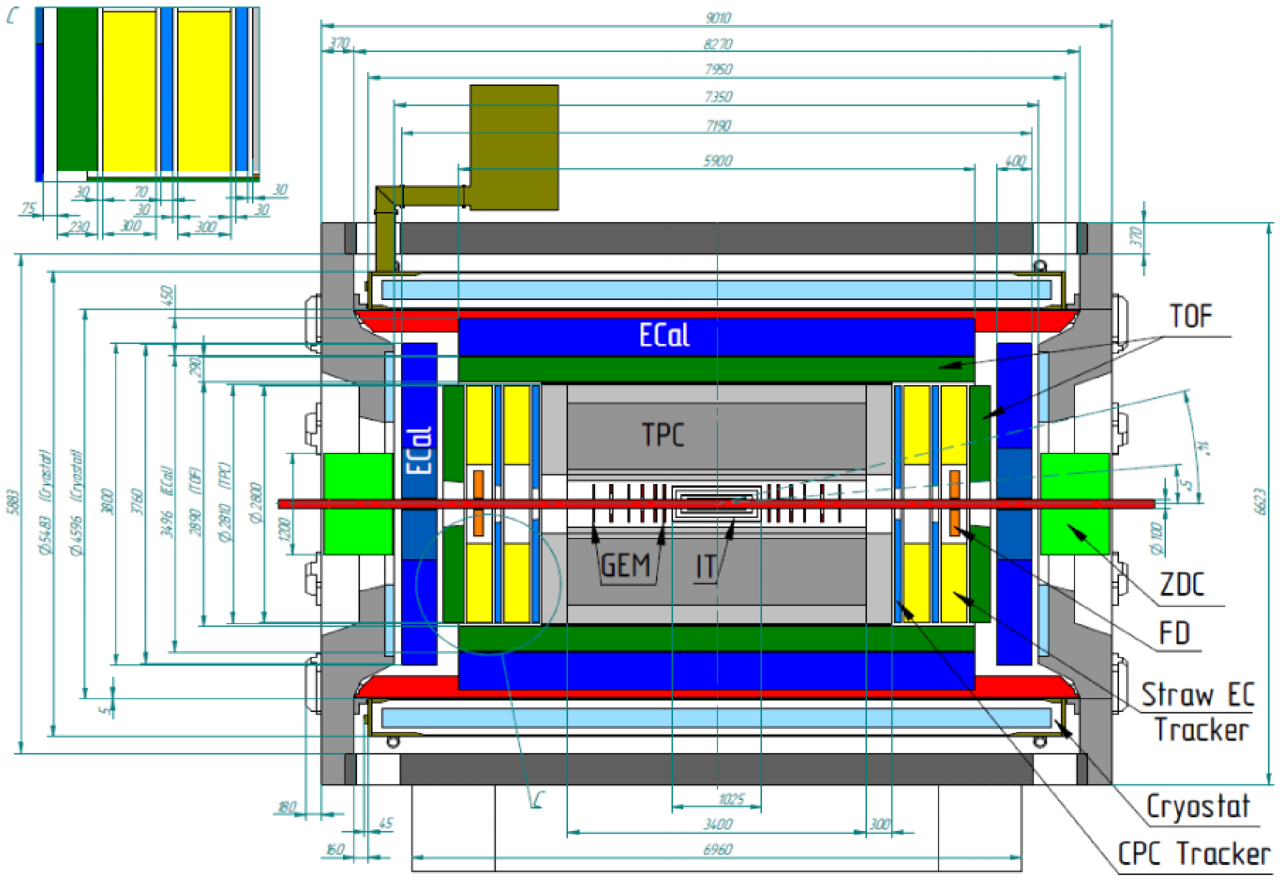

# Standard Model

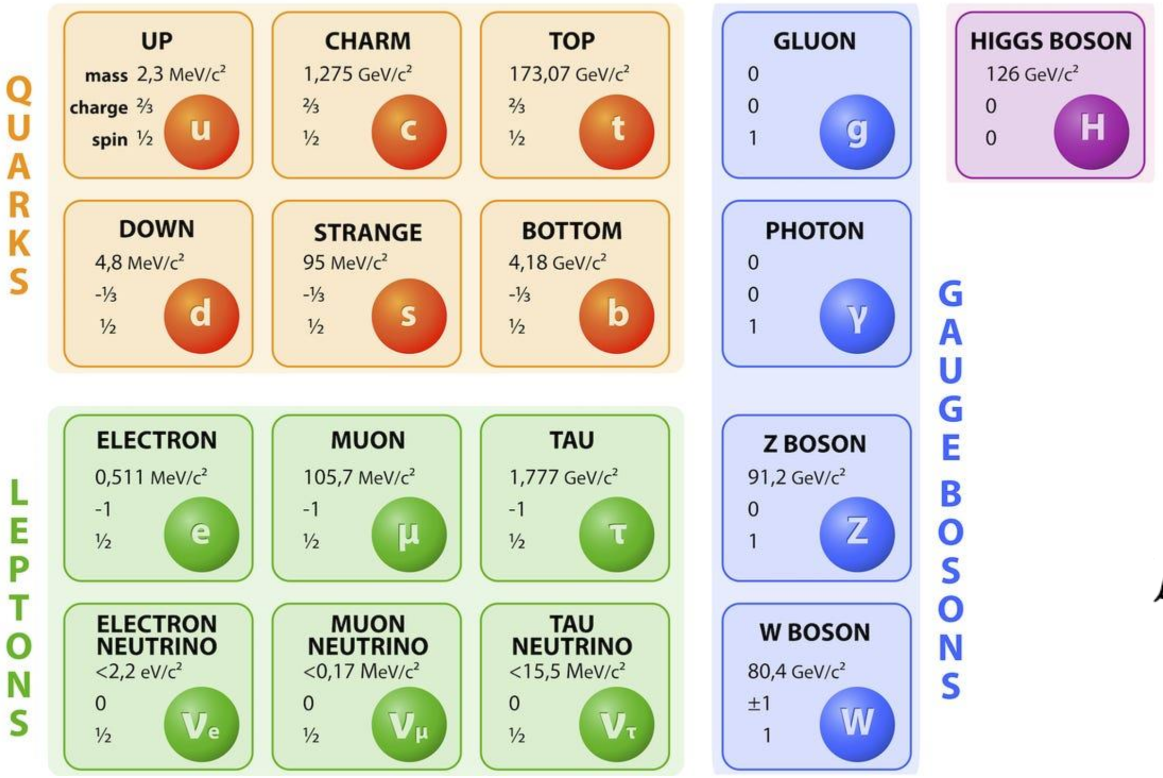


General theory of matter and fundamental interactions.

But what do we learn from it and what else is there unattended?

$$\mathcal{L} = -\frac{1}{4}F_{\mu\nu}F^{\mu\nu} + |D_\mu\phi|^2 - V(\phi) + i\bar{\psi}\hat{D}\psi + (\bar{\psi}_i Y_{ij}\psi_j\phi + \text{h.c.})$$

# Standard Model

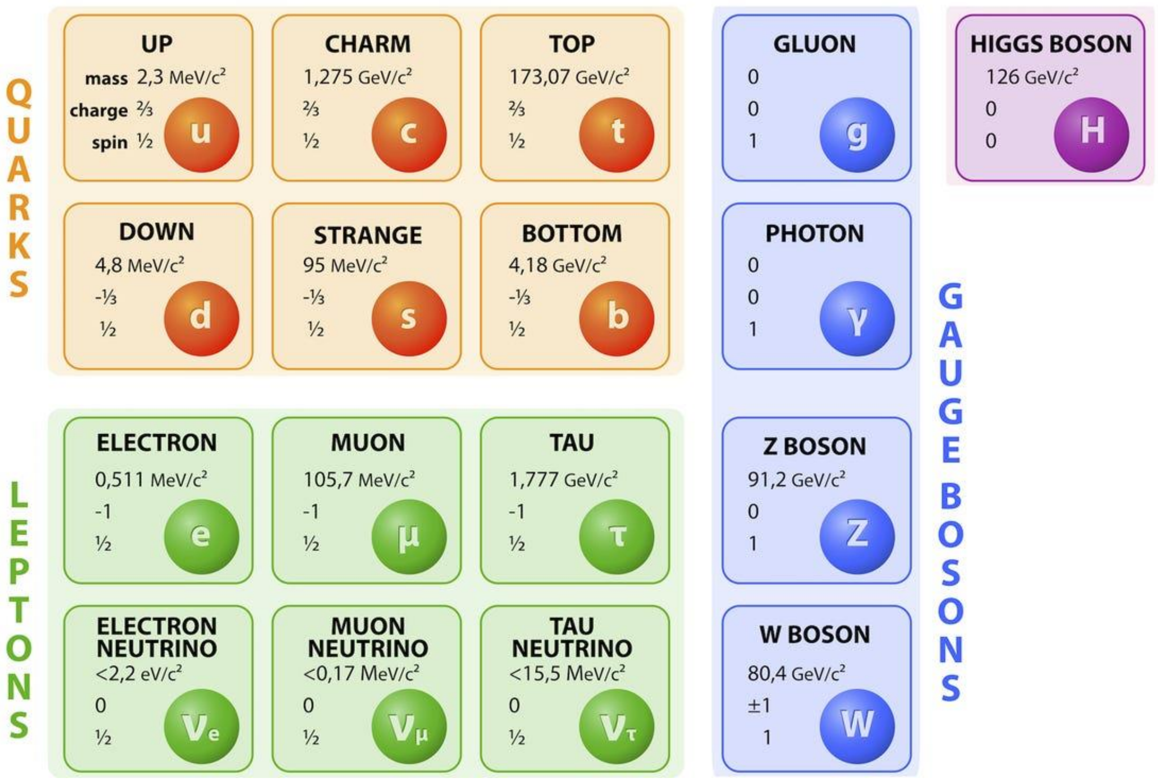


*

1

$$-\frac{1}{2}\partial_\nu g^a_\mu\partial_\nu g^a_\mu - g_s f^{abc}\partial_\mu g^a_\nu g^b_\mu g^c_\nu - \frac{1}{4}g_s^2 f^{abc}f^{ade}g^b_\mu g^c_\nu g^d_\mu g^e_\nu + \frac{1}{2}ig_s^2(\bar{q}^\sigma_i\gamma^\mu q^\sigma_j)g^a_\mu + \bar{G}^a\partial^2 G^a + g_s f^{abc}\partial_\mu\bar{G}^a G^b g^c_\mu$$

2

$$- \partial_\nu W^+_\mu\partial_\nu W^-_\mu - M^2 W^+_\mu W^-_\mu - \frac{1}{2}\partial_\nu Z^0_\mu\partial_\nu Z^0_\mu - \frac{1}{2c_w^2}M^2 Z^0_\mu Z^0_\mu - \frac{1}{2}\partial_\mu A_\nu\partial_\mu A_\nu - \frac{1}{2}\partial_\mu H\partial_\mu H - \frac{1}{2}m_h^2 H^2 - \partial_\mu\phi^+\partial_\mu\phi^- - M^2\phi^+\phi^- - \frac{1}{2}\partial_\mu\phi^0\partial_\mu\phi^0 - \frac{1}{2c_w^2}M\phi^0\phi^0 - \beta_h\left[\frac{2M^2}{g^2} + \frac{2M}{g}H + \frac{1}{2}(H^2+\phi^0\phi^0+2\phi^+\phi^-)\right] + \frac{2M^4}{g^2}\alpha_h - igc_w[\partial_\nu Z^0_\mu(W^+_\mu W^-_\nu - W^+_\nu W^-_\mu) - Z^0_\nu(W^+_\mu\partial_\nu W^-_\mu - W^-_\mu\partial_\nu W^+_\mu) + Z^0_\mu(W^+_\nu\partial_\nu W^-_\mu - W^-_\nu\partial_\nu W^+_\mu)] - igs_w[\partial_\nu A_\mu(W^+_\mu W^-_\nu - W^+_\nu W^-_\mu) - A_\nu(W^+_\mu\partial_\nu W^-_\mu - W^-_\mu\partial_\nu W^+_\mu) + A_\mu(W^+_\nu\partial_\nu W^-_\mu - W^-_\nu\partial_\nu W^+_\mu)] - \frac{1}{2}g^2 W^+_\mu W^-_\mu W^+_\nu W^-_\nu + \frac{1}{2}g^2 W^+_\mu W^-_\nu W^+_\mu W^-_\nu + g^2c_w^2(Z^0_\mu W^+_\mu Z^0_\nu W^-_\nu - Z^0_\mu Z^0_\mu W^+_\nu W^-_\nu) + g^2s_w^2(A_\mu W^+_\mu A_\nu W^-_\nu - A_\mu A_\mu W^+_\nu W^-_\nu) + g^2 s_w c_w[A_\mu Z^0_\nu(W^+_\mu W^-_\nu - W^+_\nu W^-_\mu) - 2A_\mu Z^0_\mu W^+_\nu W^-_\nu] - g\alpha[H^3 + H\phi^0\phi^0 + 2H\phi^+\phi^-] - \frac{1}{8}g^2\alpha_h[H^4 + (\phi^0)^4 + 4(\phi^+\phi^-)^2 + 4(\phi^0)^2\phi^+\phi^- + 4H^2\phi^+\phi^- + 2(\phi^0)^2H^2] - gMW^+_\mu W^-_\mu H - \frac{1}{2}g\frac{M}{c_w^2}Z^0_\mu Z^0_\mu H - \frac{1}{2}ig[W^+_\mu(\phi^0\partial_\mu\phi^- - \phi^-\partial_\mu\phi^0) - W^-_\mu(\phi^0\partial_\mu\phi^+ - \phi^+\partial_\mu\phi^0)] + \frac{1}{2}g[W^+_\mu(H\partial_\mu\phi^- - \phi^-\partial_\mu H) - W^-_\mu(H\partial_\mu\phi^+ - \phi^+\partial_\mu H)] + \frac{1}{2}g\frac{1}{c_w}(Z^0_\mu(H\partial_\mu\phi^0 - \phi^0\partial_\mu H) - ig\frac{s_w^2}{c_w}MZ^0_\mu(W^+_\mu\phi^- - W^-_\mu\phi^+) + igs_wMA_\mu(W^+_\mu\phi^- - W^-_\mu\phi^+) - ig\frac{1-2c_w^2}{2c_w}Z^0_\mu(\phi^+\partial_\mu\phi^- - \phi^-\partial_\mu\phi^+) + igs_wA_\mu(\phi^+\partial_\mu\phi^- - \phi^-\partial_\mu\phi^+) - \frac{1}{4}g^2W^+_\mu W^-_\mu[H^2 + (\phi^0)^2 + 2\phi^+\phi^-] - \frac{1}{4}g^2\frac{1}{c_w^2}Z^0_\mu Z^0_\mu[H^2 + (\phi^0)^2 + 2(2s_w^2-1)^2\phi^+\phi^-] - \frac{1}{2}g^2\frac{s_w^2}{c_w}Z^0_\mu\phi^0(W^+_\mu\phi^- + W^-_\mu\phi^+) - \frac{1}{2}ig^2\frac{s_w^2}{c_w}Z^0_\mu H(W^+_\mu\phi^- - W^-_\mu\phi^+) + \frac{1}{2}g^2s_wA_\mu\phi^0(W^+_\mu\phi^- + W^-_\mu\phi^+) + \frac{1}{2}ig^2s_wA_\mu H(W^+_\mu\phi^- - W^-_\mu\phi^+) - g^2\frac{s_w}{c_w}(2c_w^2-1)Z^0_\mu A_\mu\phi^+\phi^- - g^1s_w^2A_\mu A_\mu\phi^+\phi^-$$

3

$$- \bar{e}^\lambda(\gamma\partial + m_e^\lambda)e^\lambda - \bar{\nu}^\lambda\gamma\partial\nu^\lambda - \bar{u}^\lambda_j(\gamma\partial + m_u^\lambda)u^\lambda_j - \bar{d}^\lambda_j(\gamma\partial + m_d^\lambda)d^\lambda_j + igs_wA_\mu\left[-(\bar{e}^\lambda\gamma^\mu e^\lambda) + \frac{2}{3}(\bar{u}^\lambda_j\gamma^\mu u^\lambda_j) - \frac{1}{3}(\bar{d}^\lambda_j\gamma^\mu d^\lambda_j)\right] + \frac{ig}{4c_w}Z^0_\mu\left[(\bar{\nu}^\lambda\gamma^\mu(1+\gamma^5)\nu^\lambda) + (\bar{e}^\lambda\gamma^\mu(4s_w^2 - 1 - \gamma^5)e^\lambda) + (\bar{u}^\lambda_j\gamma^\mu(\frac{4}{3}s_w^2 - 1 - \gamma^5)u^\lambda_j) + (\bar{d}^\lambda_j\gamma^\mu(1 - \frac{8}{3}s_w^2 - \gamma^5)d^\lambda_j)\right] + \frac{ig}{2\sqrt{2}}W^+_\mu\left[(\bar{\nu}^\lambda\gamma^\mu(1+\gamma^5)e^\lambda) + (\bar{u}^\lambda_j\gamma^\mu(1+\gamma^5)C_{\lambda\kappa}d^\kappa_j)\right] + \frac{ig}{2\sqrt{2}}W^-_\mu\left[(\bar{e}^\lambda\gamma^\mu(1+\gamma^5)\nu^\lambda) + (\bar{d}^\kappa_jC^\dagger_{\lambda\kappa}\gamma^\mu(1+\gamma^5)u^\lambda_j)\right]$$

4

$$+ \frac{ig}{2\sqrt{2}}\frac{m_e^\lambda}{M}\left[-\phi^+(\bar{\nu}^\lambda(1-\gamma^5)e^\lambda) + \phi^-(\bar{e}^\lambda(1+\gamma^5)\nu^\lambda)\right] - \frac{g}{2}\frac{m_e^\lambda}{M}\left[H(\bar{e}^\lambda e^\lambda) + i\phi^0(\bar{e}^\lambda\gamma^5e^\lambda)\right] + \frac{ig}{2M\sqrt{2}}\phi^+\left[-m_d^\kappa(\bar{u}^\lambda_jC_{\lambda\kappa}(1-\gamma^5)d^\kappa_j) + m_u^\lambda(\bar{u}^\lambda_jC_{\lambda\kappa}(1+\gamma^5)d^\kappa_j\right] + \frac{ig}{2M\sqrt{2}}\phi^-\left[m_d^\lambda(\bar{d}^\lambda_jC^\dagger_{\lambda\kappa}(1+\gamma^5)u^\kappa_j) - m_u^\kappa(\bar{d}^\lambda_jC^\dagger_{\lambda\kappa}(1-\gamma^5)u^\kappa_j\right] - \frac{g}{2}\frac{m_u^\lambda}{M}H(\bar{u}^\lambda_ju^\lambda_j) - \frac{g}{2}\frac{m_d^\lambda}{M}H(\bar{d}^\lambda_jd^\lambda_j) + \frac{ig}{2}\frac{m_u^\lambda}{M}\phi^0(\bar{u}^\lambda_j\gamma^5u^\lambda_j) - \frac{ig}{2}\frac{m_d^\lambda}{M}\phi^0(\bar{d}^\lambda_j\gamma^5d^\lambda_j)$$

5

$$+ \bar{X}^+(\partial^2 - M^2)X^+ + \bar{X}^-(\partial^2 - M^2)X^- + \bar{X}^0(\partial^2 - \frac{M^2}{c_w^2})X^0 + \bar{Y}\partial^2Y + igc_wW^+_\mu(\partial_\mu\bar{X}^0X^- - \partial_\mu\bar{X}^+X^0) + igs_wW^+_\mu(\partial_\mu\bar{Y}X^- - \partial_\mu\bar{X}^+Y) + igc_wW^-_\mu(\partial_\mu\bar{X}^-X^0 - \partial_\mu\bar{X}^0X^+) + igs_wW^-_\mu(\partial_\mu\bar{X}^-Y - \partial_\mu\bar{Y}X^+) + igc_wZ^0_\mu(\partial_\mu\bar{X}^+X^+ - \partial_\mu\bar{X}^-X^-) + igs_wA_\mu(\partial_\mu\bar{X}^+X^+ - \partial_\mu\bar{X}^-X^-) - \frac{1}{2}gM\left[\bar{X}^+X^+H + \bar{X}^-X^-H + \frac{1}{c_w^2}\bar{X}^0X^0H\right] + \frac{1-2c_w^2}{2c_w}igM\left[\bar{X}^+X^0\phi^+ - \bar{X}^-X^0\phi^-\right] + \frac{1}{2c_w}igM\left[\bar{X}^0X^-\phi^+ - \bar{X}^0X^+\phi^-\right] + igMs_w\left[\bar{X}^0X^-\phi^+ - \bar{X}^0X^+\phi^-\right] + \frac{1}{2}igM\left[\bar{X}^+X^+\phi^0 - \bar{X}^-X^-\phi^0\right]$$

*Note: Thomas Gutierrez, an assistant professor of Physics at California Polytechnic State University, transcribed the Standard Model Lagrangian for the web. He derived it from Diagrammatica, a theoretical physics reference written by Nobel Laureate Martinus Veltman. In Gutierrez's dissemination of the transcript, he noted a sign error he made somewhere in the equation. Good luck finding it!

# How to extract properties of the medium

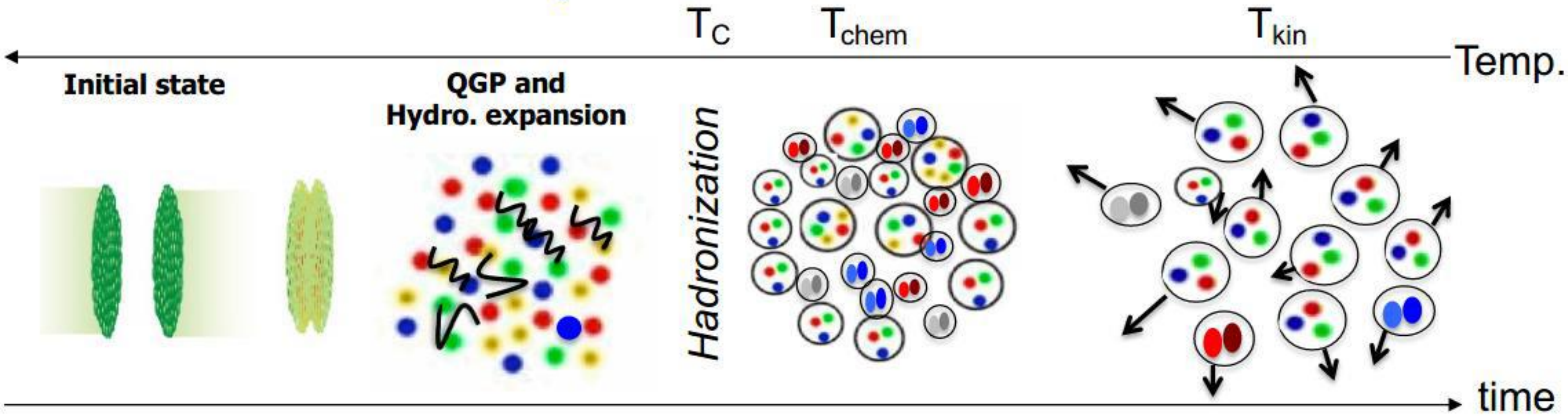


Colliding ions

Deconfined state

Chemical freeze-out
✧ Inelastic collisions cease
✧ Particle yield fixed

Kinetic freeze-out
✧ Elastic collisions cease
✧ Spectral shape fixed

Freeze-out (FO) parameters

Statistical thermal model: $T_{ch}$ and $\mu_B$

Blast-wave model: $T_{kin}$ and $\langle\beta\rangle$

**Particle Yields and Ratios:** provide Information about QCD phase diagram

# Nuclear modification of produced particles

$$R_{AA}(p_t) = \frac{\sigma_{in}^{pp}}{< N_{coll}^{AA} >} \cdot \frac{d^2N_{AA}/dp_t d\eta}{d^2\sigma_{pp}/dp_t d\eta}$$

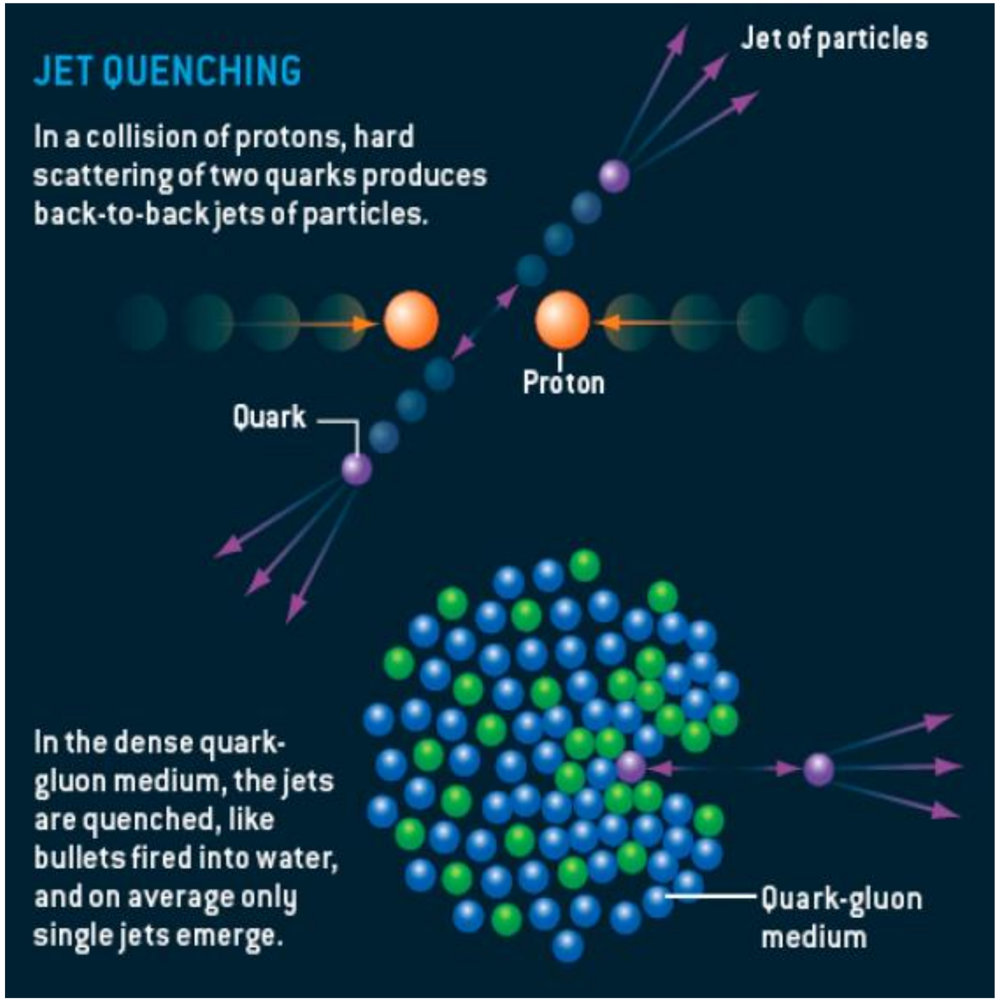


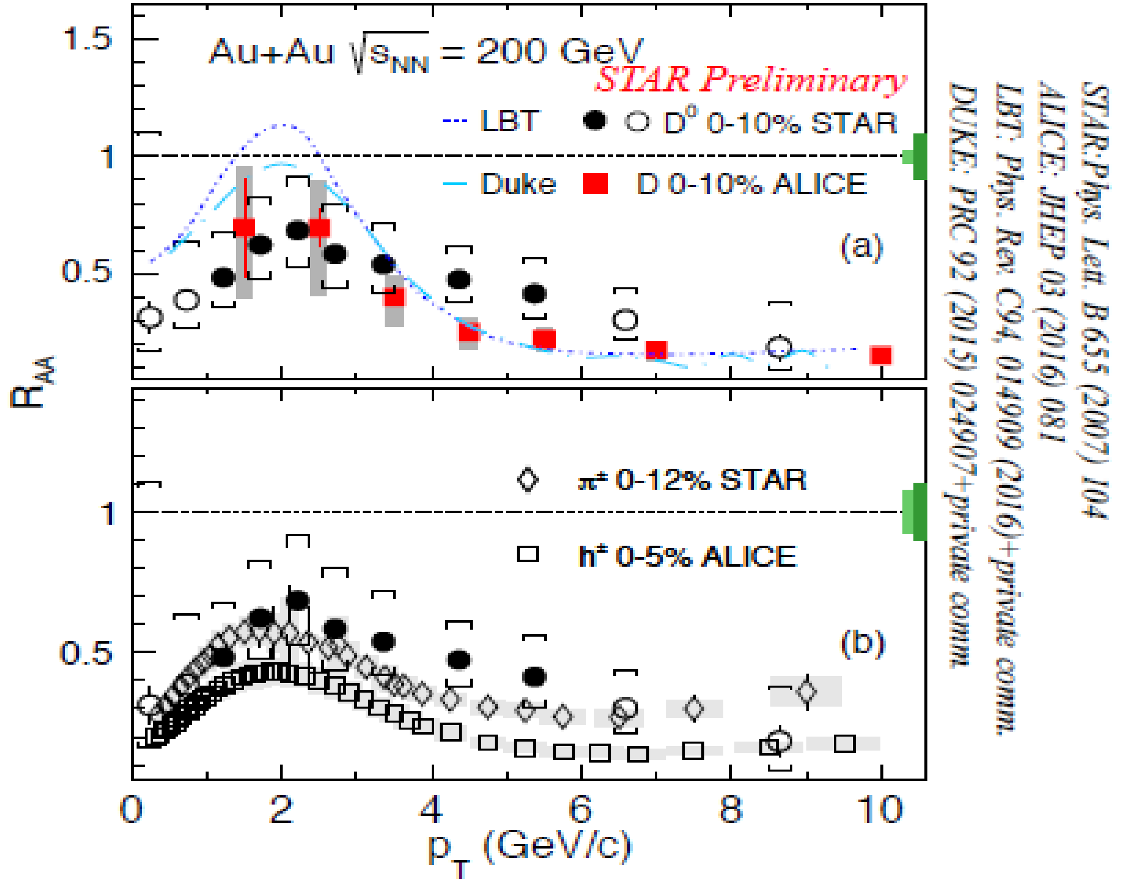

# Nuclear modification factor

$$R_{cp} = \frac{d^2N/dp_t d\eta / < N_{bin} > (central)}{d^2N/dp_t d\eta / < N_{bin} > (peripheral)}$$

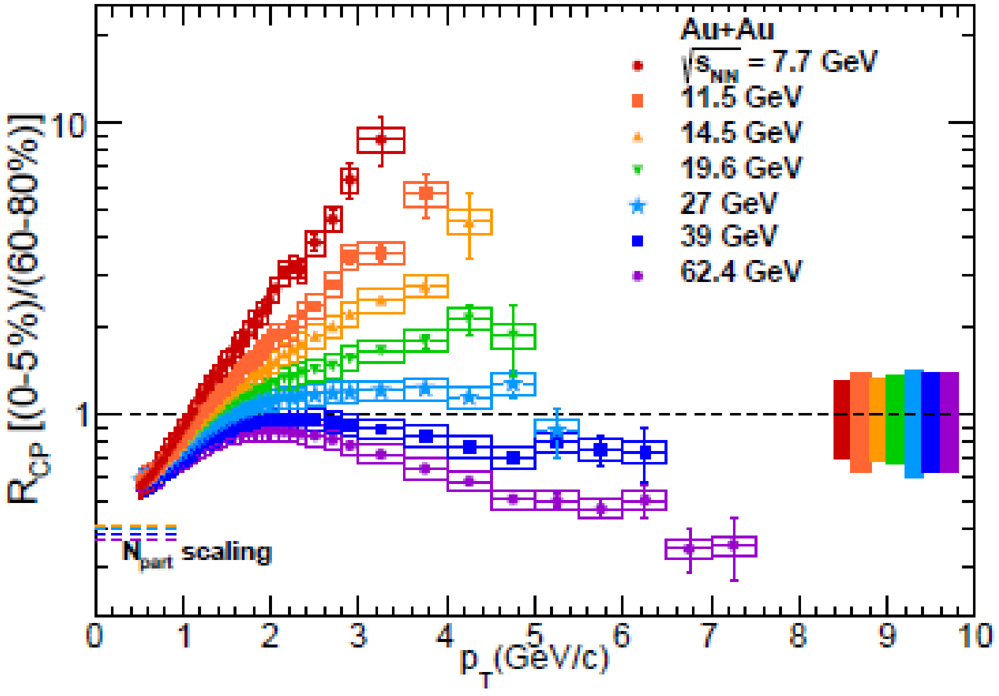


STAR, Phys. Rev. Lett. **121** (2018) 32301

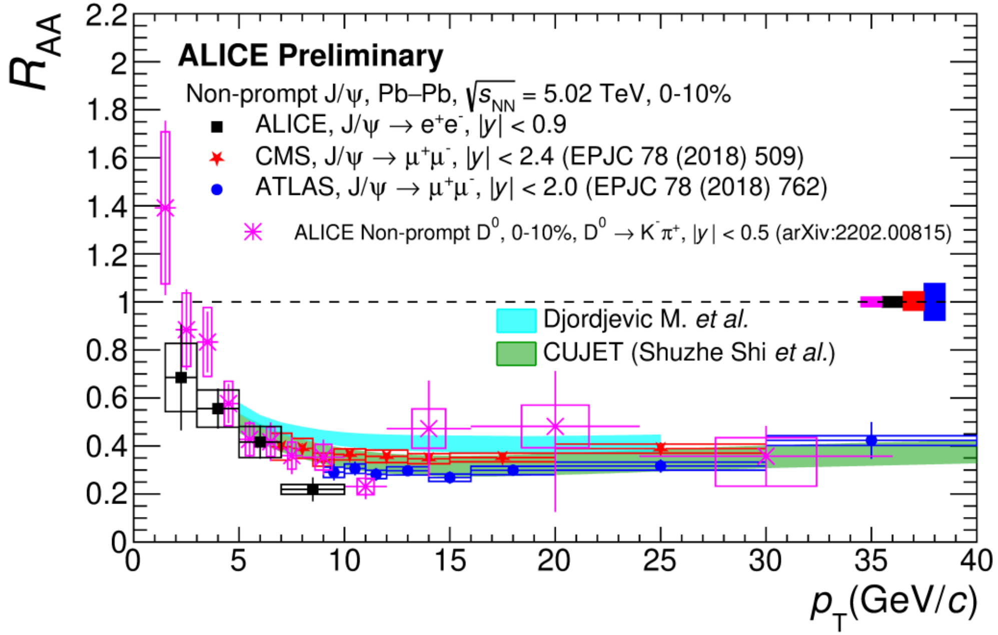


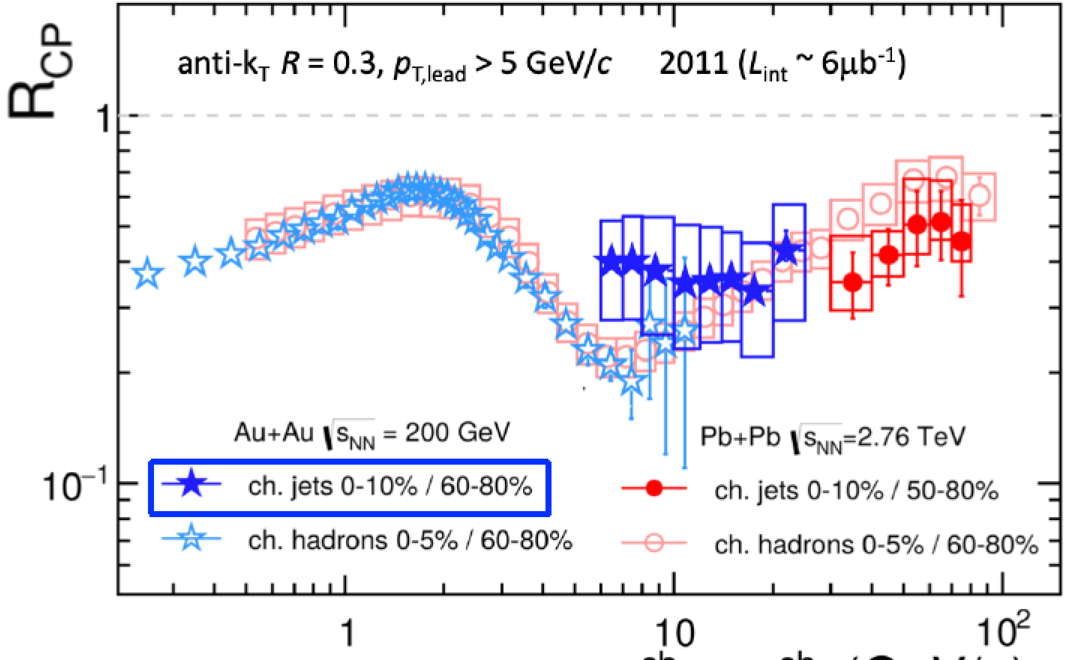


RHIC ch. hadrons: STAR, PRL 91.172302 (2003)
LHC ch. hadrons: ATLAS, JHEP09(2015) 050
LHC ch. jets: ALICE, JHEP30(2014) 013

# Hypertriton and anti-hypertriton

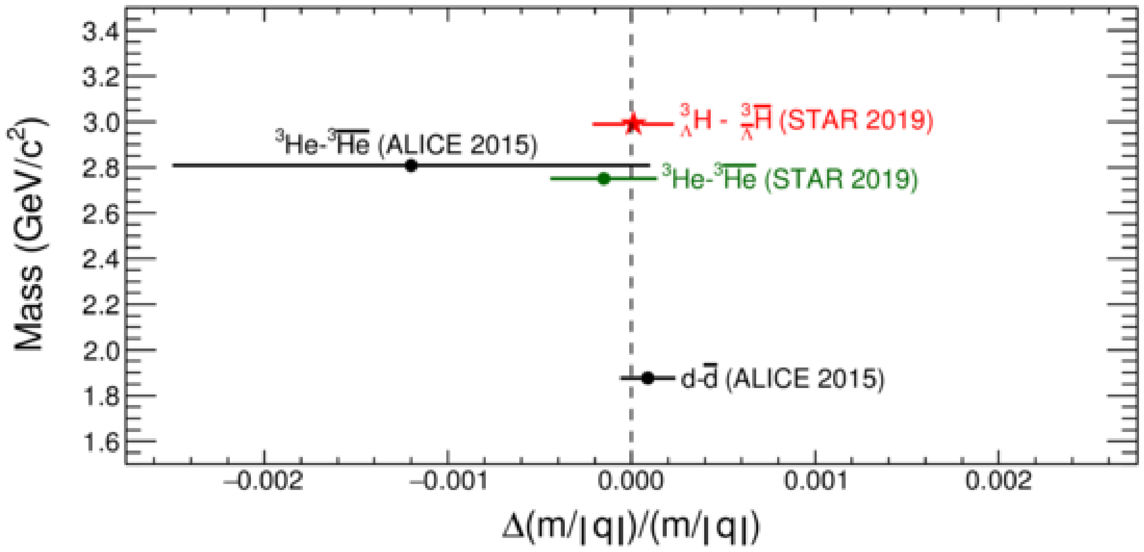


$$\frac{m_{^3_\Lambda H} - m_{^3_{\bar{\Lambda}}\bar{H}}}{m} = (0.1 \pm 2.0(\text{stat.}) \pm 1.0(\text{syst.})) \times 10^{-4}$$

This ratio allow to test the CPT symmetry from the perspective of experiment. Mass difference consistent with zero which is supporting the CPT symmetry

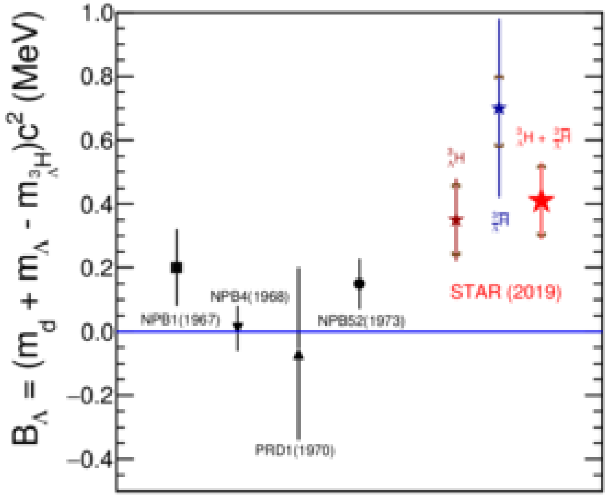


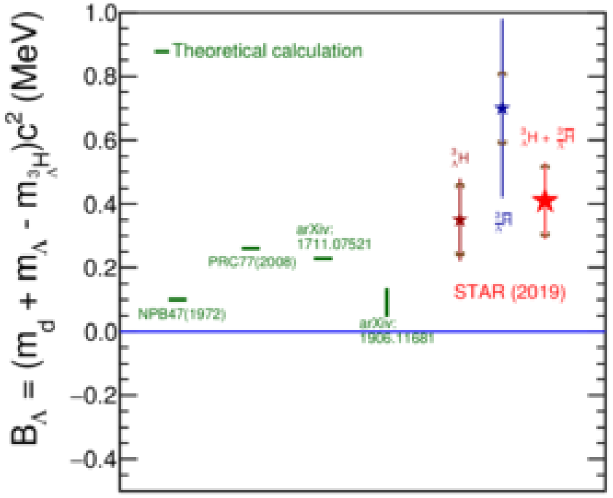


$$B_\Lambda = 0.41 \pm 0.12(stat.) \pm 0.11(syst.) MeV$$